

MASTER THESIS

SUITABLE METRICS FOR UPPER LIMB MOVEMENT SMOOTHNESS DURING STROKE RECOVERY

Bouke L. Scheltinga

FACULTY OF ELECTRICAL ENGINEERING, MATHEMATICS
AND COMPUTER SCIENCE
BIOMEDICAL SIGNALS AND SYSTEMS

EXAMINATION COMMITTEE

Dr. ir. B.F. van Beijnum
M.I. Mohamed Refai, Msc
Prof dr. G. Kwakkel
M. Saes, Msc

DOCUMENT NUMBER
BSS – 19-27

23-08-2019

UNIVERSITY OF TWENTE.

Summary

Worldwide, about 10.3 million people have a first-ever stroke each year. It is estimated that only 5-20% of the patients show complete function recovery after 6 months post stroke. Movements of stroke patients are characterized by slowness, spatial and temporal discontinuity (non-smoothness) and abnormal patterns of muscle activation. Although there are multiple hypotheses, the exact mechanism why there is a lack of smoothness is unknown. Studying movement quality, for instance change in smoothness, during stroke recovery is vital to better understand the recovery process after stroke.

Till so far, different smoothness metrics were used in research with stroke patients. It is seen that choices for the used metric are not always well motivated and even invalid metrics were introduced. In the first part of this thesis, all metrics that assess smoothness of reaching movements of stroke patients are obtained. It was seen that 31 different metrics have been used.

By critical inspection of the mathematical expression of the metrics, it was seen that some metrics were mathematically invalid as they were dependent on movement duration or movement velocity. Next, velocity profiles of reaching movements were simulated while different parameters such as peak velocity or movement duration were changed. With these simulations, was seen that 9 out of the 31 metrics seemed suitable for assessing movement smoothness. Among these suitable metrics are four dimensionless squared jerk metrics, two metrics that work in the frequency domain of the velocity profile, a metric that compares the executed movement velocity profile to a standard velocity profile by means of correlation and a metric that counts the number of peaks in the velocity profile.

As the metrics will be used with stroke patients, it is relevant to see if these metrics can capture changes in smoothness over time during the recovery of stroke patients. With clinical and kinematic data from 40 stroke subjects, measured multiple weeks after the stroke onset, two different linear mixed models using smoothness metrics were made. With these models, it was shown that the dimensionless jerk metrics performed slightly better in these models compared to the frequency spectrum based metrics.

Another important finding in this master thesis is the difference between velocity profiles of reach-to-grasp movements and pointing movements. It was seen that the reach-to-grasp movements clearly have asymmetrical velocity profiles and the minimum jerk model does not apply for these movements.

Contents

Summary	2
1 Introduction	5
1.1 Research Goal	7
1.2 Strategy and Outline	8
2 Systematic Review and Theoretical Evaluation of Movement Smoothness Metrics for Reaching Movements in Stroke	11
2.1 Abstract	12
2.2 Introduction	15
2.3 Methods	17
2.4 Results	22
2.5 Discussion	40
3 Evaluating Suitable Metrics for Movement Smoothness with Subjects Recovering after Stroke	50
3.1 Introduction	50
3.2 Methods	51
3.3 Results	54
3.4 Discussion	63
4 Discussion	67
Appendices	70
A - Search string for the different databases	70
B - Mathematical definition of metrics	73
C - Table with all metrics and users	79
D - Validation of the NOS algorithm	87

<i>CONTENTS</i>	4
E - Windows for symmetrical sub-movements	90
F - Reach-to-grasp velocity profiles	98

Chapter 1

Introduction

Worldwide, one of the main causes of adult disabilities is stroke [1]. Stroke is a phenomena where the blood flow to the brain is restricted, leading to cell death. There are two main groups of stroke types as shown in Figure 1.1. Ischemic stroke is caused by a reduced blood flow, often as a result of a blood clot. Hemorrhagic stroke is caused by a hemorrhage in the brain often caused by high blood pressure, resulting into a disruption of an artery in the brain. As most patients survive the stroke and may recover from their body impairments in the first 3 months, the biggest effect in the life of on patients and families is usually through long-term limitations in disability and restrictions in participation. Limitation of activities (disability), and reduced participation (handicap) affects about 80% of the patients [2]. The complications of the stroke are dependent of the size and location in the brain and occur within minutes after the stroke. Sudden weakness, problems with speech and paralysis are the most common symptoms seen after a stroke [3].

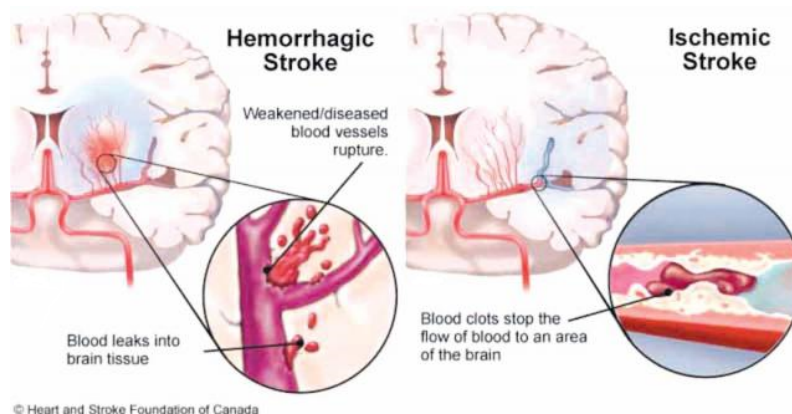


Figure 1.1: In a hemorrhagic stroke blood leaks into the brain tissue causing damage (left). In a ischemic stroke, the blood supply to the brain is restricted causing tissue damage (right).
Image from Heart and Stroke Foundation Canada [4].

Impairment of upper limb function resulting into reduced upper limb capacity is a common consequence after a stroke. These motor deficits is most evident in the limb contralateral to the side of the stroke after a meisppheric stroke [5]. Changes at motorneuron, nerve and muscle level have been observed which results in muscle weakness [6]. Further, task dependent weakness is found in hemiparetic patients. The ability of the elbow to create torque is strongly dependent on the orientation of the shoulder, which is not the case in healthy subjects [7].

Dewald et al. showed that there is a decrease in possible synergies in the paretic limb of the stroke subject which is a possible explanation of the task dependent strength [8]. It has been reported that more than 70% of stroke patients admitted to rehabilitation do have a limited reach [9]. Many subjects have a decrease in range of motion in the shoulder [10]. Van Meulen *et al.* showed that the area of range of the hand in the transversal plane at the affected side is smaller than the other side during a clinical measurement. Moreover, the area of range in daily living activities is even smaller [11].

Motor recovery after stroke is complex process and occurs probably through a combination of spontaneous and learning dependent processes. One of these processes is spontaneous neurological recovery, which is the restoring the functionality of the damaged tissue with no active treatment [12]. This process mainly occurs within the first three months after stroke with the largest improvements early after stroke and is often referred to as spontaneous neurological recovery [13]. This type of recovery would result in the same kinematic task performance as before the stroke [14]. Almost all patients show spontaneous neurological recovery following a natural logarithm pattern and occurs mainly within the first three months after stroke [2, 13]. The nature of this process is however not fully understood [15]. Further, motor recovery consists of compensation, which is the patient's ability to use an different approach compared to pre-stroke to accomplish a goal [16]. This type of recovery does not require neural repair. In the motor domain, it means that affected limbs or muscles take over the function of affected limbs or muscles [17]. The recovery pattern after stroke with the timing of different interventions is shown in figure 1.2.

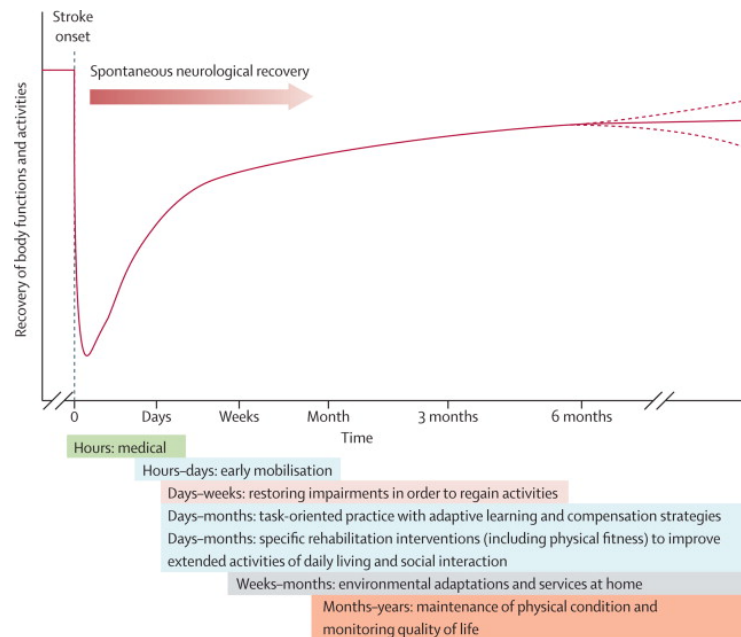


Figure 1.2: Hypothetical pattern of recovery after stroke and timing of different interventions. Image from Langhorne et al. (2011) [18]

Several longitudinal studies have shown that upper limb movements gradually recover as time proceeds in the first 6 months after stroke [19–21]. More specifically, van Kordelaar and colleagues (2014) showed that significant improvements in movement smoothness are mainly restricted to the first eight weeks after stroke onset [21]. Interestingly, this time window for significant change is similar for impairment related outcomes such as Fugl-Meyer Upper Extremity assessment [13, 22]. In addition, the lack of upper limb smoothness early post stroke is found to be highly associated with increased recruitment of sensorimotor and visual areas in whole-brain fMRI while reaching, whereas improvement in smoothness (i.e., reduction in jerk) is accompanied with an enhanced focusing of fMRI activity during stroke recovery [21]. This latter finding further supports the hypothesis that early after stroke, patients rely more on a visually and sensory controlled feed-back mechanism in their motor performance that gradually changes into a feed forward control of motor performance during upper limb recovery [21]. It is assumed that these time-dependent improvements in movement smoothness reflect behavioral restitution and are mainly driven by poorly understood processes of spontaneous neurological recovery, explaining 80 to 90% of the variance of outcome [13, 15].

Better understanding the time course of early observed improvements in quality of movement is vital for developing innovative interventions such as arm robotics, selecting appropriate outcomes and designing new trials that target true neurological repair early post stroke as it might contain information about compensation and restitution [23, 24]. But before doing that, it is important to select the correct ways to measure the quality of movement.

1.1 Research Goal

An often used measure for quality of movement is movement smoothness [24]. Smooth movements are a characteristic of skilled motor behavior [25]. Unfortunately, there is no consensus on how to measure the smoothness of movements. Many different metrics have been used in studies with stroke patients. It is believed that not all metrics used in previous studies are valid [26]. Several previous studies have compared smoothness metrics [19, 26–29]. However, these studies investigated a restricted set of smoothness metrics. Further, these studies are not objective as some recommend their own introduced metric. Currently the choice for a specific metric is not always well motivated in the study. A literature review about smoothness metrics can be of great value for researchers interested in movement smoothness to clarify the different metrics and help in choosing a metric.

Validation of the used measures is needed and can help prevent researchers from using imperfect, or worse, invalid metrics. In this master thesis, the main research question is: “What are suitable metrics for assessing movement smoothness in reaching movements of stroke patients?”

Sub-questions are created to come to an answer of this main research question. First all metrics are obtained by answering the question: “Which metrics have been used in scientific literature to assess movement smoothness in reaching of stroke subjects?”. The second sub-question is: “Which of the available metrics are valid in assessing movement smoothness?” to investigate the suitability. The last sub-question is: “Which of the valid smoothness metrics are sensitive to changes during recovery of stroke patients?”.

1.2 Strategy and Outline

Figure 1.3 gives an overview of how the research goal will be achieved. First a systematic review on the literature is done to find all metrics for movements smoothness that are used so far with reaching movements executed by stroke patients. Then, the found metrics are discussed based on the literature and assessed based on their mathematical expression. Using simulations of reaching movements, the mathematical behavior of the metrics is further investigated. This is all done in Chapter 2.

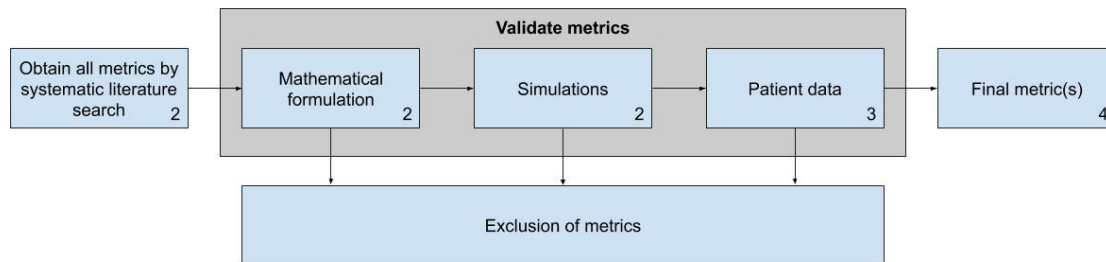


Figure 1.3: Strategy of this thesis. The number in the right bottom corner of each block represents the Chapter in which the block is addressed.

Thereafter, the metrics that were suitable to analyze movement smoothness, were applied on longitudinal patient data from 40 stroke subjects recovering from stroke. The goal here was to see if the metrics are sensitive enough to capture change in movement smoothness over time. These results are shown in Chapter 3.

To conclude in chapter 4, the results of this thesis are summarized and discussed to answer the research questions introduced at the beginning of the chapters.

References

- [1] World Health Organization. *The world health report 2003: shaping the future*. World Health Organization, 2003.
- [2] Peter Langhorne, Fiona Coupar, and Alex Pollock. “Motor recovery after stroke: a systematic review”. In: *The Lancet Neurology* 8.8 (2009), pp. 741–754.
- [3] National Heart Lung and Blood Institute. *Stroke*. 2014. URL: <https://www.nhlbi.nih.gov/health-topics/stroke#Signs,-Symptoms,-and-Complications> (visited on 01/23/2018).
- [4] Heart and Stroke Foundation of Canada. *Types of stroke*. [Online; accessed March 18, 2019]. 2010. URL: <https://www.heartandstroke.ca/stroke/what-is-stroke>.
- [5] MC Cirstea and Mindy F Levin. “Compensatory strategies for reaching in stroke”. In: *Brain* 123.5 (2000), pp. 940–953.
- [6] Daniel Bourbonnais and Sharyn Vanden Noven. “Weakness in patients with hemiparesis”. In: *American Journal of Occupational Therapy* 43.5 (1989), pp. 313–319.
- [7] Randall F Beer, Joseph D Given, and Julius PA Dewald. “Task-dependent weakness at the elbow in patients with hemiparesis”. In: *Archives of physical medicine and rehabilitation* 80.7 (1999), pp. 766–772.
- [8] Julius PA Dewald et al. “Abnormal muscle coactivation patterns during isometric torque generation at the elbow and shoulder in hemiparetic subjects”. In: *Brain* 118.2 (1995), pp. 495–510.

- [9] Catherine Dean and Fiona Mackey. “Motor assessment scale scores as a measure of rehabilitation outcome following stroke”. In: *Australian Journal of Physiotherapy* 38.1 (1992), pp. 31–35.
- [10] A Williams Andrews and Richard W Bohannon. “Decreased shoulder range of motion on paretic side after stroke”. In: *Physical Therapy* 69.9 (1989), pp. 768–772.
- [11] Fokke B van Meulen et al. “Objective evaluation of the quality of movement in daily life after stroke”. In: *Frontiers in Bioengineering and Biotechnology* 3 (2016), p. 210.
- [12] Steven C Cramer, Walter J Koroshetz, and Seth P Finklestein. “The case for modality-specific outcome measures in clinical trials of stroke recovery-promoting agents”. In: *Stroke* 38.4 (2007), pp. 1393–1395.
- [13] Gert Kwakkel, Boudewijn Kollen, and Jos Twisk. “Impact of time on improvement of outcome after stroke”. In: *Stroke* 37.9 (2006), pp. 2348–2353.
- [14] John W Krakauer et al. “Getting neurorehabilitation right: what can be learned from animal models?” In: *Neurorehabilitation and neural repair* 26.8 (2012), pp. 923–931.
- [15] Gert Kwakkel, Boudewijn Kollen, and Eline Lindeman. “Understanding the pattern of functional recovery after stroke: facts and theories”. In: *Restorative neurology and neuroscience* 22.3-5 (2004), pp. 281–299.
- [16] Julie Bernhardt et al. “Agreed definitions and a shared vision for new standards in stroke recovery research: the stroke recovery and rehabilitation roundtable taskforce”. In: *International Journal of Stroke* 12.5 (2017), pp. 444–450.
- [17] Mindy F Levin, Jeffrey A Kleim, and Steven L Wolf. “What do motor “recovery” and “compensation” mean in patients following stroke?” In: *Neurorehabilitation and neural repair* 23.4 (2009), pp. 313–319.
- [18] Peter Langhorne, Julie Bernhardt, and Gert Kwakkel. “Stroke rehabilitation”. In: *The Lancet* 377.9778 (2011), pp. 1693–1702.
- [19] Brandon Rohrer et al. “Movement smoothness changes during stroke recovery”. In: *Journal of Neuroscience* 22.18 (2002), pp. 8297–8304.
- [20] Laura Dipietro et al. “Submovement changes characterize generalization of motor recovery after stroke”. In: *Cortex* 45.3 (2009), pp. 318–324.
- [21] Joost van Kordelaar, Erwin van Wegen, and Gert Kwakkel. “Impact of time on quality of motor control of the paretic upper limb after stroke”. In: *Archives of physical medicine and rehabilitation* 95.2 (2014), pp. 338–344.
- [22] Pamela W Duncan et al. “Measurement of motor recovery after stroke. Outcome assessment and sample size requirements.” In: *Stroke* 23.8 (1992), pp. 1084–1089.
- [23] Floor Buma, Gert Kwakkel, and Nick Ramsey. “Understanding upper limb recovery after stroke”. In: *Restorative neurology and neuroscience* 31.6 (2013), pp. 707–722.
- [24] Anne Schwarz et al. “Systematic Review on Kinematic Assessments of Upper Limb Movements After Stroke”. In: *Stroke* (2019), STROKEAHA–118.
- [25] Richard A Schmidt. “A schema theory of discrete motor skill learning.” In: *Psychological review* 82.4 (1975), p. 225.
- [26] Sivakumar Balasubramanian et al. “On the analysis of movement smoothness”. In: *Journal of neuroengineering and rehabilitation* 12.1 (2015), p. 112.
- [27] Sivakumar Balasubramanian, Alejandro Melendez-Calderon, and Etienne Burdet. “A robust and sensitive metric for quantifying movement smoothness”. In: *IEEE transactions on biomedical engineering* 59.8 (2012), pp. 2126–2136.
- [28] Neville Hogan and Dagmar Sternad. “Sensitivity of smoothness measures to movement duration, amplitude, and arrests”. In: *Journal of motor behavior* 41.6 (2009), pp. 529–534.

- [29] V Rincon Montes et al. “Comparison of 4 different smoothness metrics for the quantitative assessment of movement’s quality in the upper limb of subjects with cerebral palsy”. In: *Health Care Exchanges (PAHCE), 2014 Pan American*. IEEE. 2014, pp. 1–6.

Chapter 2

Systematic Review and Theoretical Evaluation of Movement Smoothness Metrics for Reaching Movements in Stroke

This chapter is included as a Journal Article.

Systematic Review and Theoretical Evaluation of Movement Smoothness Metrics for Reaching Movements in Stroke¹

Abstract

Introduction:

Movement smoothness is an often used measure for quality of movement during reaching tasks. It is related to the continuity of a movement, independent of amplitude and duration of the movement. Studying movement quality during stroke recovery is vital to better understand the recovery process after stroke. Quantifying movement smoothness can be done using a metric for movement smoothness. Until now, over many different smoothness metrics are used in stroke research. Choices for the metrics are not always well motivated.

Objective:

The objective of this chapter is to come with a first recommendation of potentially suitable smoothness metrics based on a theoretical analysis and simulation results.

¹The findings and results of this chapter were extensively discussed during several Skype meetings and project meetings with M.I. Mohamed Refai (MIMR), Bert-Jan F. van Beijnum, Gert Kwakkel, Mique Saes, Erwin E.H. van Wegen and Carel G.M. Meskers.

Methods:

A systematic review of the literature was done to obtain an overview of available metrics of smoothness used for investigating reach-to-grasp and pointing performance post stroke. Subsequently, velocity profiles that mimic forward reaching movements were simulated. The behavior of the selected metrics was studied while parameters of the velocity profile were varied, such as movement duration, movement distance and movement segmentation. Furthermore, we investigated the effect of adding sinusoids and white noise disturbance to these velocity profiles. The suitability of different metrics to measure smoothness is discussed based on the simulations and recommendations are given.

Results:

From the systematic review, 31 different metrics were identified. From these metrics, it was seen that 16 were excluded based on their definition or units. In the simulation, another 7 metrics were excluded, resulting in 9 different valid metrics.

Conclusion:

In total 8 metrics are recommended for further analysis and research. These are: *Peaks metric*, *inverse of peak metric*, four dimensionless squared jerk metrics, *correlation metric*, and *spectral method* based on the criteria defined in this paper.

Abbreviations

AM: Acceleration metric

ARAT: Action Research Arm Test

CM: Correlation metric

CSM: Combined smoothness metric

DAJ: Dimensionless absolute jerk

DSJ_b: Dimensionless squared jerk as introduced by Balasubramanian et al. (2009)

DSJ_m: Dimensionless squared jerk as introduced by Marini et al. (2017)

DSJ_t: Dimensionless squared jerk as introduced by Teulings et al. (1997)

FMA-UE: Fugl-Meyer Motor Assessment Score for Upper Extremity

IAJ: Integrated absolute jerk

IC: Index of curvature

ICF: International Classification of Functioning, Disability, and Health

IPV: Inversed number of peaks

ISJ: Integrated squared jerk

LDAJ: Log of dimensionless absolute jerk

LDSJ_b: Log dimensionless squared jerk as introduced by Balasubramanian et al. (2012)

LDSJ_t: Log dimensionless squared jerk as introduced by van Kordelaar et al. (2014)

MAPR: Movement arrest period ratio

MIAJPS: Mean integrated absolute jerk normalized by peak speed

MSJ: Mean squared jerk

MSJMS: Mean squared jerk normalized by mean speed

MSJPS: Mean squared jerk normalized by peak speed

NOS: Number of sub-movements

NRS: Normalized reaching speed

PM: Peaks metric

PRISMA: Preferred Reporting Items for Systematic Reviews and Meta-Analyses

RMS: Root mean squared

RMSJ: Root mean squared jerk

SM: Speed metric

SPAL: Spectral arc length, as introduced by Balasubramanian et al. (2012)

SPARC: Spectral Arc Length, as introduced by Balasubramanian et al. (2015)

SPM: Spectral method

SPMR: Spectral metric

VAL: Velocity arc length

Introduction

Yearly, about 10.3 million people worldwide have a first-ever stroke and about 25.7 million stroke survivors and 6.5 million stroke-related deaths are reported (Feigin et al., 2017), making stroke the second most common cause of death and one of the main causes of acquired adult disability (Feigin et al., 2017; Langhorne et al., 2011). It is estimated that only 5-20% of the patients show complete function recovery after 6 months post stroke (Kwakkel et al., 2003). Goal-directed upper limb movements in stroke patients are characterized by slowness, spatial and temporal discontinuity (i.e., lack of smoothness) and abnormal stereotypic patterns of muscle activation also called synergies (Cirstea and Levin., 2000).

Movement smoothness is a measure of a movement quality, related to the continuity of a movement, independent of amplitude and duration of the movement (Balasubramanian et al., 2015). The lack of smoothness in movement patterns is seen as an important characteristic of affected quality of movement and often targeted in stroke rehabilitation to improve upper limb performance such as done with robotic rehabilitation devices (Schweighofer et al., 2018). A smooth movement is seen as a bell-shaped velocity profile in point-to-point reaching movements (Flash and Hogan, 1985). Reaching is defined according to the International Classification of Functioning, Disability, and Health (ICF) as *“Using the hands and arms to extend outwards and touch and grasp something, such as when reaching across a table or desk for a book”*.² Flash and Hogan (1985) found that these movements, performed by healthy subjects, can be adequately described by the minimal jerk model. Movements that do not follow the minimal jerk pattern are said to be less smooth (Balasubramanian et al., 2015). Balasubramanian et al. (2015) did point out that movement intermittencies, causing less smooth movements, can occur by two sets of factors; the first being the ability of the performer on controlling a specific task. Stroke patients often have poor motor control in upper limb movements and a decreased smoothness compared to healthy subjects (Cirstea and Levin., 2000). Secondly, smoothness is dependent on the goal of the task. A reaching task with an intermediate target will have a movement intermittency that is not the result of poor motor control but a result of the requirements of the task. Therefore, it is not possible to compare smoothness of two completely different tasks.

² <http://apps.who.int/classifications/icfbrowser/> accessed: 4-12-2018

Unfortunately, there is no consensus on how to quantify the smoothness of movements. In studies with stroke patients, many different metrics have been used and there is little consensus on the best metric to quantify smoothness (Balasubramanian et al., 2015). Furthermore, multiple definitions for similar metrics to quantify smoothness are used (Hogan and Sternad, 2009). According to Balasubramanian et al. (2012), not all used metrics are valid, for example, Jerk based metrics with meters or seconds in the units are sensitive for movement duration or movement distance. Several previous studies have compared smoothness metrics (Rohrer et al., 2002; Balasubramanian et al., 2012; Hogan and Sternad, 2009; Balasubramanian et al., 2015; Montes et al., 2014). However, these studies investigated a restricted set of smoothness metrics. Furthermore, these studies might be not objective, for example, (Balasubramanian et al., 2015) recommend the metric that they introduced.

The first research question in this paper is: “Which metrics have been used in scientific literature to assess movement smoothness in reaching of stroke subjects?”. For this purpose a systematic review is done. Metrics are subsequently classified on the basis of their underlying mathematical definition.

Secondly, we will look into the question: “Which metrics are defined in a mathematically valid and sound manner?”. To answer this, the mathematical expressions of the metrics are compared and the units are derived. Thirdly, we investigated: “How do smoothness metrics behave as the characteristics of the analyzed movement changes?” For this latter purpose, we will split up the velocity profiles in sub-movements, change movement distance and duration and add sinusoids and white noise. The findings of these evaluations will be a list of metrics that is suitable to assess movement smoothness based on the criteria defined in this study.

Materials and Methods

Literature search strategy

This systematic review was done according to the PRISMA statements (Moher et al., 2009). Scopus, Cochrane, Embase and PubMed databases were searched. The search aimed at finding papers that contained 'stroke', 'reaching' and 'movement smoothness'. The full search query is defined in Appendix A. Study screening was done by one researcher (BLS) through two levels of screening. In case of uncertainty about the inclusion of a study, it was discussed with a second author (MIMR). During the first level of screening, titles and abstracts were screened and excluded if they were not on the topic of stroke, or in a language other than English, Dutch or German. Full text was obtained for the second level of screening. We included articles where (1) reaching or aiming movements of stroke patients were studied and (2) a metric was used to determine the smoothness of this movement. For reaching, the ICF definition is used. Tasks where subjects aim for a target or object are classified as aiming movement. This target can be virtual, for example a target on screen after interaction with a robotic device. This group includes the often studied point-to-point reaching tasks. The references of the included articles were scanned for possible other relevant articles. From the included studies, the metric and its mathematical formulation used to quantify movement smoothness were extracted.

Classification of metrics

The metrics found as a result of the review were classified into different categories based on their mathematical definitions. It is expected that metrics within a category show similarities, this makes the comparison between metrics easier. First, it was determined whether the metric was in the frequency or time domain. If it was in the frequency domain, the metric was classified in the category of '*Frequency metrics*' whereas in the time domain, the metric was classified into the: 1) '*Trajectory metrics*', 2) '*Velocity metrics*', 3) '*Acceleration metrics*' or 4) '*Jerk metrics*'. For example, if a metric contained a jerk term, the metric was classified into the category of jerk metrics. Metrics that cannot be assigned to one of these categories or to more categories, will be classified in the group '*Other metrics*'.

Metrics included for simulation

An inclusion criteria was used to decide which metrics were included for the simulation. Metrics were excluded if:

1. the units contained [m] and/or [s], or
2. the metric is not reproducible from the reference, or
3. the metric is not based on velocity or a derivative of this, or
4. the metric is replaceable by another metric by
 - a. a scaling it by a dimensionless number
 - b. an addition or subtraction with a dimensionless number

These decisions will be shown in an overview table with all metrics. Exclusion reason 1 is based on the work of Hogan and Sternad (2009) where they motivate that, if a measure of movement smoothness only is desired, the units of the metric cannot contain meters or seconds. Exclusion reason 2 is introduced from practical reasons, simulations with a metric cannot be executed if the exact description or mathematical definition of that metric are missing. Exclusion reason 3 is introduced since it is impossible to derive the smoothness of a movement if only position data is used without context of the time. Exclusion reason 4 is added since it is redundant to repeat simulations that are a scaling or shifting of other metrics. In this case, the simulation is done with the metric that appeared to be the first in literature.

Movement simulations

A one second, bell shaped velocity profile with a peak speed at 0.56 m/s is created using the minimal jerk model, derived by Flash and Hogan (1985) with the equation:

$$v_{mj}(t) = \Delta \left(\frac{30t^4}{T^5} - \frac{60t^3}{T^4} + \frac{30t^2}{T^3} \right),$$

where v_{mj} is the minimal jerk velocity profile, Δ is the total reaching distance, T is the total movement time and t is the time scale from 0 till T . Flash and Hogan (1985) further confirmed that this model matches observed human planar two-joint (elbow/shoulder) arm movements. This velocity profile was used in four simulations, the *shape simulations*, *Sinus Simulation*, *Noise Simulation* and *Sub-movements Simulation*. These simulations are explained below. All created velocity profiles had a sampling frequency of 200Hz. For Δ , the value of 0.3m was chosen and for T a value of 1s to create a velocity profile which will be referred to as 'the main velocity profile'. This velocity profile is shown in Fig.1.

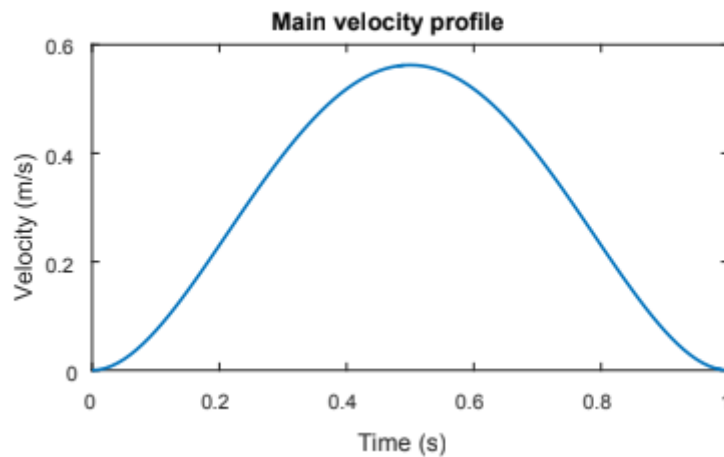


Fig. 1: The main velocity profile with peak speed at 0.56m/s and a duration of 1 second. It corresponds to a reaching movement with a distance of 0.3m.

Shape Simulations

By performing the *shape simulation*, the dependency on movement duration and moving (i.e. reaching) distance is investigated. Profiles are created with different durations ranging from 0.5 till 6.0s, with steps of 0.1s, and different reaching distance, ranging from 0.2 till 0.7m, with steps of 0.01m. A total of 2856 combinations with different durations and distances were used to calculate the outcomes of the metrics. The movement durations and distances were chosen arbitrarily, within the range of human reaching movements. A metric that only reflects movement smoothness, should not be dependent on movement duration or movement distance. Therefore, the metric outcomes should remain unchanged during this simulation. In the plot with metric, movement duration and movement distance on respectively the z-, x- and y-axis the plot should be constant on the z-axis. A metric is said to be independent of movement duration or moving distance if the changes seen in this simulation is less than 1% of the change in the sub-movement simulation.

Sinus Simulations

With the *sinus simulation*, different sinusoidal distortions are added to the main velocity profile to check the response on different frequencies and amplitudes. Frequencies between 2 and 25 Hz were used, with steps of 0.5Hz. Amplitudes were used between 0 and 0.2 m/s with steps of 0.005 m/s. A total of 1927 combinations were used. It is expected that the smoothness according to the metrics decrease with increasing amplitude for the same frequency. This simulation could imitate movements with increasingly heavy oscillations. This is further a characterization to check the sensitivity of the metrics on the different frequencies and amplitudes. When sinuses with a higher amplitude are added, the metrics should give less smooth outcomes. The relation between frequency and the metric outcome and between amplitude and metric outcome should both be monotonic, meaning that it is either entirely non-increasing, or entirely non-decreasing. For a truly monotonic relation, the derivative should not have zero crossings.

Noise Simulation

With the *noise simulation*, on top of the main velocity profile, normally distributed noise with zero mean was added with different magnitudes. Root mean square (RMS) values of the noise varied from 0 to 0.08 m/s with steps of 0.002 m/s. The noise was generated with the MATLAB function 'randn'. To improve randomness, 25 different sets of normally distributed noise for each of the different RMS values mentioned. Then, the minimal value, maximal value, mean and standard deviation was determined for each metric at each RMS value and shown. In a next simulation, the noise was filtered using a zero phase 4th order 20Hz low pass Butterworth filter. This is chosen since the SPAL metric has inherent filter properties comparable to a 20Hz low pass filter. The mean value of each metric with the filtered noise was also determined.

It is expected that added noise will decrease the quality of the performance of the metrics. This would be visible by an increase in the difference between the minimal and maximal value at a certain noise intensity, since it means that noise can induce changes in the outcome of the smoothness metric. Further it is expected that the metrics will quantify added noise as less smooth movements since noise in the velocity profile can be seen as a non-smooth addition to the main velocity profile. Metrics will be compared to the response on noise relative to each other and relative to the other simulations.

Sub-movements Simulation

As recovery after stroke proceeds, it is seen that sub-movements grow larger, fewer and more blended during stroke recovery, causing the movement to be smoother (Rohrer et al., 2004). With the *sub-movements simulation* the main velocity profile is split into sub-movements. The first sub-movement always starts at $t = 0$ seconds, when there is complete overlap between the sub-movements. The starting point for the next sub-movement is varied with the lag variable K_s between the beginning of two consecutive sub-movements. K_s is varied from 0 seconds, where the sub-movements start simultaneously till 1.2 seconds, where there 1.2 seconds between the starting points of the two sub-movements, with increments of 0.02 seconds. The outcome for the different metrics is then calculated for all different K_s values. With this simulation, the length of the movement is also increased as K_s increases. This simulation will be done with 2, 3 and 4 sub-movements. A higher number of sub-movements would mean a more segmented movement and thus a less smooth velocity profile. Therefore, it is expected that the metrics quantify the movement as less smooth as K_s increases in a monotonic trend. The monotonicity will be quantified by visual inspection of the metric curve plotted against the lag variable K_s and visual inspection of the derivative of this curve.

To summarize, a metric that (1) is independent on movement duration and movement distance, (2) is relatively insensitive to noise, (3) has a monotonic response on the sinus simulation and (4) has a monotonic response to the sub-movement simulation, would be recommended as a suitable metric for movement smoothness in point-to-point reaching task.

Results

The PRISMA flow chart (Fig. 2) shows the identified and included studies using smoothness of the upper paretic limb after stroke. After identifying 356 unique studies, 97 were included for further analysis. Metrics that have been used in these studies were classified into the 6 different groups, i.e., ‘*Trajectory metrics*’, ‘*Velocity metrics*’, ‘*Acceleration metrics*’, ‘*Jerk metrics*’, ‘*Frequency metrics*’ and ‘*Other metrics*’. The metrics in each group will be discussed separately. All metrics found in literature and their corresponding studies are shown in Appendix C. In Table 1, the found metrics are shown.

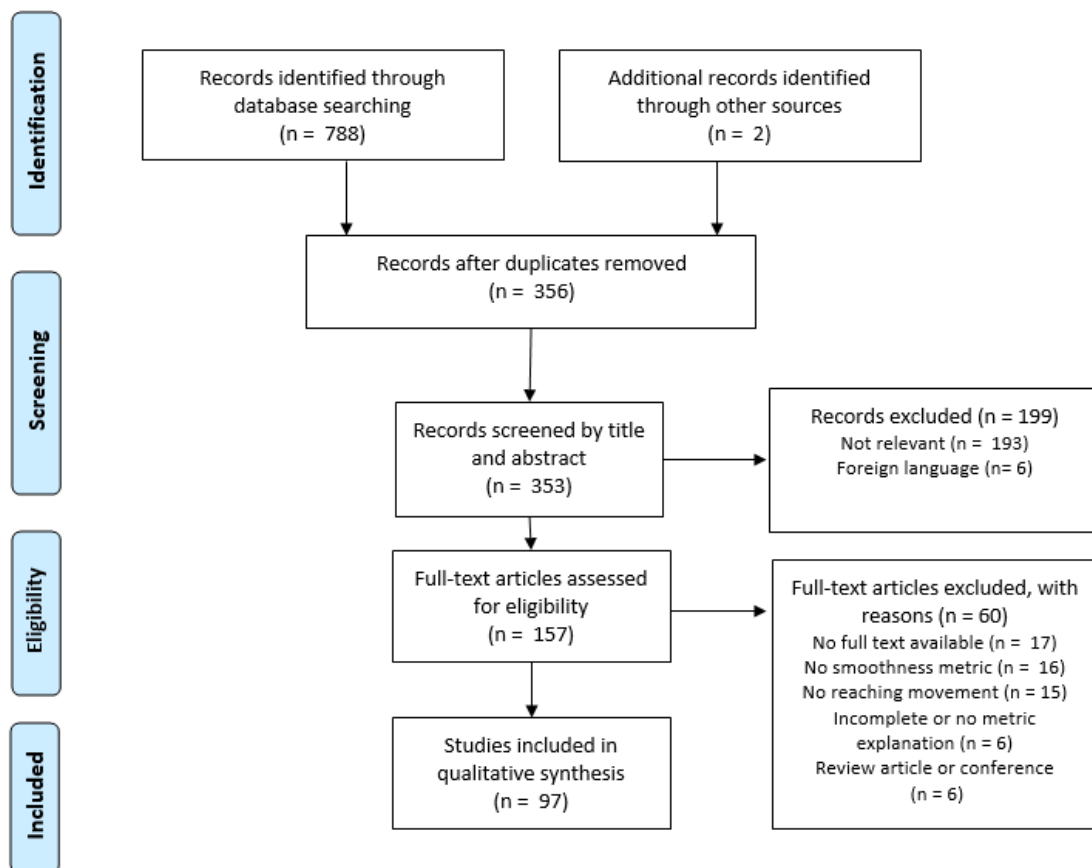


Fig. 2: PRISMA Flow chart

Table 1: Overview of smoothness metrics with units, how often it is used in literature and a brief evaluation. The different colors separate the different groups. Ordered from bottom to top as trajectory, velocity, acceleration, frequency and other metrics. Meaning of exclusion reasons: 1. the units contained [m] and/or [s], 2. the metric is not reproducible 3. the metric is not based on position or a derivative of this and 4. the metric is reproducible by another metric by scaling (a) or subtraction (b) with a dimensionless number.

Metric	Units	Usage	Evaluation	Exclusion reason for simulation	Citation
Index of curvature	[]	1	Does not contain information about movement continuity	3	Bigoni et al. (2016)
SD_XY	[]	1		3	Simonsen et al. (2017)
Number of sub-movements (NOS)	[]	1	Algorithm is not unequivocal (Liebermann et al., 2010)		Liebermann et al. (2010)
Speed metric (SM)	[]	15	Non-monotonic (Rohrer et al., 2002)		Rohrer et al. (2002)
Normalized reaching speed (NRS)	[]	2 ³	Is the same as 1-SM	4a and 4b	Mazzoleni et al. (2011)
Movement arrest period ratio (MAPR)	[]	3	Non-monotonic (Rohrer et al., 2002) and insensitive to speed fluctuations (Hogan and Sternad, 2009)		Beppu et al. (1984)
Tent metric	[]	1	Non-monotonic (Rohrer et al., 2002)	2	Rohrer et al. (2002)
Velocity arc length (VAL)	[]	1	Sensitive to noise, lack sensitivity to changes in movement arrest periods compared with SPAL (Balasubramanian et al., 2012)		Balasubramanian et al. (2012)
Correlation metric (CM)	[]	2			Krebs et al. (2001)
Number of peaks	[]	57 ⁴	Insensitive and nonrobust measure, unsuitable for practical use (Balasubramanian et al., 2012)		Brooks (1974)
Number of peaks normalized by movement duration	[s ⁻¹]	1	Dependent on duration	1	Kahn et al. (2006)
Number of peaks normalized by movement distance	[m ⁻¹]	4	Dependent on distance	1	Abdul Rahman et al. (2017)

³ Both by the same author

⁴ Slightly different algorithms were used

Inverse number of peaks and valleys (IPV)	[]	1				Pila et al. (2017)
Acceleration metric (AM)	[]	2 ³			1	Mazzoleni et al. (2011)
Integrated absolute jerk (IAJ)	[ms ⁻²]	2	Non-monotonic (Hogan and Sternad, 2009)		1	Duff et al. (2010)
Mean absolute jerk (MAJ)	[ms ⁻³]	2			1	Bigoni et al. (2016)
Mean absolute jerk normalized by peak speed (MAJPS)	[s ⁻²]	6	Non-monotonic (Rohrer et al., 2002)		1	Rohrer et al. (2002)
Integrated squared jerk (ISJ)	[m ² s ⁻⁵]	1	Hogan and Sternad (2009)		1	Laczko et al. (2017)
Root mean squared jerk metric (RMSJ)	[ms ⁻³]	1			1	Young and Marteniuk (1997)
Normalized integrated jerk (NIJ)	[ms ⁻³ √s]	1			1	Adamovich et al. (2009)
Dimensionless squared jerk (DSJ-t)	[]	12				Teulings et al. (1997)
Log dimensionless squared jerk (LDSJ-t)	[]	1	Log transformed for statistical analyses			Van Kordelaar et al. (2014)
Dimensionless squared jerk (DSJ-m)	[]	1	Only a linear scaling is different compared with DSJ-t		4a	Marini et al. (2017)
Dimensionless squared jerk (DSJ-b)	[]	1				Balasubramanian et al. (2012)
Log dimensionless squared jerk (LDSJ-b)	[]	1	Better sensitivity than DSJ-b (Balasubramanian et al., 2012), Sensitive to noise, lack sensitivity to changes in movement arrest periods compared with SPAL (Balasubramanian et al., 2012)			Balasubramanian et al. (2012)
Rotational jerk	[]	1			3	Repnik et al. (2018)
Spectral metric (SPMR)	[]	1				Strohmann et al. (2013)
Spectral method (SPM)	[]	1	Sensitive to noise (Balasubramanian et al., 2012)			Balasubramanian et al. (2009)
Spectral arc length (SPAL)	[]	8	Dependent on movement duration (Balasubramanian et al., 2015)			Balasubramanian et al. (2012)
Combined smoothness metric (CSM)	[--]	1 ⁵			1	Popović et al. (2014)

⁵ Units cannot be defined for this metric

Trajectory metrics

According to Bigoni et al. (2016) the Index of Curvature (*IC*) is representative for movement smoothness. The *IC* is the ratio between the 3D path length and the linear distance between the initial and final point of the finger. So, a straight trajectory would have an outcome of 1, while a reaching movement in a half circle would have an outcome of 1.57 (i.e. $0.5 \cdot \pi / 1$). It must be noted that this metric was calculated in other studies as well with stroke subjects (Michaelsen et al., 2001; Subramanian et al., 2007; Levin et al., 2002), however this metric was not used as a measure for movement smoothness but as 'trajectory smoothness'.

Simonsen et al. (2017) used the standard deviation of the position perpendicular to the movement direction as a 2D measure for movement smoothness (*SD_{XY}*). Movements were done while sliding the hand over the table, so the height of the hand remained constant. Therefore this measure is only in X and Y direction.

Nothing can be said about the velocity and change in velocity, which is needed to quantify smoothness, when only the shape trajectory is analyzed. Therefore it can be said that trajectory metrics are not suitable to analyze movement smoothness. These metrics are therefore excluded from the simulation, according to exclusion reason 3.

Velocity metrics

Movement arrest period ratio (*MAPR*) is defined by Beppu et al. (1984) as the proportion of time that movement speed exceeds a given percentage of the peak speed (Beppu et al., 1984). As subjects recover from a motor impairment and less movement segments occurs, the periods of movement arrest are decreased, resulting in a higher value for the metric. One drawback is that this method is not sensitive to fluctuations in speed which are higher than a chosen percentage of peak speed (Hogan and Sternad, 2009). Another drawback is that this metric has a non-monotonic response to the change in sub-movement segmentation (Rohrer et al., 2002).

The speed metric (*SM*) is the mean speed of the whole movement, normalized by the peak speed during this given movement (Rohrer et al., 2002). It is based on the fact that people with a motor impairment perform movements in a segmented way. A more severely impaired subject will have deeper valleys in the speed profile than a subject with more blending between segments, resulting in a lower value for the *SM*. A drawback is that this metric has a non-monotonic response to the change in sub-movement segmentation (Rohrer et al., 2002).

Mazzoleni et al. (2011) used the speed metric, but also introduced and used the normalized reaching speed (*NRS*). This is the ratio between the peak speed and mean speed difference, and the peak speed. However, no additional information is obtained with this metric as it is the same as $1 - SM$, and so it has the same properties as *SM*. Therefore, this metric will not be included in the following simulation.

The Tent Metric, introduced Rohrer et al. (2002) calculates the ratio between the area under an overarching (tent) profile and the area under the velocity profile. The tent profile is made by connecting peaks in the speed profile. However, the exact mathematical description is not revealed in the study (Rohrer et al., 2002) and will therefore not be evaluated in simulations in this study.

Rohrer and Hogan (2006) developed a global nonlinear minimization algorithm which can extract sub-movements from a tangential velocity profile. The number of sub-movements (*NOS*), was used by Liebermann et al. (2010) to assess smoothness in stroke subjects. However, they doubt whether such a parameterization of smoothness can be used for the diagnosis or assessment of rehabilitation effectiveness as the algorithm is ambiguous and differences can be obtained by changing boundary criteria in the algorithm. This metric is discussed and analyzed in more detail in appendix D.

The velocity arc length (*VAL*) metric was introduced by Balasubramanian et al. (2012). This metric uses the arc length of the speed profile normalized by the peak speed. It works by the principle that a bell-shaped velocity profile will have a shorter arc length than one with fluctuations in velocity. According to Balasubramanian et al. (2012), this metric is highly sensitive to noise and lacks sensitivity to changes in movement arrest periods, in contrast to the spectral arc length (*SPAL*) metric.

Krebs et al. (2001) determined the smoothness of a movement by the correlation between the velocity profile, extracted from the minimal jerk model, and the actual hand velocity profile during a straight-line movement between two targets. To this will be referred as correlation metric (*CM*). For this analysis distance from start to end point of the movement should be known as well as the movement duration. Celik et al. (2010) changed this metric slightly by changing the negative correlations to 0. With the adapted metric, they found significant correlation between the *CM* and FMA-UE and between the *CM* and ARAT. This is classified as a jerk metric since the executed velocity profile is compared with the minimal jerk model.

It is decided to include *NOS*, *SM*, *MAPR*, *VAL* and *CM* in the simulations.

Acceleration metrics

The most used metric for movement smoothness in stroke patients is the peaks metric, which is used 57 times. It is defined by Brooks (1974) as the number of local maxima in the speed profile for a given movement. Non-smooth movements are characterized by fluctuations in velocity, causing local maxima in the velocity profile. It is classified as an acceleration metric since the calculation of this metric is in the acceleration domain. A peak can be detected as a zero crossing in the acceleration domain, while the derivative of the acceleration at this zero crossing is negative. This simple metric performs well in stroke subjects performing a planar (i.e. 2D) reaching movement but is unsuitable for implementation according to Balasubramanian et al. (2012) because 1) the difficulty in detecting peaks accurately in practice, 2) the use of an ordinal scale resulting in large jumps in smoothness values and 3) the insensitivity to changes in movement arrest periods. Longhi et al. (2016) used this metric with a 3 dimensional reaching task and showed a statistically significant correlation between number of peaks and the clinical reference (Wolf Motor Function Test ability score). Occasionally, the peak metrics is referred to as the number of inversions (Schneider et al., 2007), number of reversals in velocity profile (Johnson et al., 2005) or number of sub-movements (Chang et al., 2008). Some authors normalize the number of peaks to the movement duration (Kahn et al., 2006) or to the movement distance (Abdul Rahman et al., 2017). Attention should be paid while doing this, as the metric becomes dependent on movement duration or movement distance. Therefore, these metrics are not included in the simulation, in accordance with exclusion reason 1. Some studies used the number of valleys instead of peaks (Bermúdez i Badia and Cameirão, 2012) or the sum of valleys and peaks (Mohapatra et al., 2016). These are not independent since the number of valleys is simply 'peaks-1', and peaks and valleys is 'peaks*2 - 1'. Number of valleys and number of peaks and valleys is therefore excluded from the simulation based on exclusion reason 4. Pila et al. (2017) used the inverse of the number of peaks (*IPV*) and valleys. Further, additional requirements can be applied for the peak detection algorithm. Among this is a threshold on the velocity of the peak and/or a threshold on the time interval between two consecutive peaks and/or a threshold between the velocity of a minimum and the next maximum (Casadio et al., 2009; Hussain et al., 2018).

The acceleration metric (*AM*), introduced by Mazzoleni et al. (2011) defines smoothness as the ratio between the mean acceleration and the peak acceleration. This metric increases as movements gets smoother. It is shown that this metric is increased significantly in subacute stroke patients but not in chronic stroke patients (Mazzoleni et al., 2011, 2013). It could be questioned however whether this metric is appropriate. As a point-to-point reaching movement will have zero velocity at both the beginning and end of the movement, the mean acceleration over this whole movement must be zero, meaning that the metric outcome is zero. However, in the studies of Mazzoleni et al. (2011, 2013) this outcome was not zero. As details about the algorithm are lacking, this metric is not reproducible and therefore excluded from the simulation based on exclusion reason 2.

From the category *Acceleration, peaks metric* and *IPV* are used in the simulations.

Jerk metrics

Jerk, the third time derivative of position, has often been used as a measure for smoothness (Rohrer et al., 2002; Hogan and Sternad, 2009; Teulings et al., 1997). According to Flash and Hogan (1985), a reaching task performed by healthy subjects, corresponds well to the minimal jerk model. Deviations from this minimal jerk model can result in less smooth movements. There are a lot of different variations of integrated squared jerk and integrated absolute jerk used as metrics for movement smoothness. These metrics integrate the squared or absolute jerk over the movement time. Often, the outcome is then scaled. The parameters used for scaling are movement duration, movement distance, mean velocity and peak velocity. Scaling affects the units of the metric. Although jerk metrics with units were seen in literature, these were excluded based on exclusion reason 1 and only dimensionless jerk metrics were used in the simulation. There are three types of dimensionless jerk metrics, DSJ_t , DSJ_b , DSJ_m introduced by Teulings et al. (1997), Balasubramanian et al. (2012) and Marini et al. (2017) respectively. The metrics consists of an integration of a jerk, multiplied with a normalization term. The normalization term causes the DSJ metrics to be different. Marini et al. (2017) placed the factor 0.5 outside the squared root of the jerk and is thus excluded from the simulation based on exclusion reason 4a. DSJ_b uses peak velocity in the normalization where DSJ_t uses the mean velocity.

Balasubramanian et al. (2012) took the natural logarithm of the DSJ_b metric to improve the sensitivity ($LDSJ_b$). Kordelaar et al. (2014) took the natural logarithm of DSJ_t to make their data normal distributed, introducing $LDSJ_t$. The exact description of all jerk metrics are given in Appendix B.

Repnik et al. (2018) used gyroscope data to calculate the rotational jerk. Therefore, this metric uses the jerk of the orientation (i.e. angles) instead of the position. This metric turned out to differentiate well between healthy subjects and stroke subjects. However, it did not indicate differences between movements performed with the patient's unaffected arm and normal task execution with the affected arm (Repnik et al., 2018). A potential concern of this metric is that a movement could be rotationally smooth while it is not continuous. Further, since this metric calculates metrics from the angles, it cannot be used in the simulations.

DSJ_b , $LDSJ_b$, DSJ_t and $LDSJ_t$ are the jerk metrics that will be used in the simulations.

Frequency spectrum metrics

Balasubramanian et al. (2009, 2012, 2015) has introduced three frequency spectrum based metrics that use the frequency spectrum of the velocity profile to calculate the movement smoothness. The first was the spectral method (*SPM*), which calculates the frequency spectrum of the velocity signal, normalizes the amplitude of the frequency spectrum and detects the maxima within a dynamic frequency range. Then, smoothing in the frequency domain was performed using a moving average operation. Finally, the smoothness was calculated as the sum of all the maxima detected in the normalized frequency spectrum. A lower value represents a smoother movement (Balasubramanian et al., 2009). Technical details are missing about the algorithm. Therefore, it is not completely reproducible and estimations about the spectral smoothing were necessary to reproduce it. Furthermore, in a later study Balasubramanian et al. (2012) stated that this metric is sensitive to noise as it requires detection of maxima in the frequency domain.

The second metric by Balasubramanian et al. (2012) is the spectral arc length (*SPAL*). The *SPAL* is similar to the velocity arc length metric, but then uses the length of the arc of the frequency-normalized Fourier magnitude spectrum of the velocity profile. Smoothness was defines as the length of the arc between 0Hz and a cutoff frequency of 20Hz. Later, Balasubramanian et al. (2015) adapted their *SPAL* metric by making the cutoff frequency ω_c dependent on the frequency content of the velocity profile. This was done to make the outcome of the measure independent of the movement duration, which was not the case for the *SPAL*. This version of spectral arc length is referred to as *SPARC* (SPECTRAL ARC length) (Balasubramanian et al., 2015). To our knowledge, this metric has not been used in stroke subjects and *SPARC* is therefore not evaluated in the simulations.

While Balasubramanian et al. (2009) looked at frequencies of the velocity profile of reaching movements in stroke subjects, Strohrmann et al. (2013) looked at the dominant frequency in the acceleration. In the spectral metric (*SPMR*), the acceleration profile is Fourier transformed and the energy in each 0.2Hz bin is summed and normalized. The smoothness of movement is then defined as the energy within the bin with the most energy. In this metric, a higher outcome value represents a smoother movement.

SPMR, *SPM* and *SPAL* will be used in the simulations.

Other metrics

Kostić and Popović, (2013) introduced the combined smoothness metric (*CSM*). It is not possible to classify this smoothness metric since it uses the velocity, acceleration and the jerk domain. The *CSM* consists of 4 parameters, in the first parameter, the mean negative jerk normalized by the peak speed is compared to a normal value, determined by the author. It will be 1 when it is the same as this value, if the movement has a higher jerk, the mean negative jerk will be lower and the first parameter of this metric will be lower. The second parameter contains the number of peaks. If the minimum of 1 peak is present, the outcome of this parameter will be 1. If more peaks are present, a lower value would be the result. The third contains the ratio between mean velocity and peak velocity of the movement, which is already discussed as *SM*. Lastly, there is a parameter which is the ratio of area under the curve and its convex hull, which is similar, but not the same as the Tent metric. The total metric outcome is the sum of all parameter. This metric was originally used for the kinematics of a square drawing test, but Popović et al. (2014) used it to analyze the movement smoothness of aiming movements. The *CSM* showed differences in movement smoothness changes between two different exercise programs after stroke. This metric adds a parameter with unit to a dimensionless parameter, which is mathematically doubtful. Based on exclusion reason 1, this metric is not evaluated in the simulation.

Simulation of metrics

The simulations will be discussed individually in the following subsections. In Table 2, the minimum and maximum value of each metric during all simulations are shown.

An increase in *SM*, *MAPR*, *IPV*, *SPM* and *CM* means a smoother quantification. For the other metrics an increase would mean a less smoother movement.

Table 2: Minimum and maximum of the metrics per simulation. In the last block, the change during the shape simulation is shown as percentage of the change in the sub-movement simulation (left) and the percentage change during the filtered noise simulation as a percentage of the change during the sub-movement simulation. With number of sub-movements (NOS), speed metric (SM), movement arrest period ratio (MAPR), velocity arc length (VAL), number of peaks, inverse of number of peaks and valleys (IPV), Dimensionless squared jerk (DSJt and DSJb), log of DSJt and DSJb (LDSJb and LDSJt), correlation metric (CM), spectral metric (SPMR), spectral method (SPM) and spectral arc length (SPAL)

Metric	Range	Shape		Sinus		Noise	
		Min	Max	Min	Max	Min	Max
NOS	1 - 7	1	1	1	7	1	7
SM	0 - 1	0,53	0,53	0,39	0,56	0,43	0,53
MAPR	0 - 1	0,82	0,83	0,75	0,96	0,81	0,82
VAL	-∞ - ∞	-2,00E-03	-1,64E-04	-4,93E-03	5,11E-03	-9,70E-03	3,17E-03
Peaks	1 - ∞	1	1	1	25	1	32
IPV	-∞ - 1	1,00	1,00	0,02	1,00	0,02	1,00
DSJt	0 - ∞	18,92	18,97	17,24	7850	19	4603
LDSJt	0 - ∞	2,94	2,94	2,85	8,97	2,93	8,43
DSJb	0 - ∞	203	205	159	1,89E+07	195	7,68E+06
LDSJb	0 - ∞	5,31	5,32	5,07	16,76	5,27	15,84
CM	-1 - 1	1,00	1,00	0,75	1,00	0,93	1,00
SPMR	0 - 1	0,13	0,91	0,10	0,23	0,03	0,23
SPM	0 - ∞	1,00	1,00	1,03	1,98	1,05	2,02
SPAL	0 - ∞	1,87	2,08	1,91	3,02	1,96	2,11
SPARC	0 - ∞	1,40	1,41	1,40	2,90	1,40	1,84

Metric	Range	Filtered noise		Sub-movements (N=2)		Δ as % of Δ Sub-movements	
		Min	Max	Min	Max	Shape	Filtered Noise
NOS	1 - 7	1	7	1	7	0,00	100,00
SM	0 - 1	0,43	0,55	0,40	0,55	0,62	78,03
MAPR	0 - 1	0,75	0,88	0,63	0,82	1,38	67,97
VAL	-∞ - ∞	-9,70E-03	-7,18E-03	-9,65E-03	-3,21E-03	28,47	39,14
Peaks	1 - ∞	1	16	1	2	0,00	1500,00
IPV	-∞ - 1	0,03	1,00	0,33	1,00	0,00	145,16
DSJt	0 - ∞	19	886	34	176	0,04	612,83
LDSJt	0 - ∞	2,92	6,79	3,54	5,17	0,17	237,24
DSJb	0 - ∞	191	379206	407	9670	0,02	4091,95
LDSJb	0 - ∞	5,25	12,85	6,01	9,18	0,29	239,68
CM	-1 - 1	0,96	1,00	-0,13	0,82	0,00	4,60
SPMR	0 - 1	0,03	0,23	0,15	0,34	456,42	106,64
SPM	0 - ∞	1,04	1,60	1,00	2,03	0,00	54,79
SPAL	0 - ∞	1,95	2,28	1,85	3,86	10,46	16,40
SPARC	0 - ∞	1,39	2,21	1,40	3,24	0,65	44,42

Shape simulation

Fig. 3 shows the result of the shape simulation where the metrics were tested on sensitivity for movement duration and movement distance. The horizontal axis represents the movement duration and movement distance, the vertical axes the metric. It can be seen that none of the metrics are sensitive for different movement distances. Considering the velocity metrics, *MAPR*, *VAL*, *SPAL* and *SPMR* are dependent on the movement duration as they change more than 1% of the change in the sub-movement simulation, as shown in the last column of Table 2. It is however seen that *SM*, *DSJ_t*, *LDSJ_t*, *DSJ_b* and *LDSJ_b* show dependency on movement duration but do not exceed the 1%. *NOS*, *Peaks*, *IPV*, *CM* and *SPM* show the perfect behavior in this simulation as these plots are totally flat in the z-axis, meaning that they are totally independent of movement duration and movement distance.

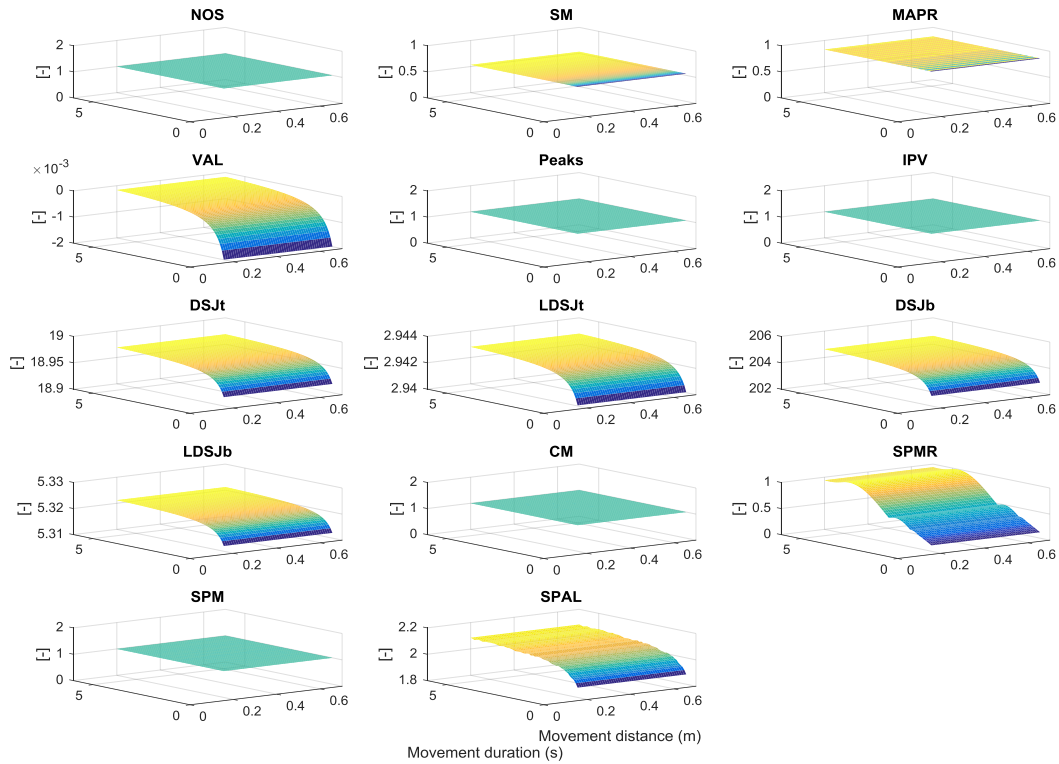


Fig. 3: Shape simulation. In this simulation the effect on the metrics of different movement durations and peak velocities is studied. The color represent the value on the z-axis. A measure for movement smoothness only is independent on movement duration and movement distance. The graph should show a flat plane like NOS. With number of sub-movements (NOS), speed metric (SM), movement arrest period ratio (MAPR), velocity arc length (VAL), number of peaks, inverse of number of peaks and valleys (IPV), Dimensionless squared jerk (DSJt and DSJb), log of DSJt and DSJb (LDSJb and LDSJt), correlation metric (CM), spectral metric (SPMR), spectral method (SPM) and spectral arc length (SPAL).

Sinus simulation

With the sinus simulation, a sinus was added to the main velocity profile. The frequency and amplitude of these sinusoids were varied and these values are plotted at the horizontal axes of Fig. 4. The metric is plotted at the vertical axes. *NOS* does not cover the whole surface of the plot, because the algorithm cannot come to a solution if more than 7 sub-movements are present, therefore the algorithm can only quantify the lower frequencies. Apart from that, it can be seen that all metrics show a decrease in smoothness as the amplitude of the added sinus increases. All metrics but *SM*, *MAPR* and *CM* show that a higher frequency results in a less smooth metric outcome for the same amplitude. *SPAL* shows no sensitivity to sinus disturbances with frequencies higher than 20Hz.

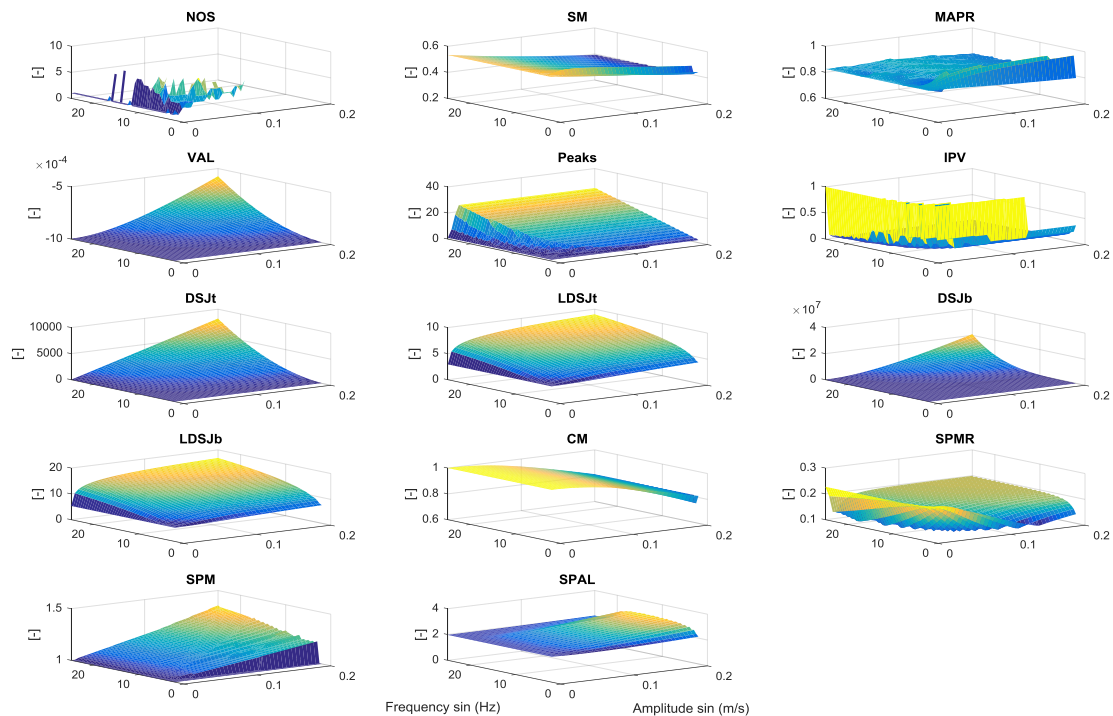


Fig. 4: Sinus simulation. Metrics were calculated with an added sinus wave with different frequencies, ranging from 2 till 25 Hz and amplitudes ranging from 0 till 0.2 m/s. This is referred to as the sinus simulation. In the top left corner, a few tested velocity profiles are shown. The metric should show a decrease in smoothness if the amplitude of the added sinus increases. With number of sub-movements (*NOS*), speed metric (*SM*), movement arrest period ratio (*MAPR*), velocity arc length (*VAL*), number of peaks, inverse of number of peaks and valleys (*IPV*), Dimensionless squared jerk (*DSJt* and *DSJb*), log of *DSJt* and *DSJb* (*LDSJb* and *LDSJt*), correlation metric (*CM*), spectral metric (*SPMR*), spectral method (*SPM*) and spectral arc length (*SPAL*)

Noise simulation

With the noise simulation, zero mean white noise was added to the main velocity profile. The RMS value of this noise was varied from 0 till 0.08 m/s and this simulation was repeated with 25 different sets of noise. The results of this simulation is shown in Fig.5, the black line represents the mean per RMS value over all noise sets, the green and blue line show the minimum and maximum value. The green line represents the mean value per metric over the filtered noise.

NOS metric is only capable of analyzing the smoothness at low noise powers till a RMS of 0.008 m/s. If the data is filtered, the metric can the number of sub-movements up to a RMS of 0.022 m/s. It was seen that *NOS* changed in this simulation over its full range (from 1 till 7). Further, all metrics except *SPMR* show a decrease in smoothness as the power of the noise is increased. All jerk metrics react strongly to this distortion compared with the other simulations. In the last column of Table 2, the change in the filtered noise simulation is shown as a percentage of the change in the sub-movement simulation. It is seen that *NOS*, *Peaks*, *IPV*, all dimensionless jerk metrics and *SPMR* change more during the noise simulation than during the sub-movement simulation (>100%), meaning that these metrics are sensitive to noise. *CM* was least sensitive.

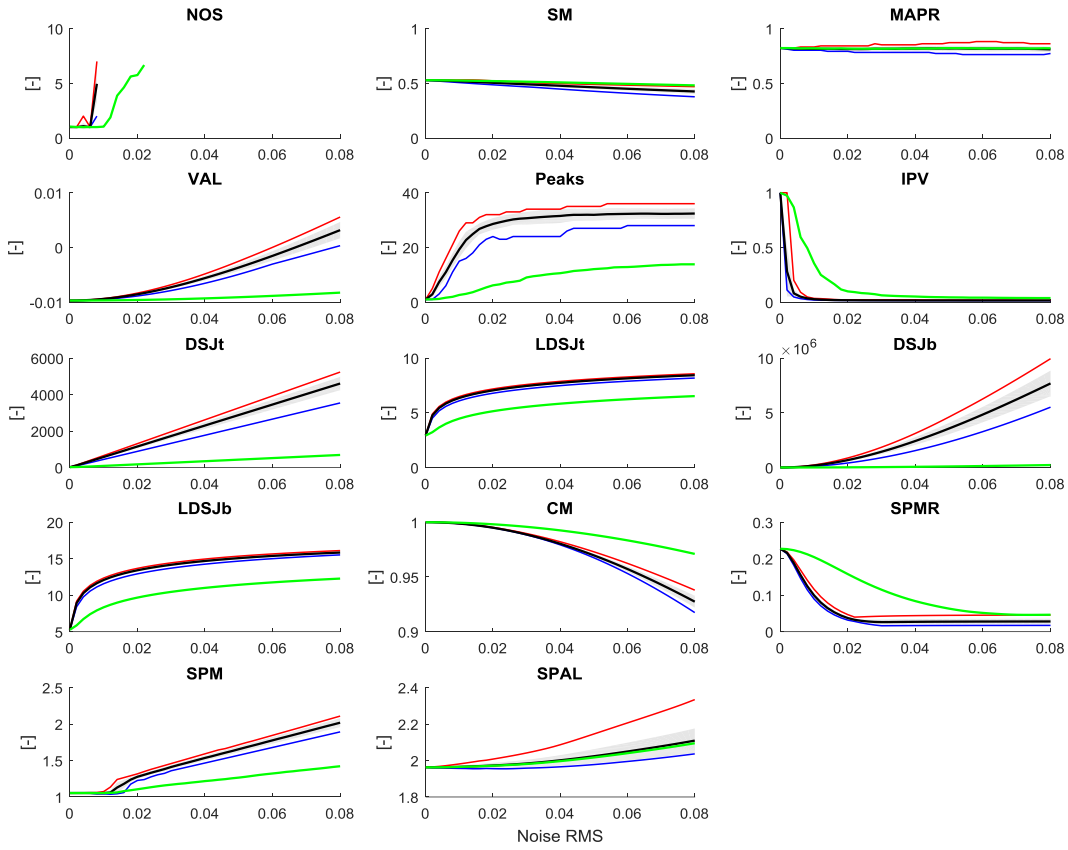


Fig. 5: Noise simulation. With this simulation, the effect of noise on the metrics is studied. The black line represents the mean value of 25 different random distributed noise sets, grey is the corresponding standard deviation. Red is the maximal value of the metric found at that RMS value and blue the minimum value. The green line shows mean value of the 25 filtered noise sets. With number of sub-movements (NOS), speed metric (SM), movement arrest period ratio (MAPR), velocity arc length (VAL), number of peaks, inverse of number of peaks and valleys (IPV), Dimensionless squared jerk (DSJt and DSJb), log of DSJt and DSJb (LDSJb and LDSJt), correlation metric (CM), spectral metric (SPMR), spectral method (SPM) and spectral arc length (SPAL)

Sub-movements simulation

With the sub-movements simulation, different velocity profiles were created by varying the lag between 2, 3 or 4 sub-movements. The effect of movement segmentation on the outcome in smoothness measures is shown in Fig. 6, on the x-axis the lag value K_s is plotted, on the y-axis the different metrics. For NOS, an increase is seen if the lag value K_s increases. This is however non-monotonic as there the graph increases, followed by a decrease. In the yellow line is seen that a score of 5 is reached while theoretically 4 would be the outcome as there were 4 sub-movements used. At $K_s = 1.2s$, the algorithm did not reach a solution. With both a higher K_s value and segmentation into more sub-movements, the solution space increases, causing the algorithm to fail.

SM and MAPR both show first an increase in smoothness, followed by a decrease in smoothness, indicating non-monotonicity. Both of these metrics do not show that much difference for the number of sub-movements. VAL, CM, SPM and SPAL show all a non-monotonic increase. For SPMR, a higher value indicates a higher smoothness. The increase of smoothness together with higher Ks value is therefore undesirable. Additionally, this metric is non-monotonic. Further, all metrics except SPMR show that splitting a movement into more sub-movements results a less smooth movement. Peaks and IPV also show a decrease of smoothness with increased movement segmentation. However, it is seen that as two peaks get separated, there is a moment where the algorithm detects a third peak. This is seen as the extra peaks at 0.3 and 0.5 seconds in the peaks and IPV metric, causing a non-monotonicity. This can however easily be prevented by adding requirements to the peak detection algorithm. All dimensionless jerk metrics show a dip at a Ks value of 1.0, so these metrics are also non-monotonic increasing.

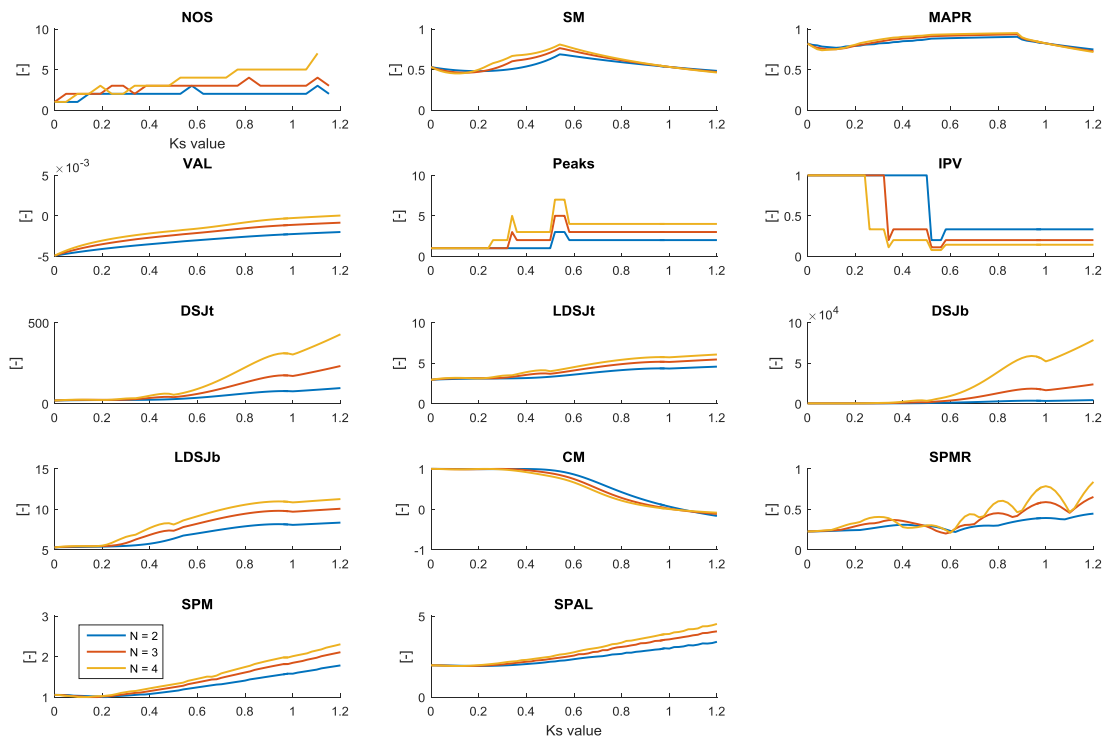


Fig. 6: With the sub-movements simulations the effect of separated sub-movements on different smoothness metrics is investigated. The colors denote for the number of sub-movements that is used. With number of sub-movements (NOS), speed metric (SM), movement arrest period ratio (MAPR), velocity arc length (VAL), number of peaks, inverse of number of peaks and valleys (IPV), Dimensionless squared jerk (DSJt and DSJb), log of DSJt and DSJb (LDSJb and LDSJt), correlation metric (CM), spectral metric (SPMR), spectral method (SPM) and spectral arc length (SPAL)

An important finding during this sub-movement simulation was that the result of the monotonicity is dependent on the shape of the velocity profile of the sub-movement. This is considered in detail in appendix E. Further, it was found that there is a difference in velocity profile of reach-to-grasp movements and movements with only reaching. This would change the velocity profile of the sub-movement and would change the result of the monotonicity in this simulation. In appendix F, reach-to-grasp movements of healthy and stroke subjects are investigated and we found that an asymmetric velocity profile was a better representation of a reach-to-grasp movement. The main implication for the work of appendices E and F are shown in Table 3.

In Table 3 it is seen that the response on the sub-movement simulation is dependent on the chosen velocity profile. It is seen that CM is always monotonic increasing with the tested symmetrical velocity profiles. However, it was not with the asymmetrical velocity profiles. For the jerk metrics, it is more complex as there are both symmetrical and asymmetrical velocity profiles where the increase of the metric is monotonic and non-monotonic respectively. It is seen that the different normalization method of the jerk metrics influences the monotonicity. The (L)DSJb metric is normalized by peak velocity while (L)DSJt is normalized by mean velocity. For the Hann and the Polynomial 2 velocity profiles it is seen that (L)DSJt increases monotonically, while (L)DSJb is not monotonically increasing. SM, MAPR and SPMR had a non-monotonic response with all velocity profiles.

In Table 4, all the metrics assessed in the simulations are shown and per simulation it is shown whether it satisfied the requirements.

Table 3 – The monotonicity of the dimensionless jerk metrics per type of velocity profile. It is seen that the monotonicity is dependent on the shape of the velocity profile used in the simulation. CM shows a non-monotonic response if the used velocity profile is asymmetrical. For the jerk metrics, a minor change in the velocity profile results in a change of the response. The complete results are shown in appendix E and F. With Dimensionless squared jerk (DSJt and DSJb), log of DSJt and DSJb (LDSJb and LDSJt) and correlation metric (CM)

Symmetrical velocity profiles	Monotonic increase of jerk metrics (Yes/No)				
	DSJt	LDSJt	DSJb	LDSJb	CM
Minimum Jerk	No	No	No	No	Yes
Hann	Yes	Yes	No	No	Yes
Blackman	Yes	Yes	Yes	Yes	Yes
Blackman Harris	Yes	Yes	Yes	Yes	Yes
Asymmetrical velocity profiles	Monotonic increase of jerk metrics (Yes/No)				
	DSJt	LDSJt	DSJb	LDSJb	CM
Polynomial 1	Yes	Yes	Yes	Yes	No
Polynomial 2	Yes	Yes	No	No	No
Beta distribution	Yes	Yes	Yes	Yes	No

Table 4 – Overview of the requirements per simulation and metrics. Yes means that the metric satisfies the requirements of the simulation, with No it does not. With number of sub-movements (NOS), speed metric (SM), movement arrest period ratio (MAPR), velocity arc length (VAL), number of peaks, inverse of number of peaks and valleys (IPV), Dimensionless squared jerk (DSJt and DSJb), log of DSJt and DSJb (LDSJb and LDSJt), correlation metric (CM), spectral metric (SPMR), spectral method (SPM) and spectral arc length (SPAL)

Metric \ Simulation	Movement duration and distance	Sinus	Sub-movements
NOS	Yes	No	No
SM	Yes*	Yes	No
MAPR	No	Yes	No
VAL	No	Yes	Yes
Peaks	Yes	Yes	Yes**
IPV	Yes	Yes	Yes**
DSJt	Yes*	Yes	Yes**
LDSJt	Yes*	Yes	Yes**
DSJb	Yes*	Yes	Yes**
LDSJb	Yes*	Yes	Yes**
CM	Yes	Yes	Yes**
SPMR	No	Yes	No
SPM	Yes	Yes	Yes
SPAL	No	Yes	Yes

*This metric is not significantly influenced by movement duration and/or distance

**There were velocity profiles where the metric changed monotonically. But not for all velocity profiles.

Discussion

To optimize therapy outcomes after stroke, it is crucial to get a better understanding in the neurological recovery after stroke (Buma et al., 2013). Kinematic measures for quality of movement can be used in gaining knowledge about recover post stroke, one of these measures is movement smoothness (Schwarz et al., 2019). However, there a lot of different metrics and it was found that some of them are invalid.

Which smoothness metric do we recommend for further research?

For the first time, all relevant 2-dimensional measures for movement smoothness of upper limb movement after stroke are included in one review. For the analysis of movement smoothness of reaching and aiming movement in stroke patients, 31 different metrics have been used and published in peer review manuscripts in the literature. It was seen that 17 metrics were not adequate in one or more of the following criteria: 1) non-dimensionless, 2) lacking a mathematical specification or 3) a scaling of another metric. Therefore, these measures are considered not appropriate to quantify movement smoothness in behavioral studies after stroke and were excluded before testing the metrics with simulated movements.

From the 14 metrics that were not excluded yet, it was seen that four metrics (*NOS SM*, *MAPR* and *SPMR*) were dependent on movement duration or increased non-monotonically as the lag between two sub-movements increased. Finally, it can be concluded that *peaks*, *IPV*, *DSJ_b*, *DSJ_t*, *LDSJ_b*, *LDSJ_t*, *CM* and *SPM* did satisfy the requirements for a suitable metric that can possibly assess smoothness of reaching tasks. Therefore the latter set of metrics is suitable for further research.

It was seen that *CM* and *SPM* were less sensitive to noise than *peaks*, *IPV* and the dimensionless jerk metrics. However, it is seen that *peaks*, *IPV* and the dimensionless jerk metrics are more sensitive in the sinus simulation. This indicates that *CM* and *SPM* are more sensitive to changes in smoothness as a result of segmentation of the task into sub-movements, while the jerk metrics, *peaks* and *IPV* are more sensitive to fluctuations in the velocity profile. From the simulations and the set-up requirements can be concluded that *CM*, *SPM*, *peaks*, *IPV*, *LDSJ_t*, *DSJ_t*, *DSJ_b* and *LDSJ_b* are suitable measures for movement smoothness.

Another interesting finding was that the integrated squared jerk is normalized to make it dimensionless (Teulings et al., 1997), but this is by our knowledge has never been done for integrated absolute jerk, in spite of it being feasible as a suitable metric. Simulations were also done with dimensionless absolute jerk (*DAJ*) and the log of dimensionless absolute jerk (*LDAJ*). *DAJ* and *LDAJ* showed similar results as the dimensionless jerk metrics found in literature.

It was already shown that *CM* is well correlated with the Action Research Arm Test (ARAT) and FMA (Celik et al., 2010). Levin et al. (2015) have shown that a greater deficit in the impaired arm results in more peaks in the velocity profile of a reaching trajectory. *IPV* is shown to be a responsive measure during a longitudinal study using a 2 degree of freedom end effector robotic device (Pilia et al., 2017).

Another finding was that there is a difference in velocity profiles between reach-to-grasp movements and aiming or pointing movements. In Appendix F it was seen that reach-to-grasp velocity profiles are asymmetrical, with the peak velocity at about 1/3 of the total movement time. Flash and Hogan (1985) however showed that point-to-point reaching tasks have a symmetrical velocity profile, matching the minimal jerk model. Focusing more on controlling the grasp at the end of the movement might explain the deceleration of the hand as it approaches the object.

The importance of standardization for smoothness measures became even more clear during the screening phase of the literature review. It was seen that the choice of the metric was often not well motivated in the studies found. Mazzoleni et al. (2011) introduced the normalized reaching speed, which is simply a scaling of the speed metric, a metric that they were using as well. Further, they introduced the acceleration metric, which is theoretically not valid as it should always be 0 for a point-to-point reaching movement. In other cases, the explanation of metrics was either unclear (Silva et al., 2014; Duff et al., 2010; Waller et al., 2008) or incomplete (Balasubramanian et al., 2009; Nakamura et al., 2008; Longhi et al., 2016), or missing completely (Kiper et al., 2016; Hondori et al., 2013). Moreover, movement smoothness was quantified by visual inspection of velocity and acceleration curves (Trombly, 1992). Kostić and Popović (2013) introduced the Combined Smoothness Metric. This metric adds up numbers with different dimensions, which is mathematically invalid. These examples show that it is highly relevant to identify suitable metrics for movement smoothness and that there is currently a lack of understanding in quantifying movement smoothness. Moreover, it was seen that a total of 54 studies used metrics that are classified as unsuitable in this study.

Movement smoothness is further relevant for other diseases than stroke such as Huntington (Hogan and Sternad, 2009) and Parkinson (Teulings et al., 1997), movement analysis in sports (Hreljac, 2000; Choi et al., 2014), and hand skills (Kahol et al., 2008). Lamothe and van Heuvelen (2012) quantified movement smoothness of the trunk during ice skating as the mean power frequency of the acceleration. This method would however not be suitable for reaching movements in stroke since it would be dependent on movement velocity.

Caplan and Gardner (2009) investigated whether stroke smoothness in rowing is an indicator of fatigue. Stroke smoothness was defined as the power of the fundamental peak as a percentage of the first ten peaks in the frequency domain of the force data. This shows that there is interest in smoothness metrics from multiple research fields.

Limitations

The literature review was restricted to studies where reaching movements were performed with stroke patients, while smoothness can be assessed in other tasks as well. Therefore, there could be suitable metrics, used in other tasks, and not included in the review. However, during the screening a few interesting papers were found and highlighted here. Osu et al. (2011) measured the movement smoothness during rhythmic tasks where a cup of water was moved from the lap to the mouth of the patient repeatedly. They calculated the three-dimensional instantaneous curvature at each time point. The metric MedianLC was the median of the negative logarithm of this curvature at all extracted time points. This 3-dimensional metric correlated with the FMA-UE and the score from the Stroke Impairment Assessment Set.

Wininger et al. (2012) assessed smoothness of self-paced, isolated elbow flexion angular trajectories from stroke patients using four different metrics. They concluded that a phase plane metric was superior to temporal domain metrics to detect deficits in performance. Although this metric is designed to quantify smoothness of angular data, the translation can be made to a measure that can quantify smoothness using positional data. This was explored outside the scope of this study and was validated using the sub-movement simulation with the minimal jerk trajectory as input. It was found that within the sub-movements simulation the response was non-monotonic. Thus, the phase plane metric would probably not be suitable to quantify movement smoothness in reaching movements as it has a non-monotonic response in the sub-movement simulation.

In the simulation with sub-movement, it was seen that small changes in the velocity profile for the sub-movement affected the monotonicity. For example, changing from a minimal jerk velocity profile to a hamming velocity profile changed the result of DSJ_t and $LDSJ_t$ from non-monotonic to monotonic.

On this same matter, a comment must be made about CM . This metric is the correlation between the minimum jerk profile and the executed velocity profile. This is based on the work of Flash and Hogan (1985) that movements are executed in in minimum jerk trajectory. But as shown, reach-to-grasp movements are not well approximated using the minimum jerk model. Therefore, this metric gave non-monotonic results during the sub-movement simulation if an asymmetrical window was used.

Recommendations

As mentioned, small changes in the velocity profile in the sub-movement simulation, can affect the outcome of the monotonicity of the metrics. Alternatives for this simulation should be considered. Currently, the complete movement is subsequently split up into two, three and four equal sub-movements and the time between these sub-movements is altered. Alternatively, this simulation can be done were not only the timing between the two sub-movements is altered, but also the ratio between the peak velocity of the sub-movements.

Although the simulations mimic features of reaching movements of stroke patients, such as slowness and sub-movement segmentation (Cirstea and Levin, 2000), it is still very different from the real velocity profiles. Furthermore, with the current simulations, it was not possible to validate 3-dimensional metrics. A validation with a longitudinal study with stroke patients recovering over time can further differentiate between different metrics and can give more insights in their behavior in real velocity profiles after stroke. Investigating its longitudinal behavior will also show which metric are most sensitive for smoothness change over time. For example, van Kordelaar et al. (2014) had a 26 weeks longitudinal study design and showed that significant improvements in movement smoothness, for a reach-to-grasp task measured by $LDSJ_t$, are mainly restricted to the first eight weeks after stroke onset. Interestingly, this time window for significant change is similar for impairment related outcomes such as FMA-UE (Duncan et al., 1992; Kwakkel et al., 2006). The task was however not executable for all participants. Therefore only patients with moderate to mild deficits in the paretic upper limb. With the inclusion of less complex movements, such as a point-to-point reaching movement without grasping, also patients with a moderate severe stroke can be represented.

A study that includes less complex movements can compare the metrics using models that can account for within and between subject relationships. Linear Mixed Models (West et al., 2014) or Hybrid models (Twisk and de Vente, 2019) can be useful modeling techniques for longitudinal data.

References

- Abdul Rahman, H., Khor, K. X., Yeong, C. F., Su, E. L. M., and Narayanan, A. L. T. (2017). The potential of iREST in measuring the hand function performance of stroke patients. *Bio-medical materials and engineering*, 28(2):105–116.
- Adamovich, S. V., Fluet, G. G., Merians, A. S., Mathai, A., and Qiu, Q. (2009). Incorporating haptic effects into three-dimensional virtual environments to train the hemiparetic upper extremity. *IEEE Transactions on Neural Systems and Rehabilitation Engineering*, 17(5):512–520.
- Balasubramanian, S., Melendez-Calderon, A., and Burdet, E. (2012). A robust and sensitive metric for quantifying movement smoothness. *IEEE transactions on biomedical engineering*, 59(8):2126–2136.
- Balasubramanian, S., Melendez-Calderon, A., Roby-Brami, A., and Burdet, E. (2015). On the analysis of movement smoothness. *Journal of neuroengineering and rehabilitation*, 12(1):112.
- Balasubramanian, S., Wei, R., Herman, R., and He, J. (2009). Robot-measured performance metrics in stroke rehabilitation. In *Complex Medical Engineering, 2009. CME. ICME International Conference on*, pages 1–6. IEEE.
- Beppu, H., Suda, M., and Tanaka, R. (1984). Analysis of cerebellar motor disorders by visually guided elbow tracking movement. *Brain*, 107(3):787–809.
- Bermúdez i Badia, S. and Cameirão, M. S. (2012). The neurorehabilitation training toolkit (ntt): A novel worldwide accessible motor training approach for at-home rehabilitation after stroke. *Stroke research and treatment*, 2012.
- Bigoni, M., Baudo, S., Cimolin, V., Cau, N., Galli, M., Pianta, L., Tacchini, E., Capodaglio, P., and Mauro, A. (2016). Does kinematics add meaningful information to clinical assessment in post-stroke upper limb rehabilitation? a case report. *Journal of physical therapy science*, 28(8):2408–2413.
- Brooks, V. B. (1974). Introductory lecture to session iii some examples of programmed limb movements. *Brain Research*, 71(2-3):299–308.
- Buma, F., Kwakkel, G., and Ramsey, N. (2013). Understanding upper limb recovery after stroke. *Restorative neurology and neuroscience*, 31(6):707–722.
- Caplan, N., & Gardner, T. N. (2009). Is stroke smoothness a reliable indicator of fatigue in ergometer rowing?. *Sports engineering*, 11(4), 207-209.
- Casadio, M., Giannoni, P., Morasso, P., and Sanguineti, V. (2009). A proof of concept study for the integration of robot therapy with physiotherapy in the treatment of stroke patients. *Clinical rehabilitation*, 23(3):217–228.
- Celik, O., O'malley, M. K., Boake, C., Levin, H. S., Yozbatiran, N., and Reistetter, T. A. (2010). Normalized movement quality measures for therapeutic robots strongly correlate with clinical motor impairment measures. *IEEE transactions on neural systems and rehabilitation engineering: a publication of the IEEE Engineering in Medicine and Biology Society*, 18(4):433.

- Chang, J.-J & Yusheng, Yang & Wu, W.-L & Guo, Lan-Yuen & Su, F.-C. (2008). The Constructs of Kinematic Measures for Reaching Performance in Stroke Patients. *Journal of Medical and Biological Engineering*, 28, 65-70.
- Choi, A., Joo, S. B., Oh, E., & Mun, J. H. (2014). Kinematic evaluation of movement smoothness in golf: relationship between the normalized jerk cost of body joints and the clubhead. *Biomedical engineering online*, 13(1), 20.
- Cirstea, M. and Levin, M. F. (2000). Compensatory strategies for reaching in stroke. *Brain*, 123(5):940-953.
- Duff, M., Chen, Y., Attygalle, S., Herman, J., Sundaram, H., Qian, G., He, J., and Rikakis, T. (2010). An adaptive mixed reality training system for stroke rehabilitation. *IEEE Transactions on Neural Systems and Rehabilitation Engineering*, 18(5):531-541.
- Duncan, P. W., Goldstein, L. B., Matchar, D., Divine, G. W., and Feussner, J. (1992). Measurement of motor recovery after stroke. outcome assessment and sample size requirements. *Stroke*, 23(8):1084-1089.
- Feigin, V. L., Forouzanfar, M. H., Krishnamurthi, R., Mensah, G. A., Connor, M., Bennett, D. A., ... & O'Donnell, M. (2014). Global and regional burden of stroke during 1990-2010: findings from the Global Burden of Disease Study 2010. *The Lancet*, 383(9913), 245-255.
- Flash, T. and Hogan, N. (1985). The coordination of arm movements: an experimentally confirmed mathematical model. *Journal of neuroscience*, 5(7):1688-1703.
- Hogan, N. and Sternad, D. (2009). Sensitivity of smoothness measures to movement duration, amplitude, and arrests. *Journal of motor behavior*, 41(6):529-534.
- Hondori, H. M., Khademi, M., Dodakian, L., Cramer, S. C., & Lopes, C. V. (2013). A spatial augmented reality rehab system for post-stroke hand rehabilitation. In *MMVR* (Vol. 184, pp. 279-285).
- Hreljac, A. (2000). Stride smoothness evaluation of runners and other athletes. *Gait & posture*, 11(3), 199-206.
- Hussain, N., Alt Murphy, M., and Sunnerhagen, K. S. (2018). Upper limb kinematics in stroke and healthy controls using target-to-target task in virtual reality. *Frontiers in neurology*, 9:300.
- Johnson, M., Wisneski, K., Hermsen, A., Smith, R., Walton, T., Hingtgen, B., McGuire, J., and Harris, G. (2005). Kinematic implications of learned non-use for robotic therapy. In *Rehabilitation Robotics, 2005. ICORR 2005. 9th International Conference on*, pages 70-73. IEEE.
- Kahn, L. E., Zygmant, M. L., Rymer, W. Z., and Reinkensmeyer, D. J. (2006). Robot-assisted reaching exercise promotes arm movement recovery in chronic hemiparetic stroke: a randomized controlled pilot study. *Journal of neuroengineering and rehabilitation*, 3(1):12.
- Kahol, K., Leyba, M. J., Deka, M., Deka, V., Mayes, S., Smith, M., ... & Panchanathan, S. (2008). Effect of fatigue on psychomotor and cognitive skills. *The American Journal of Surgery*, 195(2), 195-204.
- Kiper, P., Zucconi, C., Agostini, M., Baba, A., Dipalma, F., Berlingieri, C., ... & Turolla, A. (2016). Assessment of virtual teacher feedback for the recovery of the upper limb after a stroke. Study protocol for a randomized controlled trial. *Med Rehabil*, 20, 13-20.

- Kostić, M. D., & Popović, M. D. (2013). The modified drawing test for assessment of arm movement quality. *Journal of Automatic Control*, 21(1), 49-53.
- Krebs, H., Volpe, B., Palazzolo, J., and Rohrer, B. (2001). Interim results on the follow-up of 76. In *Integration of Assistive Technology in the Information Age: ICORR'2001, 7th International Conference on Rehabilitation Robotics*, volume 9, page 45. IOS Press.
- Kwakkel, G., Kollen, B. J., van der Grond, J., and Prevo, A. J. (2003). Probability of regaining dexterity in the flaccid upper limb: impact of severity of paresis and time since onset in acute stroke. *Stroke*, 34(9):2181-2186.
- Kwakkel, G., Kollen, B., and Twisk, J. (2006). Impact of time on improvement of outcome after stroke. *Stroke*, 37(9):2348-2353.
- Laczko, J., Scheidt, R. A., Simo, L. S., and Piovesan, D. (2017). Inter-joint coordination deficits revealed in the decomposition of endpoint jerk during goal-directed arm movement after stroke. *IEEE Transactions on Neural Systems and Rehabilitation Engineering*, 25(7):798-810.
- Lamoth, C. J., & van Heuvelen, M. J. (2012). Sports activities are reflected in the local stability and regularity of body sway: Older ice-skaters have better postural control than inactive elderly. *Gait & posture*, 35(3), 489-493.
- Langhorne, P., Bernhardt, J., & Kwakkel, G. (2011). Stroke rehabilitation. *The Lancet*, 377(9778), 1693-1702.
- Levin, M. F. (1996). Interjoint coordination during pointing movements is disrupted in spastic hemiparesis. *Brain*, 119(1), 281-293.
- Levin, M. F., Magdalon, E. C., Michaelsen, S. M., & Quevedo, A. A. (2015). Quality of grasping and the role of haptics in a 3-D immersive virtual reality environment in individuals with stroke. *IEEE Transactions on Neural Systems and Rehabilitation Engineering*, 23(6), 1047-1055.
- Levin, M. F., Michaelsen, S. M., Cirstea, C. M., and Roby-Brami, A. (2002). Use of the trunk for reaching targets placed within and beyond the reach in adult hemiparesis. *Experimental brain research*, 143(2):171-180.
- Liebermann, D. G., Levin, M. F., McIntyre, J., Weiss, P. L., and Berman, S. (2010). Arm path fragmentation and spatiotemporal features of hand reaching in healthy subjects and stroke patients. In *Engineering in Medicine and Biology Society (EMBC), 2010 Annual International Conference of the IEEE*, pages 5242-5245. IEEE.
- Longhi, M., Merlo, A., Prati, P., Giacobbi, M., & Mazzoli, D. (2016). Instrumental indices for upper limb function assessment in stroke patients: a validation study. *Journal of neuroengineering and rehabilitation*, 13(1), 52.
- Marini, F., Hughes, C. M., Squeri, V., Doglio, L., Moretti, P., Morasso, P., and Masia, L. (2017). Robotic wrist training after stroke: Adaptive modulation of assistance in pediatric rehabilitation. *Robotics and Autonomous Systems*, 91:169-178.
- Mazzoleni, S., Filippi, M., Carrozza, M., Posteraro, F., Puzzolante, L., and Falchi, E. (2011). Robot-aided therapy on the upper limb of subacute and chronic stroke patients: a biomechanical approach. In *Rehabilitation Robotics (ICORR), 2011 IEEE International Conference on*, pages 1-6. IEEE.

- Mazzoleni, S., Sale, P., Tiboni, M., Franceschini, M., Posteraro, F., and Carrozza, M. (2013). Upper limb robot-assisted therapy in chronic and subacute stroke patients: a kinematic analysis. In *Converging Clinical and Engineering Research on Neurorehabilitation*, pages 129–133. Springer.
- Michaelsen, S. M., Luta, A., Roby-Brami, A., and Levin, M. F. (2001). Effect of trunk restraint on the recovery of reaching movements in hemiparetic patients. *Stroke*, 32(8):1875–1883.
- Mohapatra, S., Harrington, R., Chan, E., Dromerick, A. W., Breceda, E. Y., and Harris-Love, M. (2016). Role of contralesional hemisphere in paretic arm reaching in patients with severe arm paresis due to stroke: a preliminary report. *Neuroscience letters*, 617:52–58.
- Moher, D., Liberati, A., Tetzlaff, J., & Altman, D. G. (2009). Preferred reporting items for systematic reviews and meta-analyses: the PRISMA statement. *Annals of internal medicine*, 151(4), 264-269.
- Montes, V. R., Quijano, Y., Quero, J. C., Ayala, D. V., and Moreno, J. P. (2014). Comparison of 4 different smoothness metrics for the quantitative assessment of movement's quality in the upper limb of subjects with cerebral palsy. In *Health Care Exchanges (PAHCE), 2014 Pan American*, pages 1–6. IEEE.
- Nakamura, T., Abreu, B. C., Patterson, R. M., Buford Jr, W. L., & Ottenbacher, K. J. (2008). Upper-limb kinematics of the presumed-to-be-unaffected side after brain injury. *The American Journal of Occupational Therapy*, 62(1), 46.
- Osu, R., Ota, K., Fujiwara, T., Otaka, Y., Kawato, M., & Liu, M. (2011). Quantifying the quality of hand movement in stroke patients through three-dimensional curvature. *Journal of neuroengineering and rehabilitation*, 8(1), 62.
- Pila, O., Duret, C., Laborne, F.-X., Gracies, J.-M., Bayle, N., and Hutin, E. (2017). Pattern of improvement in upper limb pointing task kinematics after a 3-month training program with robotic assistance in stroke. *Journal of neuroengineering and rehabilitation*, 14(1):105.
- Popović, M. D., Kostić, M. D., Rodić, S. Z., & Konstantinović, L. M. (2014). Feedback-mediated upper extremities exercise: increasing patient motivation in poststroke rehabilitation. *BioMed research international*, 2014.
- Repnik, E., Puh, U., Goljar, N., Munih, M., and Mihelj, M. (2018). Using inertial measurement units and electromyography to quantify movement during action research arm test execution. *Sensors*, 18(9):2767.
- Rohrer, B. and Hogan, N. (2006). Avoiding spurious submovement decompositions ii: a scattershot algorithm. *Biological cybernetics*, 94(5):409–414.
- Rohrer, B., Fasoli, S., Krebs, H. I., Hughes, R., Volpe, B., Frontera, W. R., Stein, J., and Hogan, N. (2002). Movement smoothness changes during stroke recovery. *Journal of Neuroscience*, 22(18):8297–8304.
- Rohrer, B., Fasoli, S., Krebs, H. I., Volpe, B., Frontera, W. R., Stein, J., & Hogan, N. (2004). Submovements grow larger, fewer, and more blended during stroke recovery. *Motor control*, 8(4), 472-483.
- Schneider, S., Schönle, P. W., Altenmüller, E., & Münte, T. F. (2007). Using musical instruments to improve motor skill recovery following a stroke. *Journal of neurology*, 254(10), 1339-1346.

- Schwarz, A., Kanzler, C. M., Lambercy, O., Luft, A. R., & Veerbeek, J. M. (2019). Systematic Review on Kinematic Assessments of Upper Limb Movements After Stroke. *Stroke*, *50*(3), 718-727.
- Schweighofer, N., Wang, C., Mottet, D., Laffont, I., Bakthi, K., Reinkensmeyer, D. J., & Rémy-Néris, O. (2018). Dissociating motor learning from recovery in exoskeleton training post-stroke. *Journal of neuroengineering and rehabilitation*, *15*(1), 89.
- Silva, F. P. D. P., Freitas, S. M. S. F. D., Silva, P. V., Banjai, R. M., & Alouche, S. R. (2014). Ipsilesional arm motor sequence performance after right and left hemisphere damage. *Journal of motor behavior*, *46*(6), 407-414.
- Simonsen, D., Popovic, M. B., Spaich, E. G., and Andersen, O. K. (2017). Design and test of a microsoft kinect-based system for delivering adaptive visual feedback to stroke patients during training of upper limb movement. *Medical & biological engineering & computing*, *55*(11):1927– 1935.
- Strohrmann, C., Labruyère, R., Gerber, C. N., van Hedel, H. J., Arnrich, B., & Tröster, G. (2013). Monitoring motor capacity changes of children during rehabilitation using body-worn sensors. *Journal of neuroengineering and rehabilitation*, *10*(1), 83.
- Subramanian, S., Knaut, L. A., Beaudoin, C., McFadyen, B. J., Feldman, A. G., and Levin, M. F. (2007). Virtual reality environments for post-stroke arm rehabilitation. *Journal of neuroengineering and rehabilitation*, *4*(1):20.
- Teulings, H.-L., Contreras-Vidal, J. L., Stelmach, G. E., and Adler, C. H. (1997). Parkinsonism reduces coordination of fingers, wrist, and arm in fine motor control. *Experimental neurology*, *146*(1):159–170.
- Trombly, C. A. (1992). Deficits of reaching in subjects with left hemiparesis: a pilot study. *American Journal of Occupational Therapy*, *46*(10), 887-897.
- Twisk, J. W., & de Vente, W. (2019). Hybrid models were found to be very elegant to disentangle longitudinal within-and between-subject relationships. *Journal of clinical epidemiology*, *107*, 66-70.
- van Kordelaar, J., van Wegen, E., and Kwakkel, G. (2014). Impact of time on quality of motor control of the paretic upper limb after stroke. *Archives of physical medicine and rehabilitation*, *95*(2):338–344.
- Waller, S. M., Liu, W., & Whittall, J. (2008). Temporal and spatial control following bilateral versus unilateral training. *Human movement science*, *27*(5), 749-758.
- West, B. T., Welch, K. B., & Galecki, A. T. (2014). *Linear mixed models: a practical guide using statistical software*. Chapman and Hall/CRC.
- Wininger, M., Kim, N. H., & Craelius, W. (2012). Reformulation in the phase plane enhances smoothness rater accuracy in stroke. *Journal of motor behavior*, *44*(3), 149-159.
- Young, R. P. and Marteniuk, R. G. (1997). Acquisition of a multi-articular kicking task: Jerk analysis demonstrates movements do not become smoother with learning. *Human Movement Science*, *16*(5):677–701.

Chapter 3

Evaluating Suitable Metrics for Movement Smoothness with Subjects Recovering after Stroke

3.1 Introduction

Movement smoothness is a quality measure of a movement, related to the continuity of a movement [1]. Several longitudinal studies have shown that upper limb movements become gradually smoother as recovery proceeds in the first 6 months after stroke [2–4]. More specifically, van Kordelaar et al (2014) showed that significant improvements in movement smoothness are mainly restricted to the first eight weeks after stroke onset. Interestingly, this time window for significant change is similar for impairment related outcomes such as the Fugl-Meyer Motor Assessment Score for Upper Extremity (FMA-UE) [5, 6]. But the exact cause of the lack of smoothness early post stroke stroke is poorly understood. It may involve poor interjoint and intermuscular coordination by increased co-activation in muscles of the paretic upper limb, causing basic synergies [7]. The joints that are coupled by this synergy cannot be mastered in isolation, resulting in a restricted movement pattern [8, 9]. Further, a decreased discharge rate of motor neurons [10] and spontaneous firing of motor units [11] may result in a lack of control in force output of the paretic limb resulting in less smooth movements. Another theory is that stroke subjects rely more on visual feedback in the end of a reach-to-grasp movement than healthy subjects [12]. This can be a result of the disrupted cortical-spinal pathways that affects the preplanning of movements [13] and selecting optimal ballistic movement strategy during functional tasks [14]. It is shown by Buma et al. (2016) that there is a relation between movement smoothness (measured with DSJ_t) and brain activation in secondary motor areas, suggesting that a decrease in smoothness results in a type of control where the movement pattern is continuously corrected, possibly based on visual and proprioceptive feedback [15]. Better understanding in the time course of early observed improvements in quality of movement is vital for developing innovative interventions such as arm robotics, selecting appropriate outcomes and designing new trials that target true neurological repair early post stroke [16]. Therefore it is important to use the appropriate metrics for quality of movement.

In the previous chapter it was found that number of peaks (*Peaks*), inversed number of peaks (*IPV*), dimensionless squared jerk metric, normalized with mean velocity (*DSJt*), dimensionless squared jerk metric, normalized with peak velocity (*DSJb*), the log of dimensionless squared jerk metrics (*LDSJb* and *LDSJt*), correlation metric (*CM*) and Spectral method (*SPM*) are the most suitable metrics for quantifying movement smoothness. *Peaks*, *IPV* and the dimensionless jerk metrics are less sensitive to movement segmentation and more sensitive for fluctuations in the velocity profile than *CM* and *SPM*. A higher sensitivity in velocity fluctuations comes with the drawback that there is a higher sensitivity to white noise compared to the other metrics.

The question answered in this chapter is: “Which of the valid smoothness metrics are sensitive to changes during recovery of stroke patients?”. A metric is said to be sensitive to measure movement smoothness in stroke subjects, if it can differentiate between changes in smoothness during the recovery after stroke. This is investigated using two different linear mixed models. In the first model, the metric is modelled as a function of time. In the second model, it is tried to model the FMA-UE score using the metrics for smoothness.

The ability of these metrics to capture smoothness changes over time in subjects recovering from stroke is important to select the most suitable metric for movement smoothness after stroke. Data from van Kordelaar et al. (2014) was made available for us to investigate the effect of progress of time on movement smoothness, the correlation between the different smoothness metrics and the correlation between FMA-UE scores and the different metrics [4]. A linear mixed model is suitable for a data set with longitudinal or repeated-measures, in which subjects are measured repeatedly over time or under different conditions [17]. This type of model consists of fixed and random coefficients. The random coefficients are subject specific while the fixed coefficients are for the whole population.

3.2 Methods

Data set

Longitudinal data of 44 patients recovering from stroke were acquired in the study by van Kordelaar et al. (2014). [4]. In the following section we summarize the dataset, further details about the dataset can be found in [4]. Data from 40 out of these 44 subjects was made available for this study.

All participants were included in the first week poststroke if they satisfied the list of requirements. These requirements consists of requirements for the type of stroke, age, type of impairments and consent. Included patients underwent clinical measurements as well as functional magnetic resonance imaging, transcranial magnetic stimulation, 3-dimensional kinematics and haptic robotics.

Included patients underwent a clinical and 3-dimensional kinematic assessment of the upper paretic limb in weeks 1, 2, 3, 4, 5, 8, 12, and 26 poststroke. The kinematic data were recorded with a portable electromagnetic motion tracking device (Polhemus Liberty¹). The setup is shown in figure 3.1. This device measures position relative to a global reference frame that has its origin in the center of its magnetic source. The x-axis was directed forward, y-axis upward and the z-axis rightward. This portable motion tracker and table were used for all measurements. The sensors were attached to the thorax and the scapula, upper arm, forearm, hand, thumb, and index finger of the non-paretic arm.

The task consisted of 2 parts. The first is a reach to grasp movement toward a block, followed by the second part; a displacement of the block toward a target location. The initial location of the block was the maximum reaching distance of the paretic arm of the participant. The different block sizes were 2.5, 5, 7.5 and 10 cm. Patients were allowed to move their trunk towards the block, however, they had to remain seated and were not allowed to slide or twist over the chair. Seven trials were recorded with each block size.

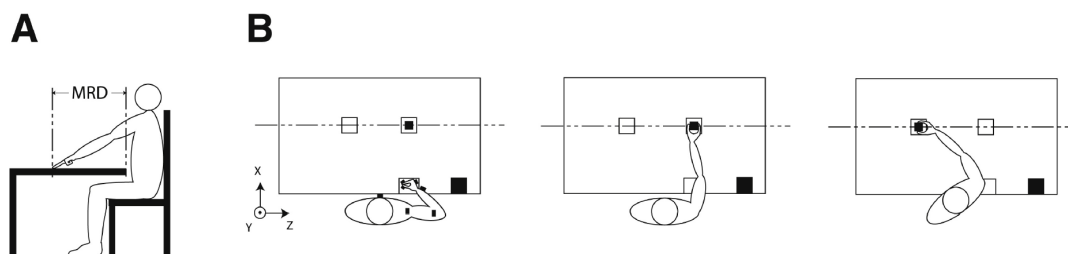


Figure 3.1: The measurement setup of the kinematic measurement with the Polhemus Liberty device (black square on bottom right corner on the table). (A) Measurement of the MRD. (B) The task execution. The position of the sensors is shown as black dots in the left panel of (B).

Adapted from van Kordelaar et al. [4]. Abbreviation: MRD, maximum reaching distance

The motor impairments were assessed using the upper extremity Fugl-Meyer Motor Assessment Score for Upper Extremity (FMA-UE) [18].

Data pre-processing

The start of the reach-to-grasp movement was defined as the moment at which the forearm sensor exceeded 5% of the peak velocity during the forward reach. The end was defined as the moment at which the forearm sensor exceeded 5% of the maximum speed during the displacement of the block. The same start and end end point marked by Kordelaar et al. (2014) were also used in this work. Thereafter, the movement was filtered using a bidirectional second-order Butterworth low-pass filter with a cutoff frequency of 20Hz, the same as Kordelaar et al. (2014) [4]. All the data analysis is done using MATLAB version 2015b².

¹Polhemus, 40 Hercules Dr, PO Box 560, Colchester, VT 05446.

²MATLAB version R2015b; MathWorks, 3 Apple Hill Dr, Natick, MA 01760-2098.

Kinematic Parameters

In Chapter 2 was concluded that *Peaks*, *IPV*, *DSJt*, *LDSJt*, *DSJb*, *LDSJb*, *CM* and *SPM* are suitable for measuring movement smoothness. These metrics are described and explained in detail in Chapter 2, and the mathematical description can be seen in appendix B.

Statistics

Correlation between metrics

Since all selected measures for smoothness should quantify smoothness, it is expected that they are correlated. The correlation between metrics for all trials, for all subjects for all weeks is calculated using the MATLAB built-in function ‘*corrcoef*’. The correlation coefficient r represents Pearsons correlation coefficient.

Random Coefficient Models

Linear regression models with only fixed coefficients can give insights in data for a single subject. When this same modelling method is used to study data from multiple subjects this model provides an estimation of the response over all subjects. This type of model however does not account for variation within subjects such as baseline values, age or gender. A random coefficient model can account for variations between subjects and is suitable to explain this type of data [17]. In the first model, the movement smoothness metrics were modelled as a function of time. It can be mathematically presented as

$$Y_{ij} = (\beta_0 + b_{0_i}) + (\beta_{1_j} + b_{1_{ij}}) \times X_{ij} + \epsilon_{ij}, \quad (3.1)$$

where Y_{ij} is the modelled smoothness metric for subject i at time point j , β_0 is a fixed intercept, b_{0_i} is a random intercept for subject i , β_{1_j} is a fixed regression coefficient for time point j , $b_{1_{ij}}$ is a random regression coefficient for subject i and time point j . Lastly, X_{ij} is a dummy variable for subject i and time point j . Week 26 was used as the reference time point (redundant variable). This dummy variable is needed since this model treated the number of weeks after stroke as a categorical variable. ϵ_{ij} specifies the residual value for subject i at time point j . The fitting is done using restricted maximum likelihood method (REML). With REML fitting it is suitable to calculate the p-values using the Satterthwaite method to derive the degrees of freedom of the models [19]. To verify the validity of the p-values, the residuals are assessed for normality using histograms and by calculating the skewness and kurtosis. Normally distributed residuals would have a skewness of approximately 0 and a kurtosis of approximately 3. Different models were built for each smoothness metric using the equation 3.1. Here, Y_{ij} denotes the smoothness metric. If the residuals of a model were not normally distributed, a transformation will be done to the input data and the model will be created again. The inverse, log and square root were used as transformation of the input data, the transformation with the residuals that were the closest to a normal distribution were used to create the final models. This was done specifically for each smoothness metric.

The fixed regression coefficients (β_{1j}) will be compared for the different metrics to see the effect of progress of time. To check the sensitivity of the models with respect to time, the r^2 values were calculated for each model and compared.

Additionally, linear mixed models were constructed to estimate the FMA-UE score using the movement smoothness metrics. The following model was used:

$$\text{FMA-UE}_{ij} = (\gamma_0 + c_{0i}) + (\gamma_1 + c_{1i}) \times Z_{ij} + \zeta_{ij}, \quad (3.2)$$

it is similar to the model in equation 3.1, however, this model estimates FMA-UE_{ij}, which is the FMA-UE score of subject i in week j . γ_0 is the fixed intercept, c_{0i} is a random intercept for subject i , γ_1 is the fixed coefficient for the metric, c_{1i} is a random regression coefficient for subject i , Z_{ij} denotes the measured smoothness metric, ζ_{ij} is here the term for the residual value for subject i at time point j . For each smoothness metric a model was made. These models are then compared by means of significance and correlation coefficient.

3.3 Results

In Table 3.1 the characteristics of the data set is shown. It can be seen that some data is missing. The proposed models can however handle missing data.

Table 3.1: Participant characteristics of the data from van Kordelaar et al. 2014, Values are n, kinematic data | FMA-UE scores, or median (interquartile range). Abbreviations: Fugl-Meyer Motor Assessment Score for Upper Extremity (FMA-UE)

Characteristics	Values
N	40
Missing data at each time point	
Wk 1	19 0
Wk 2	10 3
Wk 3	2 11
Wk 4	7 9
Wk 5	0 1
Wk 8	6 6
Wk 12	2 3
Wk 26	0 0
Clinical assessments	
FMA-UE score (0–66)	60 (50–64)

In figure 3.2 the reach-to-grasp velocity profiles of subject 14 for the first 10 trials are plotted for week 1, 2, 3 and 26. As the recovery proceeds, it can be seen that the peak velocity increases and the movement is executed in less time. Visually the trials executed in week 26 look more smooth as there are less local maxima in these profiles than the preceding weeks. The FMA-UE scores for this subject during the trials were 60, 63, 64 and 64.

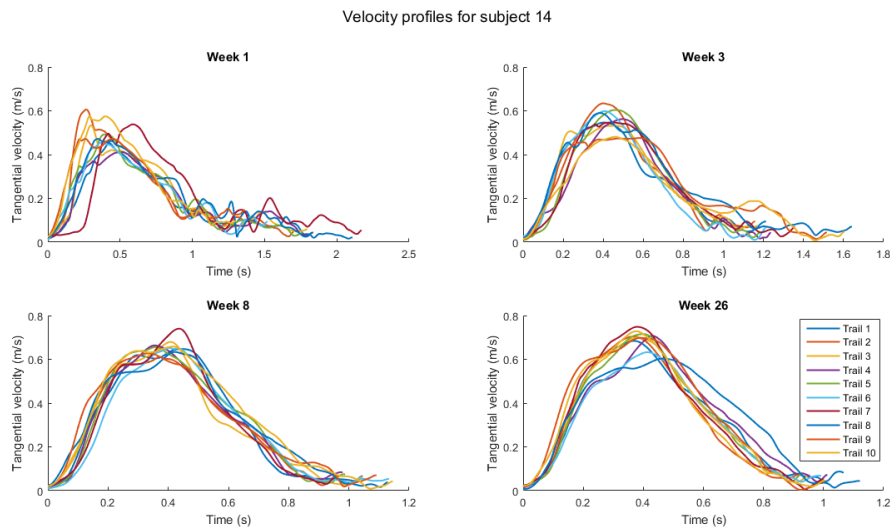


Figure 3.2: The reach-to-grasp velocity profiles of subject 14 for the first 10 trials are shown for week 1, 3, 8 and 26. It can be clearly seen that the movements become shorter and have a higher peak velocity as recovery proceeds. The FMA-UE scores for this subject during these trials were 60, 63, 64 and 64.

In figure 3.3 the different metrics and movement durations are plotted versus the FMA-UE score. For most of the metrics a trend between the two plotted variables is visible. In figure 3.4 box plots are used to show the distribution of each smoothness metric, movement duration and FMA-UE per week. Again clearly the same trend is seen that as time proceeds, the metrics show a smoother movement. *CM* is a bit different from the other metrics in a way that there is less change between week 2 and 5. Further the movements are executed in less time and the FMA-UE score increases over time, with the most change in the first four weeks after stroke. In *peaks*, it is seen that there is hardly any change over the weeks. Furthermore, it can be seen from this figure that the distributions are skewed, with outliers (as defined by Tukey (1977) [20]), in the direction of non-smoothness.

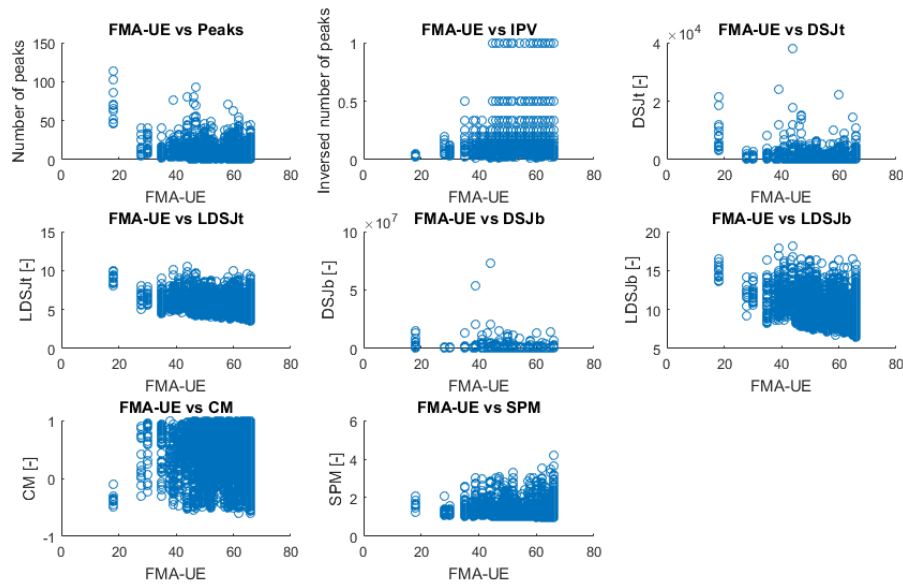


Figure 3.3: For all present weeks and all subject the data is shown here. Abbreviations: Inversed Number of peaks (IPV), Dimensionless Jerk (DSJ_t and DSJ_b), Log Dimensionless Squared Jerk ($LDSJ_t$ and $LDSJ_b$), Correlation Metric (CM), Spectral Method (SPM) and Fugl-Meyer Motor Assessment Score for Upper Extremity (FMA-UE).

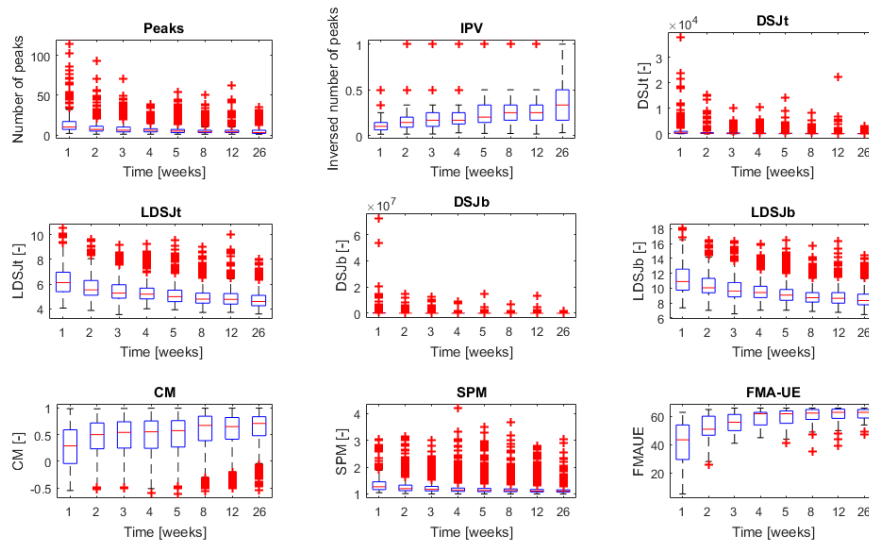


Figure 3.4: Change of metrics over time, shown in box plots. Metrics show that smoothness increases over time, movement duration decreases and Fugl-Meyer Motor Assessment Score for Upper Extremity (FMA-UE) increases mainly in the first 4 weeks after stroke. It can be seen that the distributions for the metrics and movement are skewed. Abbreviations: Inversed Number of peaks (IPV), Dimensionless Jerk (DSJ_t and DSJ_b), Log Dimensionless Squared Jerk ($LDSJ_t$ and $LDSJ_b$), Correlation Metric (CM), Spectral Method (SPM).

Correlation coefficients were calculated between the metrics and shown in table 3.2. The correlation coefficients are shown as r and represents their linear dependence. *LDSJb* has the highest correlation with FMA-UE ($r = -0.56$).

Table 3.2: Correlations between the metrics and Fugl-Meyer Motor Assessment Score for Upper Extremity (FMA-UE), shown as Pearson's correlation coefficient r . Abbreviations: Inversed Number of peaks (IPV), Dimensionless Jerk (DSJ_t and DSJ_b), Log Dimensionless Squared Jerk ($LDSJ_t$ and $LDSJ_b$), Correlation Metric (CM), Spectral Method (SPM).

	Peaks	IPV	DSJt	LDSJt	DSJb	LDSJb	CM	SPM	FMAUE
Peaks	1,00	-0,85	0,86	0,90	0,69	0,87	-0,67	0,68	-0,47
IPV	-0,85	1,00	-0,59	-0,77	-0,42	-0,77	0,58	-0,52	0,41
DSJt	0,86	-0,59	1,00	0,88	0,91	0,86	-0,60	0,76	-0,44
LDSJt	0,90	-0,77	0,88	1,00	0,70	0,98	-0,70	0,72	-0,51
DSJb	0,69	-0,42	0,91	0,70	1,00	0,71	-0,38	0,65	-0,38
LDSJb	0,87	-0,77	0,86	0,98	0,71	1,00	-0,59	0,73	-0,56
CM	-0,67	0,58	-0,60	-0,70	-0,38	-0,59	1,00	-0,53	0,14
SPM	0,68	-0,52	0,76	0,72	0,65	0,73	-0,53	1,00	-0,35
FMAUE	-0,47	0,41	-0,44	-0,51	-0,38	-0,56	0,14	-0,35	1,00

Models to predict the outcome of the smoothness metrics and movement durations, with time as input are made using equation 3.1. The histograms of the residuals of models are shown in figure 3.5. Also the value of the skewness and kurtosis are shown in this plot. In red, the fit of the normal distribution is shown. It is decided that only the model of *CM* represents a normal distribution. Transformations were applied for the other metrics and the coefficients were calculated again. It was found that for *peaks*, *IPV* and *DSJb* the log transformation had the best results and for the other metrics the inverse transformation. The type of used transform is added to the name of the metric for clarity. The prefix of *log* mean that a natural logarithmic transform is applied. *Inv* is used as prefix for the inverse transformation. The residuals after the transformations are shown in figure 3.6. The residuals seem to show acceptable normal distributions, except for *DSJb* and *SPM*, where the kurtosis is too high.

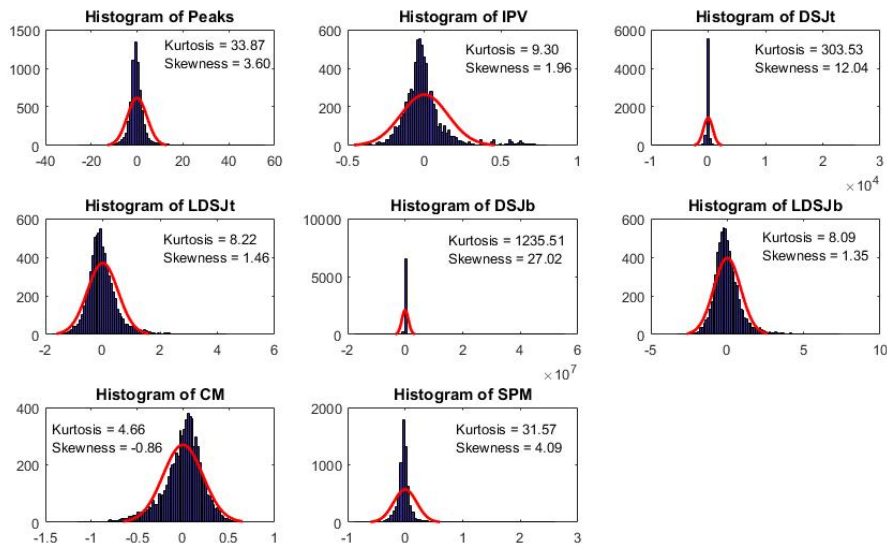


Figure 3.5: Residuals of the random coefficient models with weeks as input, with in red, a fit of a normal distribution. Also the kurtosis and skewness of the distribution is shown. Abbreviations: Inversed Number of peaks (IPV), Dimensionless Jerk (DSJ_t and DSJ_b), Log Dimensionless Squared Jerk ($LDSJ_t$ and $LDSJ_b$), Correlation Metric (CM), Spectral Method (SPM) and Fugl-Meyer Motor Assessment Score for Upper Extremity (FMA-UE).

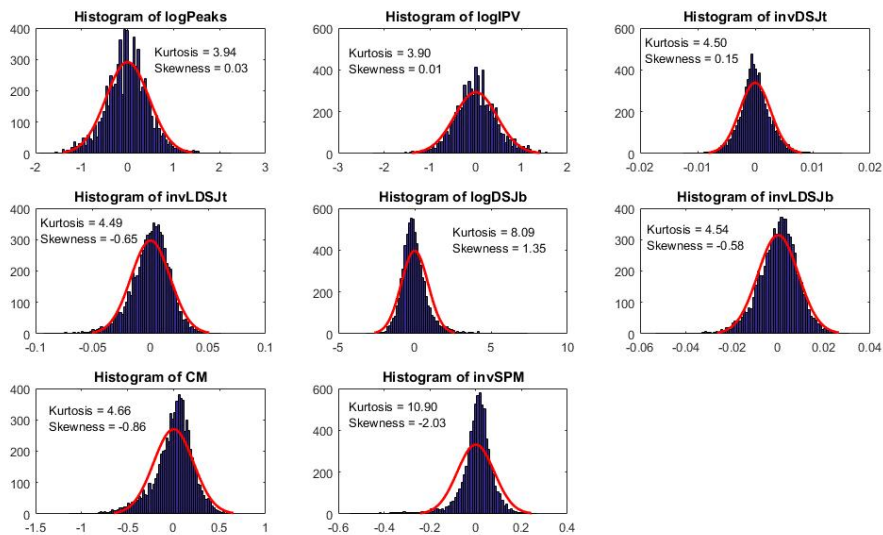


Figure 3.6: Residuals of the random coefficient models created with the log transformed input of Peaks, Peak2, SPARC and MD. In red, a fit of a normal distribution is plotted. Also the kurtosis and skewness of the distribution is shown. All distributions are assumed to be distributions except for SPARC. Preposition of log means that the log is taken, inv means that the inverse is taken. Abbreviations: Inversed Number of peaks (IPV), Dimensionless Jerk (DSJ_t and DSJ_b), Log Dimensionless Squared Jerk ($LDSJ_t$ and $LDSJ_b$), Correlation Metric (CM), Spectral Method (SPM) and Fugl-Meyer Motor Assessment Score for Upper Extremity (FMA-UE). Preposition of log and inv are the transformation by natural logarithm and inverse respectively

To evaluate the effect of progress of time, the fixed regression coefficients for time (β_{1j} in equation 3.1) are shown. The logistic pattern of recovery post stroke can be clearly seen for the different metrics. In table 3.3 these coefficients are shown, also the standard error and p-values are shown here. It can be seen from these values that all weeks differ significantly from week 26 (p-values 0.05), except for week 12 for *SPM*. The mean relative standard errors were calculated as well (SE/Coefficient) and where the lowest for *DSJ_t*, *LDSJ_t* and *LDSJ_b* (all 0.14) and the highest values were seen for *CM* and *SPM* (0.22 and 0.20 respectively).

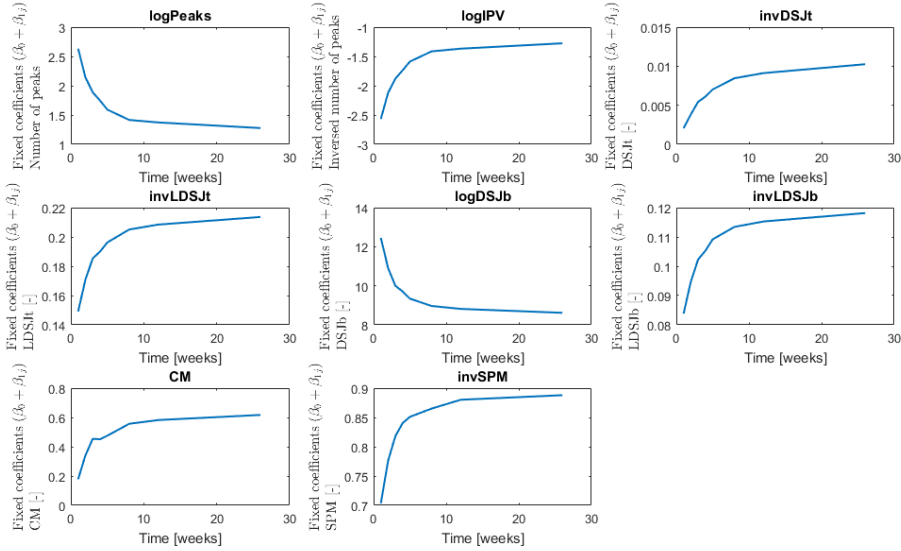


Figure 3.7: The fixed regression coefficients for time for each model are shown. The logistic pattern can be clearly seen from all graphs. Preposition of log means that the log is taken, inv means the inverse is taken. Abbreviations: Inversed Number of peaks (IPV), Dimensionless Jerk (DSJ_t and DSJ_b), Log Dimensionless Squared Jerk (LDSJ_t and LDSJ_b), Correlation Metric (CM), Spectral Method (SPM) and Fugl-Meyer Motor Assessment Score for Upper Extremity (FMA-UE). Preposition of log and inv are the transformation by natural logarithm and inverse respectively

Table 3.3: Fixed regression coefficients of recovery for the different metrics, log of movement durations and Fugl-Meyer Motor Assessment Score for Upper Extremity (FMA-UE) score. The values represent the fixed coefficients, \pm the standard error and the p-value between brackets. Abbreviations: Inversed Number of peaks (IPV), Dimensionless Jerk (DSJ_t and DSJ_b), Log Dimensionless Squared Jerk (LDSJ_t and LDSJ_b), Correlation Metric (CM), Spectral Method (SPM). Preposition of log and inv in front of the metric names are the transformation by natural logarithm and inverse respectively

Metric	logPeaks	logIPV	invDSJt	invLDSJt
r ²	0.59	0.58	0.67	0.68
Intercept	1.28E+00 \pm 7.82E-02 (<0.001)	-1.28E+00 \pm 7.79E-02 (<0.001)	1.03E-02 \pm 6.65E-04 (<0.001)	2.14E-01 \pm 3.45E-03 (<0.001)
Week 1	1.35E+00 \pm 1.41E-01 (<0.001)	-1.29E+00 \pm 1.23E-01 (<0.001)	-8.18E-03 \pm 7.00E-04 (<0.001)	-6.45E-02 \pm 5.00E-03 (<0.001)
Week 2	8.65E-01 \pm 1.01E-01 (<0.001)	-8.45E-01 \pm 9.99E-02 (<0.001)	-6.42E-03 \pm 6.16E-04 (<0.001)	-4.28E-02 \pm 4.20E-03 (<0.001)
Week 3	6.10E-01 \pm 9.28E-02 (<0.001)	-6.03E-01 \pm 9.20E-02 (<0.001)	-4.81E-03 \pm 5.69E-04 (<0.001)	-2.83E-02 \pm 3.48E-03 (<0.001)
Week 4	4.69E-01 \pm 8.26E-02 (<0.001)	-4.61E-01 \pm 8.16E-02 (<0.001)	-4.15E-03 \pm 5.18E-04 (<0.001)	-2.36E-02 \pm 3.08E-03 (<0.001)
Week 5	3.15E-01 \pm 5.47E-02 (<0.001)	-3.12E-01 \pm 5.42E-02 (<0.001)	-3.23E-03 \pm 4.19E-04 (<0.001)	-1.74E-02 \pm 2.34E-03 (<0.001)
Week 8	1.38E-01 \pm 4.94E-02 (0.008)	-1.37E-01 \pm 4.92E-02 (0.009)	-1.80E-03 \pm 4.53E-04 (<0.001)	-8.54E-03 \pm 2.28E-03 (<0.001)
Week 12	9.57E-02 \pm 3.45E-02 (0.009)	-9.14E-02 \pm 3.46E-02 (0.012)	-1.14E-03 \pm 2.63E-04 (<0.001)	-5.18E-03 \pm 1.38E-03 (<0.001)
Week 26	0*	0*	0*	0*
Metric	logDSJb	invLDSJb	CM	invSPM
r ²	0.69	0.70	0.60	0.47
Intercept	8.61E+00 \pm 1.48E-01 (<0.001)	1.18E-01 \pm 1.84E-03 (<0.001)	6.17E-01 \pm 3.46E-02 (<0.001)	8.88E-01 \pm 8.10E-03 (<0.001)
Week 1	3.84E+00 \pm 3.80E-01 (<0.001)	-3.43E-02 \pm 2.55E-03 (<0.001)	-4.39E-01 \pm 5.69E-02 (<0.001)	-1.85E-01 \pm 2.14E-02 (<0.001)
Week 2	2.29E+00 \pm 2.69E-01 (<0.001)	-2.34E-02 \pm 2.27E-03 (<0.001)	-2.76E-01 \pm 4.64E-02 (<0.001)	-1.12E-01 \pm 1.66E-02 (<0.001)
Week 3	1.39E+00 \pm 2.07E-01 (<0.001)	-1.58E-02 \pm 1.99E-03 (<0.001)	-1.63E-01 \pm 3.42E-02 (<0.001)	-7.00E-02 \pm 1.11E-02 (<0.001)
Week 4	1.09E+00 \pm 1.57E-01 (<0.001)	-1.29E-02 \pm 1.69E-03 (<0.001)	-1.66E-01 \pm 3.57E-02 (<0.001)	-4.77E-02 \pm 1.09E-02 (<0.001)
Week 5	7.26E-01 \pm 1.11E-01 (<0.001)	-8.99E-03 \pm 1.25E-03 (<0.001)	-1.42E-01 \pm 2.71E-02 (<0.001)	-3.70E-02 \pm 8.28E-03 (<0.001)
Week 8	3.51E-01 \pm 9.71E-02 (<0.001)	-4.72E-03 \pm 1.27E-03 (<0.001)	-6.03E-02 \pm 2.23E-02 (0.01)	-2.28E-02 \pm 4.95E-03 (<0.001)
Week 12	2.01E-01 \pm 6.96E-02 (0.006)	-2.87E-03 \pm 7.60E-04 (<0.001)	-3.48E-02 \pm 1.43E-02 (0.02)	-7.81E-03 \pm 4.15E-03 (0.066)
Week 26	0*	0*	0*	0*

*The values at week 26 are all 0 as this is the redundant variable.

The residuals of the FMA-UE models are shown in figure 3.8. It can be seen that the kurtosis is high (>7) for all models. Transformations did not help the residuals to become close to the normal distribution. It was therefore decided not to transform the input data. Since this model uses non-linear input data as seen in figure 3.4, it is relevant to inspect the residuals in each week. This is done in figure 3.9. It can be seen that there is no relation between the number of weeks and the magnitude of the residuals. Again a lot of outliers (as defined by Tukey (1977) [20]) are observed explaining the high value for the kurtosis.

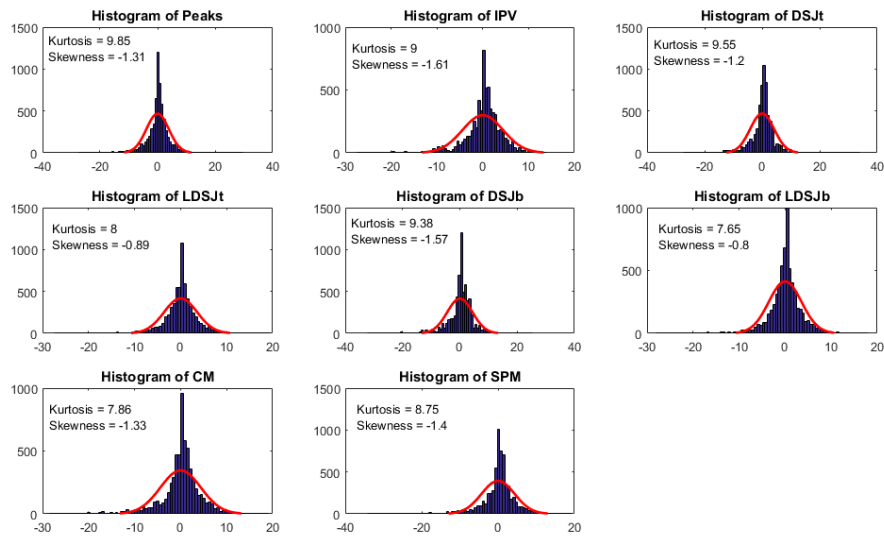


Figure 3.8: Residuals of the random coefficient models with movement smoothness or movement duration as input. Transformation hardly affected the residuals. Abbreviations: Inversed Number of peaks (IPV), Dimensionless Jerk (DSJ_t and DSJ_b), Log Dimensionless Squared Jerk ($LDSJ_t$ and $LDSJ_b$), Correlation Metric (CM), Spectral Method (SPM) and Fugl-Meyer Motor Assessment Score for Upper Extremity (FMA-UE).

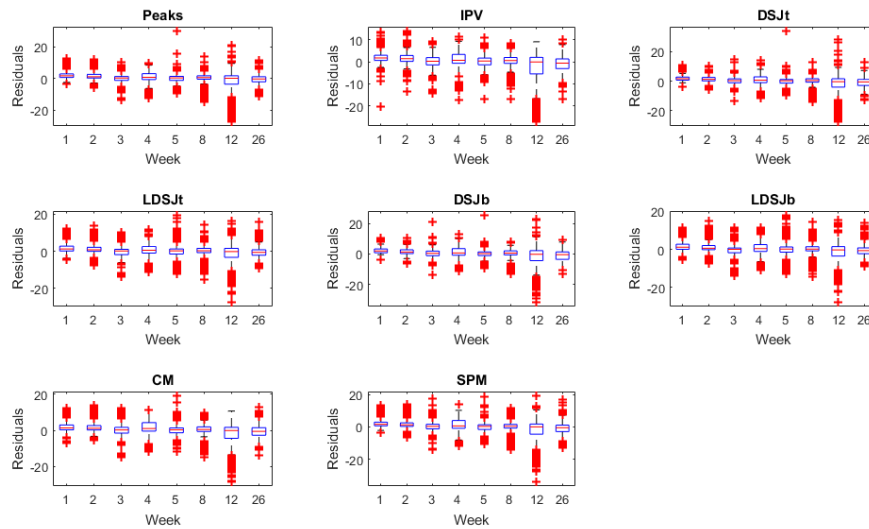


Figure 3.9: Residuals per week of the random coefficient models with movement smoothness or movement duration as input. It can be seen that there is no dependency on the residuals on the week. A lot of outliers are present, plotted in red, causing a high kurtosis. Abbreviations: Inversed Number of peaks (IPV), Dimensionless Jerk (DSJ_t and DSJ_b), Log Dimensionless Squared Jerk ($LDSJ_t$ and $LDSJ_b$), Correlation Metric (CM), Spectral Method (SPM) and Fugl-Meyer Motor Assessment Score for Upper Extremity (FMA-UE).

In table 3.4 the r^2 values and the p-values for the different models are shown. Due to the high kurtosis of the residuals of the models, these values might be improper. For *DSJb* it is seen that the p-value for the slope is >0.05 , indicating that there is no statistical significant contribution between this metric and the modelled FMA. The highest r^2 values were seen for *LDSJt* and *LDSJb*. The model of equation 3.2 was also created using only the fixed and random intercept. It was seen that the r^2 value was 0.57, and a p-value <0.001 was found.

Table 3.4: Model statistics of the linear mixed models to model the FMA-UE score. Ordinary r^2 and the p-values of the fixed effects of the model are shown. Abbreviations: Inversed Number of peaks (IPV), Log Dimensionless Jerk (*LDSJ_t* and *LDSJ_b*), Log Dimensionless Absolute Jerk (*LDAJ*), Correlation Metric (*CM*), Speed Method (*SPM*) and Fugl-Meyer Motor Assessment Score for Upper Extremity (FMA-UE).

Metric	Peaks	IPV	DSJt	LDSJt	DSJb	LDSJb	CM	SPM
r^2	0.75	0.68	0.71	0.79	0.67	0.79	0.68	0.69
pvalue intercept	<0.001	<0.001	<0.001	<0.001	<0.001	<0.001	<0.001	<0.001
pvalue slope	<0.001	<0.001	<0.001	<0.001	1.00	<0.001	<0.001	<0.001

3.4 Discussion

Which smoothness metrics are sensitive to changes during recovery of stroke patients?

The results show that all metrics change over time. All metrics except *DSJb* have a significant contribution to estimate FMA-UE compared to an intercept only model. This is an indication that *DSJb* is not sensitive to changes during stroke recovery. This result is however not conclusive as the test for significance is not valid for a model with non normally distributed residuals. Based on the results obtained with these models it can be concluded that *peaks*, *IPV*, *DSJt*, *LDSJt*, *LDSJb*, *CM* and *SPM* can be sensitive to changes in movement smoothness during stroke recovery.

If the raw data is inspected visually, it is seen that all metrics show an improvement in smoothness as a function of time. Models are created to explain the change as a function of time. It was seen that all metrics showed the same improvement patterns, this pattern was also found by van Kordelaar et al. [4]. The highest r^2 values were seen in the models that used jerk metrics. Transformations of the data was performed to create a model with (approximately) normally distributed residuals.

In the first models, where the metrics were modelled as a function of time, it was seen that the residuals for *DSJb* *SPM* were not normally distributed. After transformation of the input data using the inverse, natural logarithm and square root, the residuals still did not approximate the normal distribution. Therefore, the test of significance is not reliable for *DSJb* and *SPM*. The non-normal distribution can be explained by the box plots in figure 3.4, it is seen that the outliers span a far broader range than boxes in the boxplot, meaning that they are far out of the normally distributed range. This was also the case for *DSJb*, however, for this metrics the transformation changed this distribution while for *DSJt* and *SPM* the outliers still spanned a broader range than the boxes. If these outliers do no correspond to extreme values in FMA-UE, these will be also outliers in the residuals. In the residuals plot can clearly be seen that there are long tails, representing the outliers. Note that these values are classified as an outlier based on the normal distribution. The true distribution of the smoothness metrics is however not known and could indeed be asymmetric.

When the FMA-UE scores were modelled using the metrics as input, it was seen that the residuals did not resemble a normal distribution, even if various transformations of the input data were done. The main consequence of this fact is that the statistical tests are not reliable. In these tests was seen that implementation of *DSJb* did not have a significant contribution to the model. But since the residuals were not close to the normal distribution, the validity of these values can be questioned.

Limitations

In the study where the data was gathered, the task was not executable for all participants due to the complexity of the reach-to-grasp task. Therefore this study only represents patients with moderate to mild deficits in the paretic upper limb. This can be seen in table 3.1 as there are a total of 29 missing values in the kinematic measurements during the first two weeks. With the inclusion of less complex movements, such as a point-to-point reaching movement without grasping, also patients with a severe stroke can be represented. An additional possibility could be to give the subjects hand support during a 2-dimensional pointing task.

In the p-values of the time dependent model was seen that the metrics in week 1 until week 12 differ significantly ($\alpha = 0.05$) from the values in week 26, with an exception for week 12 in *SPM*. However, with the type of modelling that is used, the significance in change within consecutive weeks cannot be determined. By recreating the models with each time another week as redundant variable, the significance in the change per week could be determined. In this way, the sensitivity for change per week can be investigated. Another way to investigate significant change between consecutive weeks of the metrics would be a repeated measures t-test between the consecutive measurements per metric within the subjects. This method however does not take into account the change in the FMA-UE values.

Other models should be created to do a better comparison between the metrics. It would be interesting to compare the within subject behaviour of the metrics with the FMA-UE scores. As it is believed that FMA-UE reflects neurological recovery [21], metrics that show a similar behaviour as FMA-UE can possibly be an indicator of neurological recovery. A promising modeling technique to compare the within subject relationships of the metrics after stroke is the hybrid model. It is shown that hybrid models are suitable to precisely inspect between and within subject relationships in longitudinal datasets [22].

References

- [1] Sivakumar Balasubramanian et al. “On the analysis of movement smoothness”. In: *Journal of neuroengineering and rehabilitation* 12.1 (2015), p. 112.
- [2] Brandon Rohrer et al. “Movement smoothness changes during stroke recovery”. In: *Journal of Neuroscience* 22.18 (2002), pp. 8297–8304.
- [3] Laura Dipietro et al. “Submovement changes characterize generalization of motor recovery after stroke”. In: *Cortex* 45.3 (2009), pp. 318–324.
- [4] Joost van Kordelaar, Erwin van Wegen, and Gert Kwakkel. “Impact of time on quality of motor control of the paretic upper limb after stroke”. In: *Archives of physical medicine and rehabilitation* 95.2 (2014), pp. 338–344.
- [5] Pamela W Duncan et al. “Measurement of motor recovery after stroke. Outcome assessment and sample size requirements.” In: *Stroke* 23.8 (1992), pp. 1084–1089.
- [6] Gert Kwakkel, Boudewijn Kollen, and Jos Twisk. “Impact of time on improvement of outcome after stroke”. In: *Stroke* 37.9 (2006), pp. 2348–2353.
- [7] Mindy F Levin. “Interjoint coordination during pointing movements is disrupted in spastic hemiparesis”. In: *Brain* 119.1 (1996), pp. 281–293.
- [8] Thomas E Twitchell. “The restoration of motor function following hemiplegia in man”. In: *Brain* 74.4 (1951), pp. 443–480.
- [9] Joost van Kordelaar, Erwin EH van Wegen, and Gert Kwakkel. “Unraveling the interaction between pathological upper limb synergies and compensatory trunk movements during reach-to-grasp after stroke: a cross-sectional study”. In: *Experimental brain research* 221.3 (2012), pp. 251–262.
- [10] Judith J Gemperline et al. “Characteristics of motor unit discharge in subjects with hemiparesis”. In: *Muscle & Nerve: Official Journal of the American Association of Electrodiagnostic Medicine* 18.10 (1995), pp. 1101–1114.
- [11] Carol J Mottram et al. “Origins of spontaneous firing of motor units in the spastic-paretic biceps brachii muscle of stroke survivors”. In: *American Journal of Physiology-Heart and Circulatory Physiology* (2010).
- [12] Paulette M van Vliet and Martin R Sheridan. “Coordination between reaching and grasping in patients with hemiparesis and healthy subjects”. In: *Archives of physical medicine and rehabilitation* 88.10 (2007), pp. 1325–1331.
- [13] Janis J Daly et al. “Prolonged cognitive planning time, elevated cognitive effort, and relationship to coordination and motor control following stroke”. In: *IEEE Transactions on neural systems and rehabilitation engineering* 14.2 (2006), pp. 168–171.
- [14] Ruud CJ Meulenbroek, David A Rosenbaum, and Jonathan Vaughan. “Planning reaching and grasping movements: Simulating reduced movement capabilities in spastic hemiparesis”. In: *Motor Control* 5.2 (2001), pp. 136–150.
- [15] Floor E Buma et al. “Brain activation is related to smoothness of upper limb movements after stroke”. In: *Experimental brain research* 234.7 (2016), pp. 2077–2089.
- [16] Floor Buma, Gert Kwakkel, and Nick Ramsey. “Understanding upper limb recovery after stroke”. In: *Restorative neurology and neuroscience* 31.6 (2013), pp. 707–722.
- [17] Brady T West, Kathleen B Welch, and Andrzej T Galecki. *Linear mixed models: a practical guide using statistical software*. Chapman and Hall/CRC, 2014.
- [18] Axel R Fugl-Meyer et al. “The post-stroke hemiplegic patient. 1. a method for evaluation of physical performance.” In: *Scandinavian journal of rehabilitation medicine* 7.1 (1975), pp. 13–31.
- [19] Steven G Luke. “Evaluating significance in linear mixed-effects models in R”. In: *Behavior research methods* 49.4 (2017), pp. 1494–1502.

- [20] Chong Ho Yu. “Exploratory data analysis”. In: *Methods* 2 (1977), pp. 131–160.
- [21] David J Gladstone, Cynthia J Danells, and Sandra E Black. “The Fugl-Meyer assessment of motor recovery after stroke: a critical review of its measurement properties”. In: *Neurorehabilitation and neural repair* 16.3 (2002), pp. 232–240.
- [22] Jos WR Twisk and Wieke de Vente. “Hybrid models were found to be very elegant to disentangle longitudinal within-and between-subject relationships”. In: *Journal of clinical epidemiology* 107 (2019), pp. 66–70.

Chapter 4

Discussion

In Chapter 2 the question “Which metrics have been used so far to quantify movement smoothness in reaching movements of the upper limb during stroke recovery?” was addressed. We found that 31 different smoothness metrics have been used in 98 different studies. In our analysis we concluded that some proposed metrics are not applicable in many task oriented assessments. Some metrics were linearly related and could therefore be replaced by one metric. Further was seen that a metrics were mathematical invalid or the mathematical descriptions were missing. All these findings confirm the need for a standardized measure for movement smoothness or a helping guide in choosing the most suitable measure.

The second question asked in Chapter 2 was: “How do smoothness metrics behave as the characteristics of the analyzed movement changes?”. Using various simulations, the metrics were tested. It followed that number of peaks (*peaks*), the inverse of the number of peaks (*IPV*), Dimensionless Squared Jerk Normalized by mean velocity (*DSJt*), the natural logarithm of *DSJt* (*LDSJt*), Dimensionless Squared Jerk Normalized by peak velocity *DSJb*, the natural logarithm of *DSJb* (*LDSJb*), Correlation Metric (*CM*) and Spectral Method (*SPM*) showed suitable results for a metric for movement smoothness. It was however seen that in the simulation with sub-movements, a small change in the shape of the used sub-movement influences the result of the monotonicity of the metric. This was shown in Appendices E and F.

In the simulation with noise was that *peaks* and *IPV* increased with frequency and magnitude of the sinus as all metrics. However, important is that first a peak must arise before a change in the peaks metric can be captured. In figure 4.1 the minimum jerk trajectory is shown. Values for peaks, *LDSJ_t* and *SPM* are shown. On the right, a sinus with a magnitude of 0.01 added. From the shape can be seen that the movements looks less smooth, there is still only 1 peak, indicating that there is no change in smoothness according to *peaks* (and thus *IPV*). The other two metrics shown in this figure show an increase in this situation and are sensitive to this change. As this shows that this metric is insensitive for small changes in movement smoothness. This insensitivity could be unwanted, especially in later stages of stroke recovery when the progression per week is smaller.

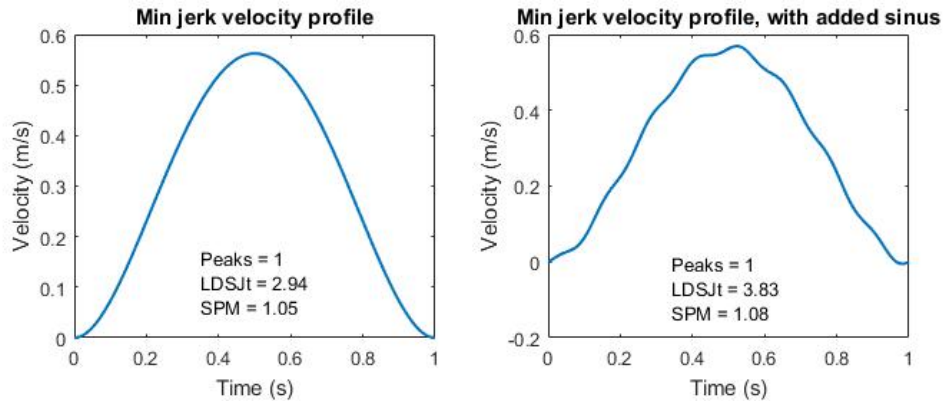


Figure 4.1: Although the velocity profile is altered by the added sinus, the peaks metric still gives 1 as outcome. For reference *LDSJt* and *SPM* are added as well, these metrics show responsiveness to that change.

The question answered in Chapter 3 was: “Which of the valid smoothness metrics are sensitive to changes during recovery of stroke patients?”. The metrics found to be suitable for measuring movement smoothness were thus applied on patient reaching. Using linear mixed models, these metrics were tested on responsiveness during the progress of time and the relation with the FMA-UE score. It was concluded that *peaks*, *IPV*, *DSJt*, *LDSJt*, *LDSJb*, *CM* and *SPM* can be sensitive to changes in movement smoothness during stroke recovery. However, some distinction between the metrics can be made. It was seen that jerk metrics had the highest r^2 values in both tested linear mixed models. Various transformations were needed before applying the models to make sure that the residuals were close to a normal distribution.

The main question of this thesis was: “What are suitable metrics for assessing movement smoothness in reaching movements of stroke patients?”. In chapters 2 and 3 was concluded that *peaks*, *IPV*, *DSJt*, *LDSJt*, *LDSJb*, *CM* and *SPM* are valid metrics and can be sensitive to capture changes during stroke recovery. However, a few recommendations can be given for choosing the right metric and further research.

Recommendations for measuring movement smoothness

In Chapter 3 was seen that transformations were needed for the input data to get the residuals close to the normal distribution. This was however not always successful and the tests for significance was in that case not reliable. Further was seen that there were not big differences between the r^2 of the models of the different metrics. To prevent these difficulties, other modelling techniques are interesting to investigate. A promising modeling technique to compare within subject relationships of the metrics after stroke is the hybrid model [1].

CM, used in this thesis is based on literature that human reaching is according to the minimum jerk model [2]. Then the correlation is calculated between the velocity profile of the subject and the minimum jerk model of that specific task. It was however shown in Appendix F that the movement of a reach-to-grasp does not follow the minimum jerk profile but is asymmetrical. But the *CM* still calculates the correlation with the symmetrical velocity profile. A new *CM* that calculates the correlation with an asymmetrical velocity profile instead would be an interesting metric to study for reach-to-grasp movements.

To get more insights into normal values for movement smoothness for the various metrics, it would be interesting to analyze velocity profiles of healthy subjects. As far we now, there are no values standard values for movement smoothness in healthy subjects. Knowing what would be values for healthy subject can give a better feeling for clinicians working with movement smoothness.

Although more metrics are suitable to measure movement smoothness, the choice can also be dependent on the type the measurements that is done. In Chapter 2 it was explained that the metrics can be classified into velocity-, acceleration-, jerk metrics and metrics in the frequency domain. If inertial measurement units are used for the measurements, it would be less suitable to use velocity metric or a metric based on velocity in the frequency domain (*SPM*), as integration to velocity will cause errors. Therefore it would be better to use an acceleration metric or to differentiate and use a jerk metric.

Another important note is that the goal of the analyzed movement should be known. A reaching movement to a target cannot be compared with a reaching movement with an intermediate target. This is also confirmed by the finding that a reach-to-grasp velocity profile has different values for smoothness than point-to-point reaching movements.

References

- [1] Jos WR Twisk and Wieke de Vente. “Hybrid models were found to be very elegant to disentangle longitudinal within-and between-subject relationships”. In: *Journal of clinical epidemiology* 107 (2019), pp. 66–70.
- [2] Tamar Flash and Neville Hogan. “The coordination of arm movements: an experimentally confirmed mathematical model”. In: *Journal of neuroscience* 5.7 (1985), pp. 1688–1703.

Appendix A – Search string for the different databases

PubMed

#1 Stroke patients

"Stroke"[Mesh] OR "Stroke Rehabilitation"[Mesh] OR cva[tiab] OR cvas[tiab] OR poststroke*[tiab] OR post-stroke*[tiab] OR stroke*[tiab] OR apoplex*[tiab] OR cerebrovascular diseases*[tiab] OR cerebrovascular accident*[tiab] OR cerebrovascular disorder*[tiab] OR ((brain*[tiab] OR cerebr*[tiab] OR cerebell*[tiab] OR intracran*[tiab] OR intracerebral*[tiab] OR vertebrobasilar*[tiab]) AND vascular*[tiab] AND (disease[tiab] OR diseases[tiab] OR accident*[tiab] OR disorder*[tiab])) OR ((brain*[tiab] OR cerebr*[tiab] OR cerebell*[tiab] OR intracran*[tiab] OR intracerebral*[tiab] OR vertebrobasilar*[tiab]) AND (haemorrhag*[tiab] OR hemorrhag*[tiab] OR ischemi*[tiab] OR ischaemi*[tiab] OR infarct*[tiab] OR haematoma*[tiab] OR hematoma*[tiab] OR bleed*[tiab]))

#2 Kinetics and kinematics

((("Movement"[Mesh:NoExp] OR "Motion"[Mesh] OR "Spatio-Temporal Analysis"[Mesh] OR "Kinetics"[Mesh] OR Kinematic*[tiab] OR kinetic*[tiab] OR angle*[tiab] OR motion[tiab] OR acceler*[tiab] OR deceler*[tiab] OR rotation[tiab] OR velocity*[tiab] OR speed*[tiab] OR spatiotemporal[tiab]))

#3 Upper limb kinetics and kinematics

OR "Upper Extremity"[Mesh] OR Upper Extremit*[tiab] OR Upper Limb*[tiab] OR arm[tiab] OR arms[tiab] OR shoulder[tiab] OR elbow*[tiab] OR forearm*[tiab] OR wrist*[tiab] OR hand[tiab] OR hands[tiab] OR finger*[tiab] OR thumb*[tiab]

#4 Smoothness

Smooth*

All articles with #1 AND #2 AND #3 AND #4 were retrieved.

Scopus

#1 Stroke

TITLE-ABS-KEY (cva OR cvas OR poststroke* OR stroke* OR apoplex* OR ((brain* OR cerebr* OR cerebell* OR intracran* OR intracerebral* OR vertebrobasilar*) AND vascular* AND (disease OR diseases OR accident* OR disorder*)) OR (cerebrovascular* AND (disease OR diseases OR accident* OR disorder*)) OR ((brain* OR cerebr* OR cerebell* OR intracran* OR intracerebral* OR vertebrobasilar*) AND (haemorrhag* OR hemorrhag* OR ischemi* OR ischaemi* OR infarct* OR haematoma* OR hematoma* OR bleed*)))

#2 Kinetics and kinematics

TITLE-ABS-KEY (movement OR motion OR kinematic* OR kinetic* OR angle* OR motion OR acceler* OR deceler* OR rotation OR velocity* OR speed* OR spatiotemporal)

#3 Upper extremity

TITLE-ABS-KEY ("Upper Extremit*" OR "Upper Limb*" OR arm OR arms OR shoulder OR elbow* OR forearm* OR wrist* OR hand OR hands OR finger* OR thumb*)

#4 Smoothness

TITLE-ABS-KEY (smooth*)

All articles with #1 AND #2 AND #3 AND #4 were retrieved.

Cochrane Library**#1 Stroke patients**

cva OR cvas OR poststroke* OR stroke* OR apoplex* OR ((brain* OR cerebr* OR cerebell* OR intracran* OR intracerebral* OR vertebrobasilar*) AND vascular* AND (disease OR diseases OR accident* OR disorder*)) OR (cerebrovascular* AND (disease OR diseases OR accident* OR disorder*)) OR ((brain* OR cerebr* OR cerebell* OR intracran* OR intracerebral* OR vertebrobasilar*) AND (haemorrhag* OR hemorrhag* OR ischemi* OR ischaemi* OR infarct* OR haematoma* OR hematoma* OR bleed*))

#2 Reach and grasp

reach* OR coordination OR grasp* OR grip* OR "Upper Extremit*" OR "Upper Limb*" OR arm OR arms OR shoulder OR elbow* OR forearm* OR wrist* OR hand OR hands OR finger* OR thumb*

#3 Upper limb kinetics and kinematics

Movement OR Motion OR Mechanical OR biomechanic* OR Kinematic* OR kinetic* OR angle* OR motion OR acceler* OR deceler* OR rotation OR velocity* OR speed* OR spatiotemporal

#4 Smoothness

Smooth*

All articles with #1 AND #2 AND #3 AND #4 were retrieved.

Embase**#1 Stroke patients**

'cerebrovascular accident'/exp OR cva:ab,ti OR cvas:ab,ti OR stroke:ab,ti OR apoplex*:ab,ti OR poststroke*:ab,ti OR ((brain*:ab,ti OR cerebr*:ab,ti OR cerebell*:ab,ti OR intracran*:ab,ti OR intracerebral*:ab,ti OR vertebrobasilar*:ab,ti) AND vascular*:ab,ti AND (disease:ab,ti OR diseases:ab,ti OR accident*:ab,ti OR disorder*:ab,ti)) OR (cerebrovascular*:ab,ti AND (disease:ab,ti OR diseases:ab,ti OR accident*:ab,ti OR disorder*:ab,ti)) OR ((brain*:ab,ti OR cerebr*:ab,ti OR cerebell*:ab,ti OR intracran*:ab,ti OR intracerebral*:ab,ti OR vertebrobasilar*:ab,ti) AND (haemorrhag*:ab,ti OR hemorrhag*:ab,ti OR ischemi*:ab,ti OR ischaemi*:ab,ti OR infarct*:ab,ti OR haematoma*:ab,ti OR hematoma*:ab,ti OR bleed*:ab,ti))

#2 Reach and grasp

reach*:ti,ab OR coordination:ti,ab OR grasp*:ti,ab OR grip*:ti,ab OR 'upper limb'/exp OR 'Upper Extremit*':ti,ab OR 'Upper Limb*':ti,ab OR arm:ti,ab OR arms:ti,ab OR shoulder:ti,ab OR elbow*:ti,ab OR forearm*:ti,ab OR wrist*:ti,ab OR hand:ti,ab OR hands:ti,ab OR finger*:ti,ab OR thumb*:ti,ab

#3 Kinetics and kinematics

'movement (physiology)'/de OR 'limb movement'/de OR 'arm movement'/exp OR 'hand movement'/exp OR 'motion'/de OR 'velocity'/exp OR 'mechanics'/de OR 'biomechanics'/exp OR 'force'/exp OR 'kinematics'/exp OR 'kinetics'/de OR 'torque'/exp OR 'temporal analysis'/exp OR 'spatial analysis'/de OR torque*:ti,ab OR biomechanic*:ti,ab OR Kinematic*:ti,ab OR kinetic*:ti,ab OR angle*:ti,ab OR force*:ti,ab OR motion:ti,ab OR acceler*:ti,ab OR deceler*:ti,ab OR rotation:ti,ab OR velocity*:ti,ab OR speed*:ti,ab OR spatiotemporal:ti,ab

#4 Smoothness

Smooth*:ti,ab

All articles with #1 AND #2 AND #3 AND #4 NOT ('animal'/exp NOT 'human'/exp) were retrieved.

Appendix B – Mathematical definition of metrics

Peaks metric (PM), introduced by Brooks (1974)

$$PM = \#\{v_{\text{maxima}}\},$$

Where v_{maxima} is defined as

$$v(t): \dot{v}(t) = 0 \text{ and } \ddot{v}(t) < 0,$$

Where $v(t)$, $\dot{v}(t)$, and $\ddot{v}(t)$ are respectively the first, second and third time derivative of position.

Peaks metric normalized by peak speed is defined by

$$PM_{ps} = \frac{PM}{v_{\text{peak}}},$$

peaks metric normalized by movement duration is defined by

$$PM_{md} = \frac{PM}{T}$$

and *Inverse number of peaks and valleys* is defined by

$$PM_{inv} = \frac{1}{(PM * 2) - 1}$$

where PM is the number of peaks, defined earlier, v_{peak} is the peak velocity within the movement and T is the total movement duration. Note here that the number of peaks and valleys is defined as $(PM * 2) - 1$.

Speed metric (SM), introduced by Rohrer et al. (2002).

$$SM = \frac{v_{\text{mean}}}{v_{\text{peak}}}$$

Where v_{mean} and v_{peak} are respectively the mean and peak velocity of the whole movement.

Movement arrest period ratio (MAPR), introduced by Beppu et al. (1984).

$$MAPR = \frac{t(v \geq F \cdot v_{\text{peak}})}{T},$$

where F is the fraction that is taken from the peak velocity to calculate the threshold and T is the total duration. Rohrer et al. (2002) used a F-value of 0.1.

Normalized reaching speed (NRS), introduced by Mazzoleni et al. (2011).

$$NRS = \frac{v_{peak} - v_{mean}}{v_{peak}}$$

Velocity arc length (VAL), introduced by Balasubramanian et al. (2012)

$$VAL = -\ln \left(\int_{t_1}^{t_2} \sqrt{\left(\frac{1}{t_2 - t_1}\right)^2 + \left(\frac{d\hat{v}}{dt}\right)^2} dt \right),$$

$$\hat{v}(t) = \frac{v(t)}{v_{peak}}.$$

t_1 and t_2 are the time points at the start and end of the movement.

Number of sub-movements (NOS), introduced by Rohrer and Hogan (2006). This algorithm fits the velocity profile by a combination of minimal jerk velocity profiles. This is done by using MATLAB's function `fmincon` and minimizing the error function

$$\epsilon = \frac{\int |F(t) - G(t)| dt}{\int |G(t)| dt},$$

where $G(t)$ is the movement speed profile and $F(t)$ is the fitted speed profile.

$$F(t) = \sum_{i=1}^{Ns} v_{mji}(t) \text{ where,}$$

$$v_{mji}(t) = \begin{cases} 0 & \text{if } t < T_{s_i} \\ 0 & \text{if } t > T_{s_i} + T_i \\ \text{else } \Delta_i \left(\frac{30(t-T_{s_i})^4}{T_i^5} - \frac{60(t-T_{s_i})^3}{T_i^4} + \frac{30(t-T_{s_i})^2}{T_i^3} \right) \end{cases}$$

With N_s the number of sub-movements, v_{mj} the minimal jerk speed profile, Δ the sub-movement distance, T the sub-movement duration and T_s the sub-movement time shift. Subscript i denotes the i th sub-movement. Δ , T_s and T are minimized, while the function was ten times initialized at random points within the solution space, with $N_s = 1$. For Δ the solution space is between 0 and 1 meter, for T between 0.01 and 3 seconds and for T_s between 0 seconds and the total duration of the movement. If the error was below 0.02, the optimization is finished, else, 1 is added to N_s and the optimization continues. Further, the minimization was aborted if N_s was greater than 7. In that case, there was no optimized solution. Finally, NOS gives the number of subtracted sub-movements N_s , which is the measure for smoothness. A more detailed explanation is given in Appendix D.

Acceleration metric (AM) introduced by Mazzoleni et al. (2011)

$$AM = \frac{\ddot{x}_{mean}}{\ddot{x}_{peak}},$$

where \ddot{x} is the second derivative of $x(t)$ with respect to time, which is the acceleration.

Integrated absolute jerk (IAJ) introduced by Duff et al. (2010).

$$\eta_{iaj} = \int_{t_1}^{t_2} |\ddot{x}(t)| dt$$

where $\ddot{x}(t)$ is the third derivative of $x(t)$ with respect to time, which is the jerk.

Mean absolute jerk (MAJ) introduced by Bigoni et al. (2016).

$$\eta_{maj} = \frac{1}{t_2 - t_1} \int_{t_1}^{t_2} |\ddot{x}(t)| dt$$

Mean absolute jerk, normalized by peak speed (MAJPS), introduced by Rohrer et al. (2002).

$$\eta_{majps} = \frac{1}{v_{peak}(t_2 - t_1)} \int_{t_1}^{t_2} \ddot{x}(t)^2 dt.$$

Integrated squared jerk (ISJ), introduced by Laczko et al. (2017).

$$\eta_{isj} = \int_{t_1}^{t_2} \ddot{x}(t)^2 dt.$$

Root mean squared jerk (RMSJ) introduced by Young and Marteniuk (1997).

$$\eta_{rmsj} = \sqrt{\frac{1}{(t_2 - t_1)} \int_{t_1}^{t_2} \ddot{x}(t)^2 dt.}$$

Dimensionless squared jerk (DSJ_t) as introduced by Teulings et al. (1997).

$$\eta_{dsj-t} = \sqrt{\frac{1}{2} \frac{(t_2 - t_1)^3}{v_{mean}^2} \int_{t_1}^{t_2} \ddot{x}(t)^2 dt.}$$

Log dimensionless squared jerk (LDSJ_l) as introduced by van Kordelaar et al. (2012).

$$\eta_{\text{lds-j-t}} = \ln \left(\sqrt{\frac{1}{2} \frac{(t_2 - t_1)^3}{v_{\text{mean}}^2} \int_{t_1}^{t_2} \ddot{x}(t)^2 dt} \right).$$

Dimensionless squared jerk (DSJ_m) as introduced by Marini et al. (2017).

$$\eta_{\text{dsj-m}} = \frac{1}{2} \sqrt{\frac{(t_2 - t_1)^3}{v_{\text{mean}}^2} \int_{t_1}^{t_2} \ddot{x}(t)^2 dt},$$

Note that this one is actually the same as the Dimensionless squared jerk as introduced by Teulings et al. (1997). Possibly due to an inattentiveness, they placed the 1/2 in front of the square root resulting in a value which is $\sqrt{\frac{1}{2}}$ higher.

Normalized integrated jerk (NIJ) as introduced by Adamovich et al. (2009)

$$\eta_{\text{nij}} = \sqrt{\frac{1}{2} \frac{(t_2 - t_1)^3}{v_{\text{mean}}^2} \int_{t_1}^{t_2} \ddot{x}(t)^2 dt}.$$

Dimensionless squared jerk (DSJ_b) as introduced by Balasubramanian et al. (2012).

$$\eta_{\text{dsj-b}} = \frac{(t_2 - t_1)^3}{v_{\text{peak}}^2} \int_{t_1}^{t_2} \ddot{x}(t)^2 dt.$$

Log dimensionless squared jerk (LDSJ_b) as introduced by Balasubramanian et al. (2012).

$$\eta_{\text{lds-j-b}} = \ln \left(\frac{(t_2 - t_1)^3}{v_{\text{peak}}^2} \int_{t_1}^{t_2} \ddot{x}(t)^2 dt \right),$$

Correlation metric (CM) introduced by Krebs et al. (2001). First the minimum jerk speed profile is calculated by

$$v_{\text{mj}}(t) = \Delta \left(\frac{30t^4}{T^5} - \frac{60t^3}{T^4} + \frac{30t^2}{T^3} \right),$$

$$v_{\text{norm}}(t) = \frac{v(t)}{v_{\text{peak}}},$$

where $v(t)$ is the hand speed, $v_{\text{mj}}(t)$ is the minimal jerk speed profile. Δ is the distance of the reaching movement. T is the duration of the reaching movement.

Then, the correlation coefficient is calculated in the standard form as

$$\rho = \frac{\sum[(v_{norm} - \bar{v}_{norm})(v_{mj} - \bar{v}_{mj})]}{\sqrt{(\sum[(v_{norm} - \bar{v}_{norm})^2 \sum(v_{mj} - \bar{v}_{mj})^2])}}$$

Where \bar{v}_{norm} and \bar{v}_{mj} are the mean values of the normalized hand speed and minimum jerk speed profile.

Rotational jerk, introduced by Repnik et al. (2018)

$$\eta_{rot} = \log \sqrt{\frac{(t_2 - t_1)^5}{2\theta^p} \int_{t_1}^{t_2} \left\| \frac{d^2\omega(t)}{dt^2} \right\|^2 dt},$$

where t_1 is the beginning of the movement, t_2 the end of the movement, $\omega(t)$ is the hand angular velocity vector and parameter θ^p normalizes the jerk index with angular displacement of the rotation movement.

Spectral metric (SPMR) introduced by Strohrmann et al. (2013)

$$\begin{aligned} V(\omega) &= \text{fft}(v(t)) \\ \bar{V}(\omega) &= \frac{V(\omega)}{\sum_{\forall\omega}\{V(\omega)\}} \\ SPMR &= \max_{\forall\omega}\{V(\omega)\}, \end{aligned}$$

Where $\text{fft}(v(t))$ is the fast Fourier transform operation. The parameters are in this transformation are chosen such that each bin in the frequency domain is equal to 0.2Hz

Spectral method (SPM) introduced by Balasubramanian et al. (2009).

$$\begin{aligned} V(\omega) &= \text{fft}(\tilde{v}(t)) \\ \bar{V}(\omega) &= \frac{V(\omega)}{\max_{\forall\omega}\{V(\omega)\}} \\ SPM &= \sum \text{Maxima}_{\bar{V}(\omega)} \in [0, \omega_c] \text{ with,} \\ \omega_c &= \min(\omega) \mid \bar{V}(\omega) < 0.01 \end{aligned}$$

where $\tilde{v}(t)$ is the zero padded version of $v(t)$, $V(\omega)$ is the Fourier magnitude spectrum of $\tilde{v}(t)$, and $[0, \omega_c]$ is the frequency band occupied by the given movement. Before detecting the maxima, spectral smoothing was done using a moving average filter using a window size of 5 samples.

Spectral arc length (SPAL) introduced by Balasubramanian et al. (2012).

$$SPAL = - \int_0^{\omega_c} \sqrt{\left(\frac{1}{\omega_c}\right)^2 + \left(\frac{d\hat{V}(\omega)}{d\omega}\right)^2} d\omega,$$

$$\hat{V}(\omega) = \frac{V(\omega)}{V(0)},$$

where $V(\omega)$ is the Fourier magnitude spectrum of $v(t)$, and $[0, \omega_c]$ is the frequency band occupied by the given movement

Spectral arc length (SPARC) as introduced by Balasubramanian et al. (2015) uses the same formula as the SPAL. However, to determine ω_c the following additional formula is used

$$\omega_c \triangleq \min \left\{ \omega_c^{max}, \min \left\{ \omega, \hat{V}(r) < \bar{V} \quad \forall r > \omega \right\} \right\}.$$

Osu et al. (2011) introduced the *MedianLC* metric to calculate the smoothness of rhythmic reaching movements. This metric calculates first the three-dimensional instantaneous curvature at each time point using the following formula:

$$\kappa^2 = \frac{(\dot{x}^2 + \dot{y}^2 + \dot{z}^2)(\ddot{x}^2 + \ddot{y}^2 + \ddot{z}^2) - (\dot{x}\ddot{x} + \dot{y}\ddot{y} + \dot{z}\ddot{z})^2}{(\dot{x}^2 + \dot{y}^2 + \dot{z}^2)^3},$$

Then to calculate the smoothness, the $-\log$ of curvature κ was taken. Then the timepoints where the tangential velocity exceeds 50mm/s were extracted. The median of $-\log(\kappa)$ was taken at the extracted points as the smoothness metric MedianLC.

Combined smoothness metric (CSM), introduced by Kostić and Popović, (2013)

$$CSM = e^{(J_h + J_i)} + e^{(P_h + P_i)} + \frac{V_i}{V_h} + \frac{T_i}{T_h},$$

Where J_i is the mean negative jerk, normalized by peak velocity, P_i is the number of peaks in the velocity profile, V_i is the ratio of mean velocity and peak velocity and T_i is the ratio of area under the velocity profile and its convex hull. The terms J_h, P_h, V_h and T_h are the normal values, determined by the authors. Respectively 1.15, 1, 0.5 and 0.9. were the values used by Kostić and Popović (2013).

Appendix C – Table with all metrics and users

Metric	Category	References
Index of curvature	Trajectory	Bigoni, M., Baudo, S., Cimolin, V., Cau, N., Galli, M., Pianta, L., ... & Mauro, A. (2016). Does kinematics add meaningful information to clinical assessment in post-stroke upper limb rehabilitation? A case report. <i>Journal of physical therapy science</i> , 28(8), 2408-2413.
SD_XY	Trajectory	Simonsen, D., Popovic, M. B., Spaich, E. G., & Andersen, O. K. (2017). Design and test of a Microsoft Kinect-based system for delivering adaptive visual feedback to stroke patients during training of upper limb movement. <i>Medical & biological engineering & computing</i> , 55(11), 1927-1935.
Number of submovements (NOS)	Velocity	Liebermann, D. G., Levin, M. F., McIntyre, J., Weiss, P. L., & Berman, S. (2010, August). Arm path fragmentation and spatiotemporal features of hand reaching in healthy subjects and stroke patients. In <i>Engineering in Medicine and Biology Society (EMBC), 2010 Annual International Conference of the IEEE</i> (pp. 5242-5245). IEEE.
Speed metric (SM)	Velocity	Rohrer, B., Fasoli, S., Krebs, H. I., Hughes, R., Volpe, B., Frontera, W. R., ... & Hogan, N. (2002). Movement smoothness changes during stroke recovery. <i>Journal of Neuroscience</i> , 22(18), 8297-8304.
		Liebermann, D. G., Levin, M. F., McIntyre, J., Weiss, P. L., & Berman, S. (2010, August). Arm path fragmentation and spatiotemporal features of hand reaching in healthy subjects and stroke patients. In <i>Engineering in Medicine and Biology Society (EMBC), 2010 Annual International Conference of the IEEE</i> (pp. 5242-5245). IEEE.
		Mazzoleni, S., Filippi, M., Carrozza, M. C., Posteraro, F., Puzzolante, L., & Falchi, E. (2011, June). Robot-aided therapy on the upper limb of subacute and chronic stroke patients: a biomechanical approach. In <i>Rehabilitation Robotics (ICORR), 2011 IEEE International Conference on</i> (pp. 1-6). IEEE.
		Stoquart, G., Gilliaux, M., Lejeune, T., Detrembleur, C., Sapin, J., & Dehez, B. (2012). A robotic device as a sensitive quantitative tool to assess upper limb impairments in stroke patients: a preliminary prospective cohort study. <i>European Journal of Physical and Rehabilitation Medicine: a journal of physical medicine and rehabilitation after pathological events</i> , 48(49).
		Mazzoleni, S., Sale, P., Tiboni, M., Franceschini, M., Posteraro, F., & Carrozza, M. C. (2013). Upper limb robot-assisted therapy in chronic and subacute stroke patients: a kinematic analysis. In <i>Converging Clinical and Engineering Research on Neurorehabilitation</i> (pp. 129-133). Springer, Berlin, Heidelberg.
		Giacobbe, V., Krebs, H. I., Volpe, B. T., Pascual-Leone, A., Rykman, A., Zeiarati, G., ... & Edwards, D. J. (2013). Transcranial direct current stimulation (tDCS) and robotic practice in chronic stroke: the dimension of timing. <i>NeuroRehabilitation</i> , 33(1), 49-56.
		Christopher, S. M., & Johnson, M. J. (2014, August). Task-oriented robot-assisted stroke therapy of paretic limb improves control in a unilateral and bilateral functional drink task: A case study. In <i>Engineering in Medicine and Biology Society (EMBC), 2014 36th Annual International Conference of the IEEE</i> (pp. 1194-1197). IEEE.
		Colombo, R., Cusmano, I., Sterpi, I., Mazzone, A., Delconte, C., & Pisano, F. (2014). Test-retest reliability of robotic assessment measures for the evaluation of upper limb recovery. <i>IEEE Transactions on Neural Systems and Rehabilitation Engineering</i> , 22(5), 1020-1029.
		Yoo, D. H., & Kim, S. Y. (2015). Effects of upper limb robot-assisted therapy in the rehabilitation of stroke patients. <i>Journal of physical therapy science</i> , 27(3), 677-679.
		Adams, R. J., Lichter, M. D., Krepkovich, E. T., Ellington, A., White, M., & Diamond, P. T. (2015). Assessing upper extremity motor function in practice of virtual activities of daily living. <i>IEEE Transactions on Neural Systems and Rehabilitation Engineering</i> , 23(2), 287-296.
		Duret, C., Courtial, O., & Grosmaire, A. G. (2016). Kinematic measures for upper limb motor assessment during robot-mediated training in patients with severe sub-acute stroke. <i>Restorative neurology and neuroscience</i> , 34(2), 237-245.
		Colombo, R., Pisano, F., Delconte, C., Mazzone, A., Griioni, G., Castagna, M., ... & Pistarini, C. (2017). Comparison of exercise training effect with different robotic devices for upper limb rehabilitation: a retrospective study. <i>European journal of physical and rehabilitation medicine</i> , 53(2), 240-248.
		Xu, C., Li, S., Wang, K., Hou, Z., & Yu, N. (2017, July). Quantitative assessment of paretic limb dexterity and interlimb coordination during bilateral arm rehabilitation training. In <i>Rehabilitation Robotics (ICORR), 2017 International Conference on</i> (pp. 634-639). IEEE.

		Dipietro, L., Krebs, H. I., Volpe, B. T., Stein, J., Bever, C., Mernoff, S. T., ... & Hogan, N. (2012). Learning, not adaptation, characterizes stroke motor recovery: evidence from kinematic changes induced by robot-assisted therapy in trained and untrained task in the same workspace. <i>IEEE Transactions on Neural Systems and Rehabilitation Engineering</i> , 20(1), 48-57.
		Shin, J. H., Park, G., & Cho, D. Y. (2017). Cognitive-motor interference on upper extremity motor performance in a robot-assisted planar reaching task among patients with stroke. <i>Archives of physical medicine and rehabilitation</i> , 98(4), 730-737.
Normalized reaching speed (NRS)	Velocity	Mazzoleni, S., Filippi, M., Carrozza, M. C., Posteraro, F., Puzzolante, L., & Falchi, E. (2011, June). Robot-aided therapy on the upper limb of subacute and chronic stroke patients: a biomechanical approach. In <i>Rehabilitation Robotics (ICORR)</i> , 2011 IEEE International Conference on (pp. 1-6). IEEE.
		Mazzoleni, S., Buono, L., Dario, P., & Posteraro, F. (2014, August). Upper limb robot-assisted therapy in subacute and chronic stroke patients: Preliminary results on initial exposure based on kinematic measures. In <i>Biomedical Robotics and Biomechatronics (2014 5th IEEE RAS & EMBS International Conference on (pp. 265-269). IEEE.</i>
Movement arrest period ratio (MAPR)	Velocity	Rohrer, B., Fasoli, S., Krebs, H. I., Hughes, R., Volpe, B., Frontera, W. R., ... & Hogan, N. (2002). Movement smoothness changes during stroke recovery. <i>Journal of Neuroscience</i> , 22(18), 8297-8304.
		Liebermann, D. G., Levin, M. F., McIntyre, J., Weiss, P. L., & Berman, S. (2010, August). Arm path fragmentation and spatiotemporal features of hand reaching in healthy subjects and stroke patients. In <i>Engineering in Medicine and Biology Society (EMBC)</i> , 2010 Annual International Conference of the IEEE (pp. 5242-5245). IEEE.
		Adams, R. J., Lichter, M. D., Krepkovich, E. T., Ellington, A., White, M., & Diamond, P. T. (2015). Assessing upper extremity motor function in practice of virtual activities of daily living. <i>IEEE Transactions on Neural Systems and Rehabilitation Engineering</i> , 23(2), 287-296.
Tent metric	Velocity	Rohrer, B., Fasoli, S., Krebs, H. I., Hughes, R., Volpe, B., Frontera, W. R., ... & Hogan, N. (2002). Movement smoothness changes during stroke recovery. <i>Journal of Neuroscience</i> , 22(18), 8297-8304.
Velocity arc length (VAL)	Velocity	Balasubramanian, S., Melendez-Calderon, A., Roby-Brami, A., & Burdet, E. (2015). On the analysis of movement smoothness. <i>Journal of neuroengineering and rehabilitation</i> , 12(1), 112.
Number of peaks	Acceleration	Levin, Mindy F., et al. "Quality of grasping and the role of haptics in a 3-D immersive virtual reality environment in individuals with stroke." <i>IEEE Transactions on Neural Systems and Rehabilitation Engineering</i> 23.6 (2015): 1047-1055.
		Tropea, P., Cesqui, B., Monaco, V. I. T. O., Aliboni, S. A. R. A., Posteraro, F., & Micera, S. (2013). Effects of the alternate combination of "error-enhancing" and "active assistive" robot-mediated treatments on stroke patients. <i>IEEE journal of translational engineering in health and medicine</i> , 1, 2100109-2100109.
		Kahn, L. E., Zygmant, M. L., Rymer, W. Z., & Reinkensmeyer, D. J. (2001). Effect of robot-assisted and unassisted exercise on functional reaching in chronic hemiparesis. <i>REHABILITATION INST OF CHICAGO IL</i> .
		Rohrer, B., Fasoli, S., Krebs, H. I., Hughes, R., Volpe, B., Frontera, W. R., ... & Hogan, N. (2002). Movement smoothness changes during stroke recovery. <i>Journal of Neuroscience</i> , 22(18), 8297-8304.
		Kamper, D. G., McKenna-Cole, A. N., Kahn, L. E., & Reinkensmeyer, D. J. (2002). Alterations in reaching after stroke and their relation to movement direction and impairment severity. <i>Archives of physical medicine and rehabilitation</i> , 83(5), 702-707.
		Chang, J. J., Tung, W. L., Wu, W. L., & Su, F. C. (2006). Effect of bilateral reaching on affected arm motor control in stroke—with and without loading on unaffected arm. <i>Disability and rehabilitation</i> , 28(24), 1507-1516.
		Casadio, M., Giannoni, P., Morasso, P., & Sanguineti, V. (2009). A proof of concept study for the integration of robot therapy with physiotherapy in the treatment of stroke patients. <i>Clinical rehabilitation</i> , 23(3), 217-228.
		Colombo, R., Sterpi, I., Mazzone, A., Delconte, C., Minuco, G., & Pisano, F. (2010). Measuring changes of movement dynamics during robot-aided neurorehabilitation of stroke patients. <i>IEEE Transactions on Neural Systems and Rehabilitation Engineering</i> , 18(1), 75-85.
		Senesac, C. R., Davis, S., & Richards, L. (2010). Generalization of a modified form of repetitive rhythmic bilateral training in stroke. <i>Human movement science</i> , 29(1), 137-148.
		Chalmers, N., Glasgow, J., & Scott, S. (2011, August). Dynamic Time Warping as a spatial assessment of sensorimotor impairment resulting from stroke. In <i>Engineering in Medicine and Biology Society, EMBC</i> , 2011 Annual International Conference of the IEEE (pp. 8235-8238). IEEE.

		Murphy, M. A., Willén, C., & Sunnerhagen, K. S. (2011). Kinematic variables quantifying upper-extremity performance after stroke during reaching and drinking from a glass. <i>Neurorehabilitation and neural repair</i> , 25(1), 71-80.
		Bustrén, E. L., Sunnerhagen, K. S., & Alt Murphy, M. (2017). Movement kinematics of the ipsilesional upper extremity in persons with moderate or mild stroke. <i>Neurorehabilitation and neural repair</i> , 31(4), 376-386.
		Bermúdez i Badia, S., & Cameirão, M. S. (2012). The neurorehabilitation training toolkit (ntt): A novel worldwide accessible motor training approach for at-home rehabilitation after stroke. <i>Stroke research and treatment</i> , 2012.
		Frisoli, A., Sotgiu, E., Procopio, C., Bergamasco, M., Chisari, C., Lamola, G., & Rossi, B. (2012, June). Training and assessment of upper limb motor function with a robotic exoskeleton after stroke. In <i>Biomedical Robotics and Biomechanics (BioRob)</i> , 2012 4th IEEE RAS & EMBS International Conference on (pp. 1782-1787). IEEE.
		Murphy, M. A., Willén, C., & Sunnerhagen, K. S. (2011). Kinematic Variables Quantifying Upper-Extremity Performance After Stroke During Reaching and Drinking From a Glass. <i>Neurorehabilitation and Neural Repair</i> , 25(1), 71–80. https://doi.org/10.1177/1545968310370748
		Alt Murphy, M., Willén, C., & Sunnerhagen, K. S. (2012). Movement kinematics during a drinking task are associated with the activity capacity level after stroke. <i>Neurorehabilitation and neural repair</i> , 26(9), 1106-1115.
		Frisoli, A., Procopio, C., Chisari, C., Creatini, I., Bonfiglio, L., Bergamasco, M., ... & Carboncini, M. C. (2012). Positive effects of robotic exoskeleton training of upper limb reaching movements after stroke. <i>Journal of neuroengineering and rehabilitation</i> , 9(1), 36.
		Mazzoleni, S., Sale, P., Tiboni, M., Franceschini, M., Posteraro, F., & Carrozza, M. C. (2013). Upper limb robot-assisted therapy in chronic and subacute stroke patients: a kinematic analysis. In <i>Converging Clinical and Engineering Research on Neurorehabilitation</i> (pp. 129-133). Springer, Berlin, Heidelberg.
		Metrot, J., Froger, J., Hauret, I., Mottet, D., van Dokkum, L., & Laffont, I. (2013). Motor recovery of the ipsilesional upper limb in subacute stroke. <i>Archives of physical medicine and rehabilitation</i> , 94(11), 2283-2290.
		Mazzoleni, S., Buono, L., Dario, P., & Posteraro, F. (2014, August). Upper limb robot-assisted therapy in subacute and chronic stroke patients: Preliminary results on initial exposure based on kinematic measures. In <i>Biomedical Robotics and Biomechanics (2014 5th IEEE RAS & EMBS International Conference on</i> (pp. 265-269). IEEE.
		van Dokkum, L., Hauret, I., Mottet, D., Froger, J., Métrot, J., & Laffont, I. (2014). The contribution of kinematics in the assessment of upper limb motor recovery early after stroke. <i>Neurorehabilitation and neural repair</i> , 28(1), 4-12.
		Colombo, R., Cusmano, I., Sterpi, I., Mazzone, A., Delconte, C., & Pisano, F. (2014). Test–retest reliability of robotic assessment measures for the evaluation of upper limb recovery. <i>IEEE Transactions on Neural Systems and Rehabilitation Engineering</i> , 22(5), 1020-1029.
		Mohapatra, S., Harrington, R., Chan, E., Dromerick, A. W., Breceda, E. Y., & Harris-Love, M. (2016). Role of contralesional hemisphere in paretic arm reaching in patients with severe arm paresis due to stroke: a preliminary report. <i>Neuroscience letters</i> , 617, 52-58.
		Park, H., Kim, S., Winstein, C. J., Gordon, J., & Schweighofer, N. (2016). Short-duration and intensive training improves long-term reaching performance in individuals with chronic stroke. <i>Neurorehabilitation and neural repair</i> , 30(6), 551-561.
		Longhi, M., Merlo, A., Prati, P., Giacobbi, M., & Mazzoli, D. (2016). Instrumental indices for upper limb function assessment in stroke patients: a validation study. <i>Journal of neuroengineering and rehabilitation</i> , 13(1), 52.
		Bigoni, M., Baudo, S., Cimolin, V., Cau, N., Galli, M., Pianta, L., ... & Mauro, A. (2016). Does kinematics add meaningful information to clinical assessment in post-stroke upper limb rehabilitation? A case report. <i>Journal of physical therapy science</i> , 28(8), 2408-2413.
		Gulde, P., Hughes, C. M. L., & Hermsdörfer, J. (2017). Effects of stroke on ipsilesional end-effector kinematics in a multi-step activity of daily living. <i>Frontiers in human neuroscience</i> , 11, 42.
		Colombo, R., Pisano, F., Delconte, C., Mazzone, A., Gironi, G., Castagna, M., ... & Pistarini, C. (2017). Comparison of exercise training effect with different robotic devices for upper limb rehabilitation: a retrospective study. <i>European journal of physical and rehabilitation medicine</i> , 53(2), 240-248.
		Hussain, N., Alt Murphy, M., & Sunnerhagen, K. S. (2018). Upper limb kinematics in stroke and healthy controls using target-to-target task in virtual reality. <i>Frontiers in neurology</i> , 9, 300.
		Tomita, Y., Mullick, A. A., & Levin, M. F. (2018). Reduced Kinematic Redundancy and Motor Equivalence During Whole-Body Reaching in

		Individuals With Chronic Stroke. <i>Neurorehabilitation and neural repair</i> , 32(2), 175-186.
		Van Dokkum, L. E., Le Bars, E., Mottet, D., Bonafé, A., Menjot de Champfleur, N., & Laffont, I. (2018). Modified Brain Activations of the Nondamaged Hemisphere During Ipsilesional Upper-Limb Movement in Persons With Initial Severe Motor Deficits Poststroke. <i>Neurorehabilitation and neural repair</i> , 32(1), 34-45.
		Schneider, S., Schönle, P. W., Altenmüller, E., & Münte, T. F. (2007). Using musical instruments to improve motor skill recovery following a stroke. <i>Journal of neurology</i> , 254(10), 1339-1346.
		Amengual, J. L., Rojo, N., de Las Heras, M. V., Marco-Pallarés, J., Grau-Sánchez, J., Schneider, S., ... & Rubio, F. (2013). Sensorimotor plasticity after music-supported therapy in chronic stroke patients revealed by transcranial magnetic stimulation. <i>PLoS One</i> , 8(4), e61883.
		Cha, Y. J., Yoo, E. Y., Jung, M. Y., Park, S. H., Park, J. H., & Lee, J. (2015). Effects of mental practice with action observation training on occupational performance after stroke. <i>Journal of Stroke and Cerebrovascular Diseases</i> , 24(6), 1405-1413.
		Johnson, M. J., Wisneski, K., Hermsen, A., Smith, R. O., Walton, T., Hingtgen, B., ... & Harris, G. F. (2005). Kinematic implications of learned non-use for robotic therapy. In <i>Rehabilitation Robotics, 2005. ICORR 2005. 9th International Conference on</i> (pp. 70-73). IEEE.
		Pila, O., Duret, C., Laborne, F. X., Gracies, J. M., Bayle, N., & Hutin, E. (2017). Pattern of improvement in upper limb pointing task kinematics after a 3-month training program with robotic assistance in stroke. <i>Journal of neuroengineering and rehabilitation</i> , 14(1), 105.
		Wu, C. Y., Trombly, C. A., Lin, K. C., & Tickle-Degnen, L. (2000). A kinematic study of contextual effects on reaching performance in persons with and without stroke: influences of object availability. <i>Archives of physical medicine and rehabilitation</i> , 81(1), 95-101.
		Chang, J.-J & Yusheng, Yang & Wu, W.-L & Guo, Lan-Yuen & Su, F.-C. (2008). The Constructs of Kinematic Measures for Reaching Performance in Stroke Patients. <i>Journal of Medical and Biological Engineering</i> . 28. 65-70.
		Mazzoleni, S., Filippi, M., Carrozza, M. C., Posteraro, F., Puzzolante, L., & Falchi, E. (2011, June). Robot-aided therapy on the upper limb of subacute and chronic stroke patients: a biomechanical approach. In <i>Rehabilitation Robotics (ICORR), 2011 IEEE International Conference on</i> (pp. 1-6). IEEE.
		Massie, C. L., & Malcolm, M. P. (2012). Instructions emphasizing speed improves hemiparetic arm kinematics during reaching in stroke. <i>NeuroRehabilitation</i> , 30(4), 341-350.
		Lee, D. H., Kim, W. J., Oh, J. S., & Chang, M. (2015). Taping of the elbow extensor muscle in chronic stroke patients: comparison between before and after three-dimensional motion analysis. <i>Journal of physical therapy science</i> , 27(7), 2101-2103.
		Casadio, M., Morasso, P., Ide, A. N., Sanguineti, V., & Giannoni, P. (2009). Measuring functional recovery of hemiparetic subjects during gentle robot therapy. <i>Measurement</i> , 42(8), 1176-1187.
		Park, J. H., Yoo, E., Chung, B., & Jung, M. (2009). Effects of vocalization on elbow motion during reaching in persons with hemiparetic stroke. <i>NeuroRehabilitation</i> , 25(2), 123-128.
		Tsao, C. C., & Mirbagheri, M. M. (2007). Upper limb impairments associated with spasticity in neurological disorders. <i>Journal of neuroengineering and rehabilitation</i> , 4(1), 45.
		Murphy, M. A., Murphy, S., Persson, H. C., Bergström, U. B., & Sunnerhagen, K. S. (2018). Kinematic Analysis Using 3D Motion Capture of Drinking Task in People With and Without Upper-extremity Impairments. <i>JoVE (Journal of Visualized Experiments)</i> , (133), e57228.
		Trombly, C. A., & Wu, C. Y. (1999). Effect of rehabilitation tasks on organization of movement after stroke. <i>American Journal of Occupational Therapy</i> , 53(4), 333-344.
		Wu, C. Y., Chou, S. H., Chen, C. L., Kuo, M. Y., Lu, T. W., & Fu, Y. C. (2009). Kinematic analysis of a functional and sequential bimanual task in patients with left hemiparesis: intra-limb and interlimb coordination. <i>Disability and rehabilitation</i> , 31(12), 958-966.
		Ribeiro Coqueiro, P., de Freitas, S. M. S. F., e Silva, A., Mendes, C., & Alouche, S. R. (2014). Effects of direction and index of difficulty on aiming movements after stroke. <i>Behavioural neurology</i> , 2014.
		Balasubramanian, S., Melendez-Calderon, A., & Burdet, E. (2012). A robust and sensitive metric for quantifying movement smoothness. <i>IEEE transactions on biomedical engineering</i> , 59(8), 2126-2136.

		Singh, T., Perry, C. M., Fritz, S. L., Fridriksson, J., & Herter, T. M. (2018). Eye Movements Interfere With Limb Motor Control in Stroke Survivors. <i>Neurorehabilitation and neural repair</i> , 32(8), 724-734.
		Schweighofer, N., Wang, C., Mottet, D., Laffont, I., Bakthi, K., Reinkensmeyer, D. J., & Rémy-Néris, O. (2018). Dissociating motor learning from recovery in exoskeleton training post-stroke. <i>Journal of neuroengineering and rehabilitation</i> , 15(1), 89.
		Richards, L., Senesac, C., McGuirk, T., Woodbury, M., Howland, D., Davis, S., & Patterson, T. (2008). Response to intensive upper extremity therapy by individuals with ataxia from stroke. <i>Topics in stroke rehabilitation</i> , 15(3), 262-271.
		Bensmail, D., Robertson, J. V., Fermanian, C., & Roby-Brami, A. (2010). Botulinum toxin to treat upper-limb spasticity in hemiparetic patients: analysis of function and kinematics of reaching movements. <i>Neurorehabilitation and neural repair</i> , 24(3), 273-281.
		Dipietro, L., Krebs, H. I., Volpe, B. T., Stein, J., Bever, C., Mernoff, S. T., ... & Hogan, N. (2012). Learning, not adaptation, characterizes stroke motor recovery: evidence from kinematic changes induced by robot-assisted therapy in trained and untrained task in the same workspace. <i>IEEE Transactions on Neural Systems and Rehabilitation Engineering</i> , 20(1), 48-57.
		Alt Murphy, M., Willén, C., & Sunnerhagen, K. S. (2013). Responsiveness of upper extremity kinematic measures and clinical improvement during the first three months after stroke. <i>Neurorehabilitation and neural repair</i> , 27(9), 844-853.
		Pila, O., Duret, C., Gracies, J. M., Francisco, G. E., Bayle, N., & Hutin, É. (2018). Evolution of upper limb kinematics four years after subacute robot-assisted rehabilitation in stroke patients. <i>International Journal of Neuroscience</i> , 1-10.
		Wu, C. Y., Yang, C. L., Chuang, L. L., Lin, K. C., Chen, H. C., Chen, M. D., & Huang, W. C. (2012). Effect of therapist-based versus robot-assisted bilateral arm training on motor control, functional performance, and quality of life after chronic stroke: a clinical trial. <i>Physical Therapy</i> , 92(8), 1006-1016.
Number of peaks normalized by movement duration	Acceleration	Kahn, L. E., Zygmant, M. L., Rymer, W. Z., & Reinkensmeyer, D. J. (2006). Robot-assisted reaching exercise promotes arm movement recovery in chronic hemiparetic stroke: a randomized controlled pilot study. <i>Journal of neuroengineering and rehabilitation</i> , 3(1), 12.
Number of peaks normalized by movement distance	Acceleration	Abdul Rahman, H., Khor, K. X., Yeong, C. F., Su, E. L. M., & Narayanan, A. L. T. (2017). The potential of iRest in measuring the hand function performance of stroke patients. <i>Bio-medical materials and engineering</i> , 28(2), 105-116.
		Wu, C. Y., Chuang, L. L., Lin, K. C., Chen, H. C., & Tsay, P. K. (2011). Randomized trial of distributed constraint-induced therapy versus bilateral arm training for the rehabilitation of upper-limb motor control and function after stroke. <i>Neurorehabilitation and neural repair</i> , 25(2), 130-139.
		Wu, C. Y., Yang, C. L., Chuang, L. L., Lin, K. C., Chen, H. C., Chen, M. D., & Huang, W. C. (2012). Effect of therapist-based versus robot-assisted bilateral arm training on motor control, functional performance, and quality of life after chronic stroke: a clinical trial. <i>Physical Therapy</i> , 92(8), 1006-1016.
		Ching-yi Wu, Chieh-ling Yang, Li-ling Chuang, Keh-chung Lin, Hsieh-ching Chen, Ming-de Chen, Wan-chien Huang: Effect of Therapist-Based Versus Robot-Assisted Bilateral Arm Training on Motor Control, Functional Performance, and Quality of Life After Chronic Stroke: A Clinical Trial, <i>Physical Therapy</i> , Volume 92, Issue 8, 1 August 2012
Inverse number of peaks and valleys (IPV)	Acceleration	Pila, O., Duret, C., Laborne, F. X., Gracies, J. M., Bayle, N., & Hutin, E. (2017). Pattern of improvement in upper limb pointing task kinematics after a 3-month training program with robotic assistance in stroke. <i>Journal of neuroengineering and rehabilitation</i> , 14(1), 105.
Acceleration metric (AM)	Acceleration	Mazzoleni, S., Filippi, M., Carrozza, M. C., Posteraro, F., Puzzolante, L., & Falchi, E. (2011, June). Robot-aided therapy on the upper limb of subacute and chronic stroke patients: a biomechanical approach. In <i>Rehabilitation Robotics (ICORR), 2011 IEEE International Conference on</i> (pp. 1-6). IEEE.
		Mazzoleni, S., Sale, P., Tiboni, M., Franceschini, M., Posteraro, F., & Carrozza, M. C. (2013). Upper limb robot-assisted therapy in chronic and subacute stroke patients: a kinematic analysis. In <i>Converging Clinical and Engineering Research on Neurorehabilitation</i> (pp. 129-133). Springer, Berlin, Heidelberg.
Integrated absolute jerk (IAJ)	Jerk	Duff, M., Chen, Y., Attygalle, S., Herman, J., Sundaram, H., Qian, G., ... & Rikakis, T. (2010). An adaptive mixed reality training system for stroke rehabilitation. <i>IEEE Transactions on Neural Systems and Rehabilitation Engineering</i> , 18(5), 531-541.

Mean absolute jerk (MAJ)	Jerk	Bigoni, M., Baudo, S., Cimolin, V., Cau, N., Galli, M., Pianta, L., ... & Mauro, A. (2016). Does kinematics add meaningful information to clinical assessment in post-stroke upper limb rehabilitation? A case report. <i>Journal of physical therapy science</i> , 28(8), 2408-2413.
		Szczęśna, A., & Błaszczyzyn, M. (2017, July). Quantitative analysis of arm movement smoothness. In <i>AIP Conference Proceedings</i> (Vol. 1863, No. 1, p. 400002). AIP Publishing.
Mean absolute jerk normalized by peak speed (MAJPS)	Jerk	Rohrer, B., Fasoli, S., Krebs, H. I., Hughes, R., Volpe, B., Frontera, W. R., ... & Hogan, N. (2002). Movement smoothness changes during stroke recovery. <i>Journal of Neuroscience</i> , 22(18), 8297-8304.
		Tropea, P., Cesqui, B., Monaco, V. I. T. O., Aliboni, S. A. R. A., Posteraro, F., & Micera, S. (2013). Effects of the alternate combination of "error-enhancing" and "active assistive" robot-mediated treatments on stroke patients. <i>IEEE journal of translational engineering in health and medicine</i> , 1, 2100109-2100109.
		Mazzoleni, S., Filippi, M., Carrozza, M. C., Posteraro, F., Puzzolante, L., & Falchi, E. (2011, June). Robot-aided therapy on the upper limb of subacute and chronic stroke patients: a biomechanical approach. In <i>Rehabilitation Robotics (ICORR), 2011 IEEE International Conference on</i> (pp. 1-6). IEEE.
		Mazzoleni, S., Buono, L., Dario, P., & Posteraro, F. (2014, August). Upper limb robot-assisted therapy in subacute and chronic stroke patients: Preliminary results on initial exposure based on kinematic measures. In <i>Biomedical Robotics and Biomechatronics (2014 5th IEEE RAS & EMBS International Conference on</i> (pp. 265-269). IEEE.
		Balasubramanian, S., Melendez-Calderon, A., & Burdet, E. (2012). A robust and sensitive metric for quantifying movement smoothness. <i>IEEE transactions on biomedical engineering</i> , 59(8), 2126-2136.
		Dipietro, L., Krebs, H. I., Volpe, B. T., Stein, J., Bever, C., Mernoff, S. T., ... & Hogan, N. (2012). Learning, not adaptation, characterizes stroke motor recovery: evidence from kinematic changes induced by robot-assisted therapy in trained and untrained task in the same workspace. <i>IEEE Transactions on Neural Systems and Rehabilitation Engineering</i> , 20(1), 48-57.
		Merians, A. S., Fluet, G. G., Qiu, Q., & Adamovich, S. V. (2009, June). Robotically facilitated training of the hemiparetic upper extremity as an integrated functional unit in virtual environments. In <i>Virtual Rehabilitation International Conference, 2009</i> (pp. 185-188). IEEE.
Integrated squared jerk (ISJ)	Jerk	Laczko, J., Scheidt, R. A., Simo, L. S., & Piovesan, D. (2017). Inter-joint coordination deficits revealed in the decomposition of endpoint jerk during goal-directed arm movement after stroke. <i>IEEE Transactions on Neural Systems and Rehabilitation Engineering</i> , 25(7), 798-810.
Root mean squared jerk metric (RMSJ)	Jerk	Song, R., Tong, K. Y., & Hu, X. L. (2008). Evaluation of velocity-dependent performance of the spastic elbow during voluntary movements. <i>Archives of physical medicine and rehabilitation</i> , 89(6), 1140-1145.
Normalized integrated jerk (NIJ)	Jerk	Adamovich, S. V., Fluet, G. G., Merians, A. S., Mathai, A., & Qiu, Q. (2009). Incorporating haptic effects into three-dimensional virtual environments to train the hemiparetic upper extremity. <i>IEEE Transactions on Neural Systems and Rehabilitation Engineering</i> , 17(5), 512-520.
Dimensionless squared jerk (DSJ-t)	Jerk	Chang, J. J., Tung, W. L., Wu, W. L., & Su, F. C. (2006). Effect of bilateral reaching on affected arm motor control in stroke—with and without loading on unaffected arm. <i>Disability and rehabilitation</i> , 28(24), 1507-1516.
		Chang, J.-J & Yusheng, Yang & Wu, W.-L & Guo, Lan-Yuen & Su, F.-C. (2008). The Constructs of Kinematic Measures for Reaching Performance in Stroke Patients. <i>Journal of Medical and Biological Engineering</i> . 28. 65-70.
		Tavernese, E., Paoloni, M., Mangone, M., Mandic, V., Sale, P., Franceschini, M., & Santilli, V. (2013). Segmental muscle vibration improves reaching movement in patients with chronic stroke. A randomized controlled trial. <i>NeuroRehabilitation</i> , 32(3), 591-599.
		Bartolo, M., De Nunzio, A. M., Sebastiano, F., Spicciato, F., Tortola, P., Nilsson, J., & Pierelli, F. (2014). Arm weight support training improves functional motor outcome and movement smoothness after stroke. <i>Functional neurology</i> , 29(1), 15.
		Buma, F. E., van Kordelaar, J., Raemaekers, M., van Wegen, E. E., Ramsey, N. F., & Kwakkel, G. (2016). Brain activation is related to smoothness of upper limb movements after stroke. <i>Experimental brain research</i> , 234(7), 2077-2089.
		Kato, N., Tanaka, T., Sugihara, S., Shimizu, K., & Kudo, N. (2016). A study of the effect of visual depth information on upper limb movement by use of measurement of smoothness. <i>Journal of physical therapy science</i> , 28(4), 1134-1141.

		Scano, A., Chiavenna, A., Malosio, M., Molinari Tosatti, L., & Molteni, F. (2017). Muscle synergies-Based characterization and clustering of Poststroke Patients in reaching Movements. <i>Frontiers in bioengineering and biotechnology</i> , 5, 62.
		Xu, C., Li, S., Wang, K., Hou, Z., & Yu, N. (2017, July). Quantitative assessment of paretic limb dexterity and interlimb coordination during bilateral arm rehabilitation training. In <i>Rehabilitation Robotics (ICORR), 2017 International Conference on</i> (pp. 634-639). IEEE.
		Osumi, M., Sumitani, M., Otake, Y., & Morioka, S. (2018). A “matched” sensory reference can guide goal-directed movements of the affected hand in central post-stroke sensory ataxia. <i>Experimental brain research</i> , 236(5), 1263-1272.
		Mazzoleni, S., Tran, V. D., Dario, P., & Posteraro, F. (2018). Wrist Robot-Assisted Rehabilitation Treatment in Subacute and Chronic Stroke Patients: From Distal-to-Proximal Motor Recovery. <i>IEEE Transactions on Neural Systems and Rehabilitation Engineering</i> , 26(9), 1889-1896.
		Merians, A. S., Fluet, G. G., Qiu, Q., Saleh, S., Lafond, I., Davidow, A., & Adamovich, S. V. (2011). Robotically facilitated virtual rehabilitation of arm transport integrated with finger movement in persons with hemiparesis. <i>Journal of neuroengineering and rehabilitation</i> , 8(1), 27.
		Bensmail, D., Robertson, J. V., Fermanian, C., & Roby-Brami, A. (2010). Botulinum toxin to treat upper-limb spasticity in hemiparetic patients: analysis of function and kinematics of reaching movements. <i>Neurorehabilitation and neural repair</i> , 24(3), 273-281.
Log Dimensionless squared jerk (LDSJ-t)	Jerk	van Kordelaar, J., van Wegen, E., & Kwakkel, G. (2014). Impact of time on quality of motor control of the paretic upper limb after stroke. <i>Archives of physical medicine and rehabilitation</i> , 95(2), 338-344.
Dimensionless squared jerk (DSJ-m)	Jerk	Marini, F., Hughes, C. M., Squeri, V., Doglio, L., Moretti, P., Morasso, P., & Masia, L. (2017). Robotic wrist training after stroke: Adaptive modulation of assistance in pediatric rehabilitation. <i>Robotics and Autonomous Systems</i> , 91, 169-178.
Dimensionless squared jerk (DSJ-b)	Jerk	Balasubramanian, S., Melendez-Calderon, A., & Burdet, E. (2012). A robust and sensitive metric for quantifying movement smoothness. <i>IEEE transactions on biomedical engineering</i> , 59(8), 2126-2136.
Log dimensionless squared jerk (LDSJ-b)	Jerk	Balasubramanian, S., Melendez-Calderon, A., & Burdet, E. (2012). A robust and sensitive metric for quantifying movement smoothness. <i>IEEE transactions on biomedical engineering</i> , 59(8), 2126-2136.
Rotational jerk	Jerk	Repnik, E., Puh, U., Goljar, N., Muni, M., & Mihelj, M. (2018). Using Inertial Measurement Units and Electromyography to Quantify Movement during Action Research Arm Test Execution. <i>Sensors</i> , 18(9), 2767.
Correlation metric (CM)	Velocity	Daly, J. J., Hogan, N., Perepezko, E. M., Krebs, H. I., Rogers, J. M., Goyal, K. S., ... & Ruff, R. L. (2005). Response to upper-limb robotics and functional neuromuscular stimulation following stroke. <i>Journal of rehabilitation research & development</i> , 42(6).
		Celik, O., O'malley, M. K., Boake, C., Levin, H. S., Yozbatiran, N., & Reistetter, T. A. (2010). Normalized movement quality measures for therapeutic robots strongly correlate with clinical motor impairment measures. <i>IEEE transactions on neural systems and rehabilitation engineering: a publication of the IEEE Engineering in Medicine and Biology Society</i> , 18(4), 433.
Spectral metric (SPMR)	Frequency	Strohrmann, C., Labruyère, R., Gerber, C. N., van Hedel, H. J., Arnrich, B., & Tröster, G. (2013). Monitoring motor capacity changes of children during rehabilitation using body-worn sensors. <i>Journal of neuroengineering and rehabilitation</i> , 10(1), 83.
Spectral method (SPM)	Frequency	Balasubramanian, S., Wei, R., Herman, R., & He, J. (2009, April). Robot-measured performance metrics in stroke rehabilitation. In <i>Complex Medical Engineering, 2009. CME. ICME International Conference on</i> (pp. 1-6). IEEE.
Spectral arc length (SPAL)	Frequency	Cusmano, I., Colombo, R., Sterpi, I., Mazzone, A., Delconte, C., & Pisano, F. (2014). Inter-session Reliability of Robot-Measured Parameters for the Evaluation of Upper Limb Recovery. In <i>Replace, Repair, Restore, Relieve—Bridging Clinical and Engineering Solutions in Neurorehabilitation</i> (pp. 313-319). Springer, Cham.
		Balasubramanian, S., Melendez-Calderon, A., & Burdet, E. (2012). A robust and sensitive metric for quantifying movement smoothness. <i>IEEE transactions on biomedical engineering</i> , 59(8), 2126-2136.
		Colombo, R., Cusmano, I., Sterpi, I., Mazzone, A., Delconte, C., & Pisano, F. (2014). Test–retest reliability of robotic assessment measures for the evaluation of upper limb recovery. <i>IEEE Transactions on Neural Systems and Rehabilitation Engineering</i> , 22(5), 1020-1029.
		Hussain, A., Dailey, W., Hughes, C., Budhota, A., Gamage, W. K. C., Vishwanath, D. A., ... & Campolo, D. (2015, August). Quantitative motor assessment of upperlimb after unilateral stroke: a preliminary feasibility study

		with H-Man, a planar robot. In Rehabilitation Robotics (ICORR), 2015 IEEE International Conference on (pp. 654-659). IEEE.
		Hussain, A., Budhota, A., Hughes, C. M. L., Dailey, W. D., Vishwanath, D. A., Kuah, C. W., ... & Burdet, E. (2016). Self-paced reaching after stroke: A quantitative assessment of longitudinal and directional sensitivity using the H-man planar robot for upper limb neurorehabilitation. <i>Frontiers in neuroscience</i> , 10, 477.
		Colombo, R., Pisano, F., Delconte, C., Mazzone, A., Grioni, G., Castagna, M., ... & Pistarini, C. (2017). Comparison of exercise training effect with different robotic devices for upper limb rehabilitation: a retrospective study. <i>European journal of physical and rehabilitation medicine</i> , 53(2), 240-248.
		Repnik, E., Puh, U., Goljar, N., Munih, M., & Mihelj, M. (2018). Using Inertial Measurement Units and Electromyography to Quantify Movement during Action Research Arm Test Execution. <i>Sensors</i> , 18(9), 2767.
		Budhota, A., Hussain, A., Hughes, C., Hansen, C., Kager, S., Vishwanath, D. A., ... & Campolo, D. (2016, June). Role of EMG as a complementary tool for assessment of motor impairment. In <i>Biomedical Robotics and Biomechanics (BioRob)</i> , 2016 6th IEEE International Conference on (pp. 692-697). IEEE.
Spectral arc length (SPARC)	Frequency	Balasubramanian, S., Melendez-Calderon, A., Roby-Brami, A., & Burdet, E. (2015). On the analysis of movement smoothness. <i>Journal of neuroengineering and rehabilitation</i> , 12(1), 112.
Combined smoothness metric (CSM)	Other	Popović, M. D., Kostić, M. D., Rodić, S. Z., & Konstantinović, L. M. (2014). Feedback-mediated upper extremities exercise: increasing patient motivation in poststroke rehabilitation. <i>BioMed research international</i> , 2014.

Appendix D – Validation of the global nonlinear minimization algorithm

How does the algorithm work?

Rohrer and Hogan (2006) developed a scattershot-type global nonlinear minimization algorithm which can extract sub-movements from a tangential velocity profile [1]. This algorithm was used by Liebermann et al. (2010) to assess smoothness in stroke subjects, they however doubt whether such a parameterization of smoothness can be used for the diagnosis or assessment of rehabilitation effectiveness as the algorithm is not unequivocal and differences can be obtained by changing boundary criteria in the algorithm [2].

Since only these two publications about this algorithm are published and exact details are lacking about the validity of this algorithm, there is some extra research done about this algorithm. This algorithm fits the velocity profile by a combination of minimal jerk velocity profiles. This is done by using MATLAB's function *fmincon* and minimizing the error function

$$\epsilon = \frac{\int |F(t) - G(t)|dt}{\int |G(t)|dt},$$

where $G(t)$ is the movement speed profile and $F(t)$ is the fitted speed profile

$$F(t) = \sum_{i=1}^{Ns} v_{mj_i}(t) \text{ where,}$$

$$v_{mj_i}(t) = \begin{cases} 0 & \text{if } t < T_{s_i} \\ 0 & \text{if } t > T_{s_i} + T_i \\ \text{else } \Delta_i \left(\frac{30(t-T_{s_i})^4}{T_i^5} - \frac{60(t-T_{s_i})^3}{T_i^4} + \frac{30(t-T_{s_i})^2}{T_i^3} \right) \end{cases}$$

with Ns the number of sub-movements, v_{mj} the minimal jerk speed profile, Δ the sub-movement distance, T the sub-movement duration, T_s the sub-movement time shift. Subscript i denotes the i th sub-movement. Δ , T_s and T are minimized, while the function was ten times initialized at random points within the solution space, with $Ns = 1$. For Δ the solution space is between 0 and 1 meter, for T between 0.01 and 3 seconds and for T_s between 0 and 3 seconds. If the error was below 0.02, the optimization is finished, else, 1 is added to Ns and the optimization continues. As three parameters are fitted for each sub-movement, the complexity of the optimization increases if more sub-movements were present. A complex optimization is more likely to end in a local minimum while more local minima are present since the solution space is bigger. For this reason, in this appendix a small analysis of the reliability of this algorithm is done.

Is the algorithm reliable?

To analyze the reliability, a velocity profile was created using the minimum jerk model, with sub-movement duration of 1 second, spacing of 0.5 seconds between the sub-movements and a total movement distance of 0.4 meter. The number of sub-movements was changed from 5 to 10. The reliability was calculated as the number of times that the error was <0.02 divided by the number of iterations, multiplied by 100%. As the number of submovements increased, also the number of iterations was increased for a more accurate result.

In table D.1 can be seen that for 5 and 6 sub-movements the reliability is still above 80%. For 7 sub-movements it decreased to 20.8%. If this algorithm is ran to calculate the number of sub-movements for a subject trail, always 10 iterations are done. So with 7 sub-movements, it can be said that there is a chance not to find the correct solution of $(1 - 0.208)^{10} = 9.7\%$. For 8 sub-movements, this chance increased to 36%. Therefore, it was decided to fit profiles up to 7 sub-movements. After that, the algorithm was aborted. In figure A.1a the error after each optimization is shown for the situation with eight sub-movements. It was chosen in the rest of this work to only go to a maximal of 7 submovements. Further remarkable is that for 9 and 10 sub-movements together, a solution with an error <0.02 was only reached once. This can be dedicated to the high degree of complexity of the optimization with respectively 27 and 30 parameters. The result of 250 optimization iterations with 8 sub-movements is shown in figure D.1a

Table D.1: Results of the reliability test of the Number of Sub-movements algorithm. It can be seen that the reliability decreases heavily from 6 sub-movements.

Number of submovements	Iterations	Values <0.02	Min error	Reliability (%)
5	10	8	0,0078	80
6	10	9	0,0086	90
7	250	52	0,0067	20,8
8	250	24	0,015	9,6
9	250	1	0,013	0,4
10	250	0	0,0299	0

Another drawback of this algorithm are the computational costs. The simulation with eight sub-movements and 250 iteration costed 21 minutes. With ten sub-movements it even increased to over 30 minutes. Further, it was seen that it is ineffective to fit velocity profiles with noise. As shown in figure D.1b the algorithm tries to fit the noise by adding small sub-movements (dotted black lines). It is however impossible to reach a low error term in the optimization with only 7 sub-movements. If noise is present, no solution can be found for this algorithm and it is not possible to calculate a value for movement smoothness.

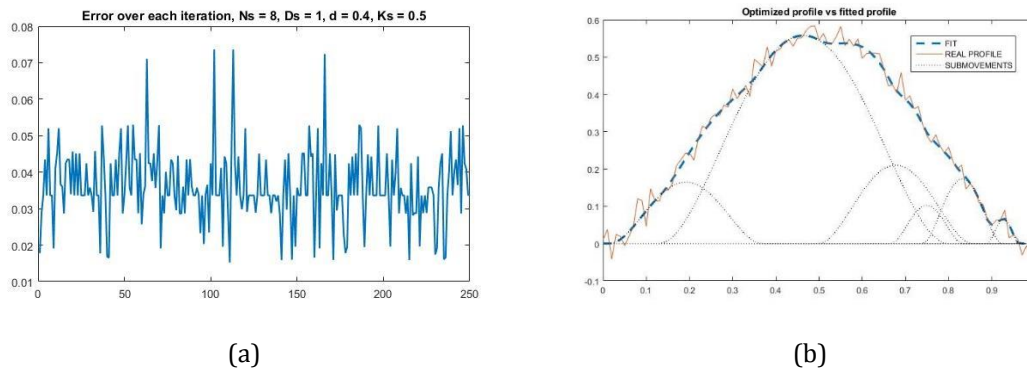


Figure D.1: (a) the error at y-axis after each optimization (x-axis) with eight sub-movements. (b) it is ineffective for this algorithm to fit noisy velocity profiles.

Based on the results presented here, it is decided to perform the optimization to a maximum of 7 sub-movements. If no suitable solution was found with 7 sub-movements, the algorithm was not capable of quantifying smoothness of the movement.

Can the algorithm be enhanced?

There is space for enhancement of this algorithm. An improvement would be to apply more requirements to the solution to decrease the number of possible solutions. The time lag between two consecutive sub-movements in this algorithm can be 0 seconds, where testing this during the optimization would not be relevant as this means that there is no separation between sub-movements and it cannot be detected. This enhancement might reduce the computation time needed.

Although this is a minor improvement, I do not see improvements to significantly reduce the complexity of this optimization and decrease the computational time needed to complete the analyses of movement smoothness.

References

- [1] Brandon Rohrer and Neville Hogan. "Avoiding spurious submovement decompositions II: a scattershot algorithm". In: *Biological cybernetics* 94.5 (2006), pp. 409–414.
- [2] Dario G Liebermann et al. "Arm path fragmentation and spatiotemporal features of hand reaching in healthy subjects and stroke patients". In: *2010 Annual International Conference of the IEEE Engineering in Medicine and Biology*. IEEE. 2010, pp. 5242–5245.

Appendix E - Window comparison for symmetrical sub-movements

To see the effect of different underlying velocity profiles on the calculation of smoothness, this 'mini report' is written. There are 3 sections: (1) Window selection, (2) Simulations with sub-movements and (3) Inspection of velocity profiles.

In (1) Window selection the different windows are introduced and velocity profiles are created using these windows. Further the acceleration and jerk of these windows is plotted. In (2) Simulations, the sub-movement simulation is done with 4 selected windows. In (3) the velocity profiles are shown. After each short section the findings are noted.

Main finding: the monotonicity of the sub-movements simulation is dependent on the chosen underlying sub-movement. If a wide sub-movement is chosen, such as the minimum jerk model, the results of the simulation would show that there is a non-monotonic increase. While a narrow underlying sub-movement in the same simulation would show a monotonic increase.

In this 'mini report' the same abbreviations are used as in the paper. Monotonic is defined as 'no zero crossing in the derivative of the sub-movement simulation'.

1. Window selection

All MATLAB default windows with a 0, or nearly 0 (<0.001) derivative at the first sample and have a bell shape (triangles, rectangles and sync shapes are excluded):

- Blackman
- Blackmanharris
- Bohmanwin
- Hamming
- Hann
- Nuttallwin
- Parzenwin
- Taylorwin

Additionally, a window is created using the cosines function, multiplied by -1, and 1 was added to create the bell shape. This is cosine is added after short discussion with people in the group Biomechanical Engineering group. They use this type of velocity profiles as reference profiles.

These windows and the minimal jerk trajectory are investigated to use as sub-movement. The windows are normalized in a way that the duration is 1 second (201 samples at 200Hz), have a minimum value of 0 m/s and the and the integral is 0.3m. In Figure E.1 the windows are shown. In Figure E.2 and E.3 respectively the acceleration and jerk of these windows are plotted.

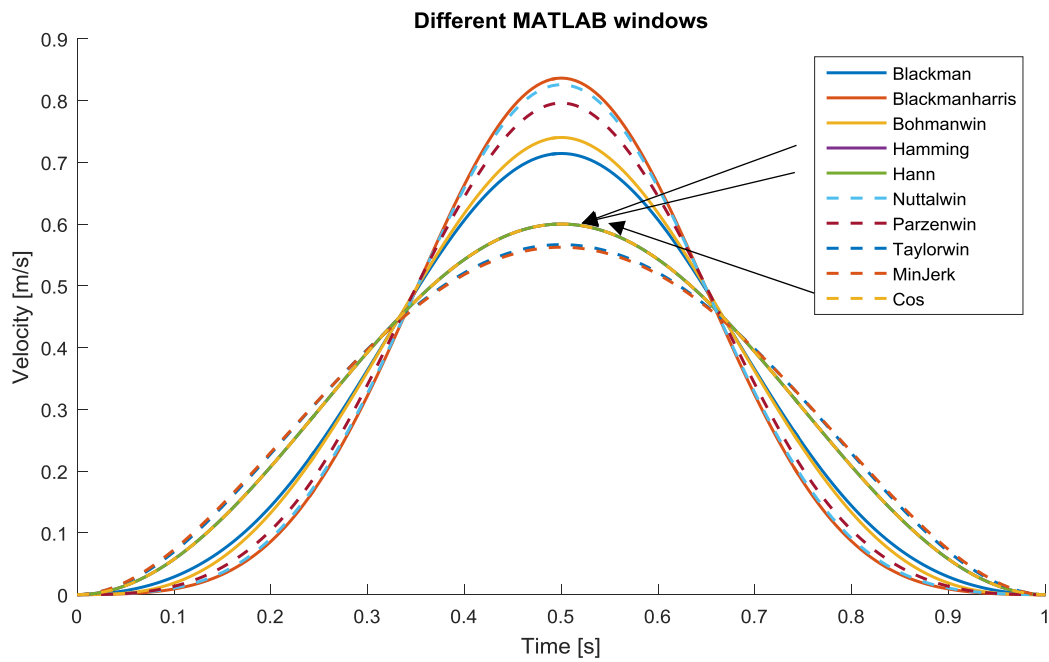


Figure E.1 - The different MATLAB windows

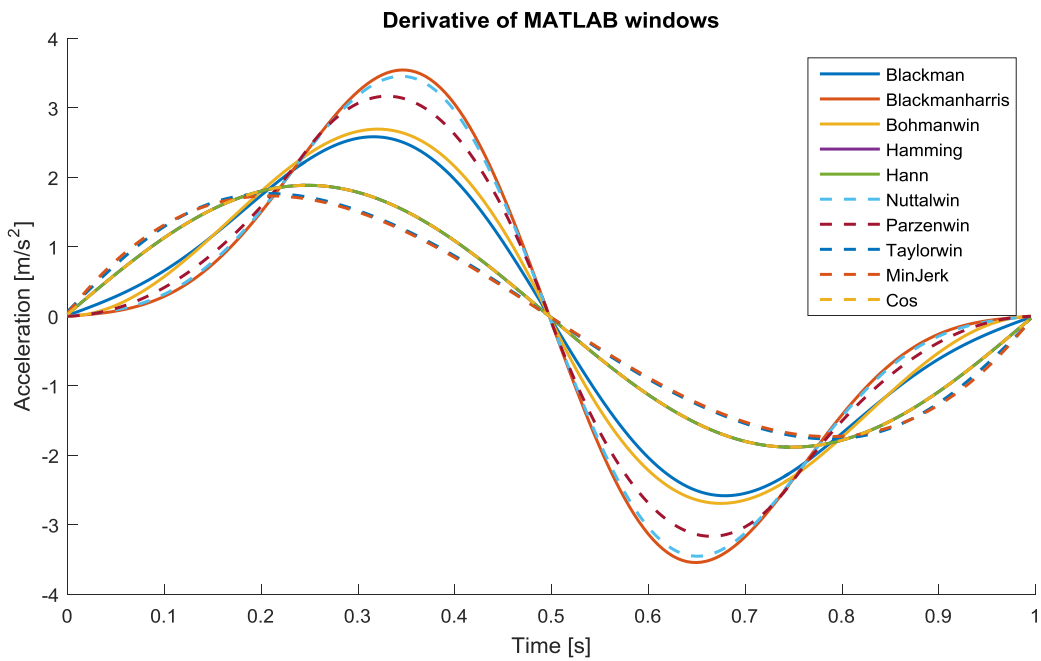


Figure E.2 - Acceleration of the MATLAB windows

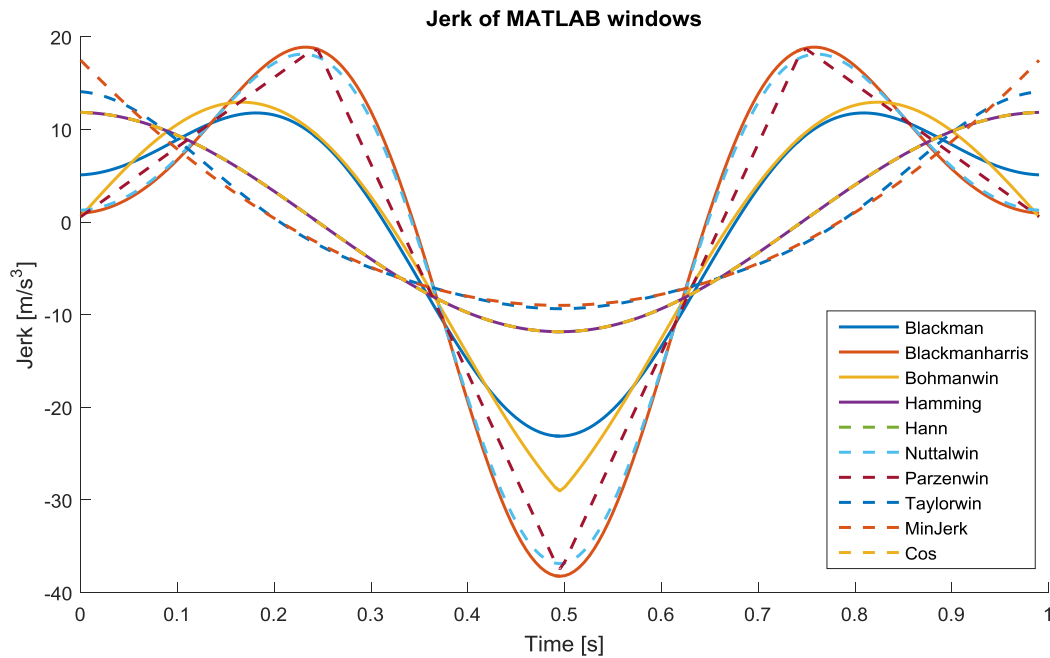


Figure E.3 - Jerk of the MATLAB windows

Findings:

- Hann, Hamming and Cos are completely overlapping (not visible in the Figure E, although arrows are drawn). Hann and Hamming are the same due to the normalization.
- Taylorwin and MinJerk are nearly equal. Main difference is seen in the jerk values at 0 and 1s.
- Taylorwin, MinJerk, Hann and Hamming have a higher derivative during the first 0.2 seconds and a lower maximum derivative
- MinJerk has both the minimal integrated squared jerk as integrated absolute jerk.

2. Simulations with sub-movements

Based on these findings, the following windows are chosen to do the sub-movements simulation: MinJerk, Hann, Blackman and Blackmanharris. This set includes the windows with the minimum (MinJerk) and maximum (Blackmanharris) peak acceleration. In other words, the more wider and more narrow velocity profiles.

Simulations are done with 1, 2, 3 and 4 sub-movements. This result are shown in respectively Figure E. 4, 5, 6 and 7. In the top left, also integrated squared jerk (ISJ) is added. This might help to explain the dips in the dimensionless jerk metrics. On the horizontal axis the lag is shown, lag is the time between the starting points of two consecutive sub-movements. 61 different values for lag have been used between 0 and 1.2. In Figure E.8 the derivative of Figure E.7 is shown. Monotonicity can be defined as no zero crossings in the derivative.

Findings:

- For 1 sub-movement (N=1) it is remarkable that there is a lot of difference between the jerk value of MinJerk profile and Blackmanharris (63 vs 310 m²/s⁵). Obviously, this is also seen for the other jerk metrics. Effect on SM, MAPR, SPARC and CM is relatively small. No difference seen is here for Peaks and IPV.
- For 2 sub-movements (N=2) it is seen that the ‘N+1 peaks phenomena’ occurs with the MinJerk sub-movements. The combination of 2 sub-movements induces a third peak at 0.5s. This is at the moment that the overlap is exactly half of the sub-movement. This was also reported in literature (Rohrer et al., 2002). For the Hann sub-movement, the velocity profile is completely horizontal. The peaks detecting algorithm detect this period as all peaks, thus a high value is obtained here.
- In DSJt and DSJb clearly a dip is seen with the MinJerk sub-movement at 1 second. This is also seen in ISJ for this sub-movement.
- In LDSJt and LDSJb all sub-movements except MinJerk have a dip around 0.3 seconds.
- For 3 sub-movements an extra peak in the DSJ metrics can be seen compared to the simulation with 2 sub-movements.
- There is not that much change when the simulation of 3 and 4 sub-movements are compared. For the N=4 situation, also the derivative is plotted in Figure E.8.
- In DSJt and DSJb a zero crossing in the derivative is seen for the MinJerk sub-movement at 0.5 and 1 seconds. Hann window has also a zero crossing at 1 second in DSJb.

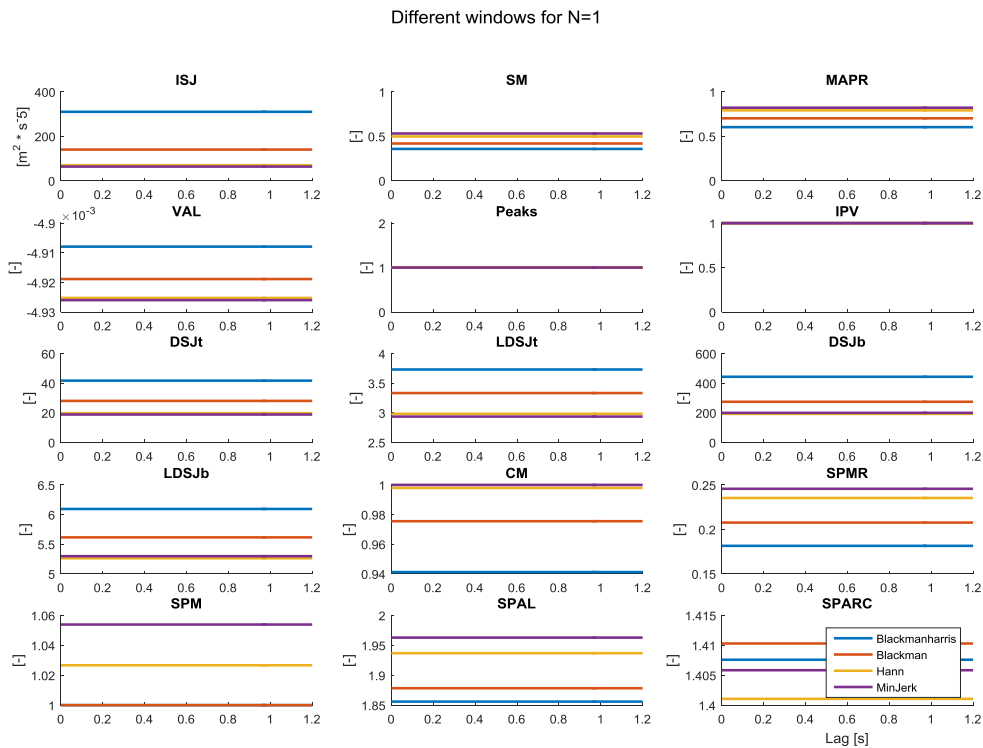


Figure E.4 - 1 sub-movement simulation. With integrated squared jerk (ISJ), speed metric (SM), movement arrest period ratio (MAPR), velocity arc length (VAL), number of peaks, inverse of number of peaks and valleys (IPV), Dimensionless squared jerk (DSJt and DSJb), log of DSJt and DSJb (LDSJb and LDSJt), correlation metric (CM), spectral metric (SPMR), spectral method (SPM), spectral arc length (SPAL) and spectral arc length with threshold (SPARC)

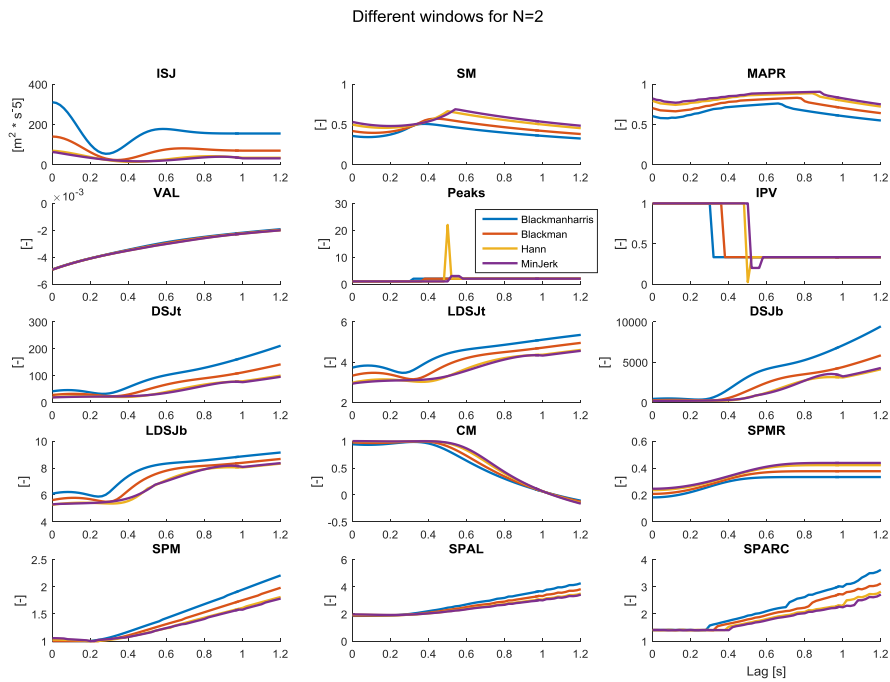


Figure E.5 - 2 sub-movements simulation. With integrated squared jerk (ISJ), speed metric (SM), movement arrest period ratio (MAPR), velocity arc length (VAL), number of peaks, inverse of number of peaks and valleys (IPV), Dimensionless squared jerk (DSJt and DSJb), log of DSJt and DSJb (LDSJb and LDSJt), correlation metric (CM), spectral metric (SPMR), spectral method (SPM), spectral arc length (SPAL) and spectral arc length with threshold (SPARC)

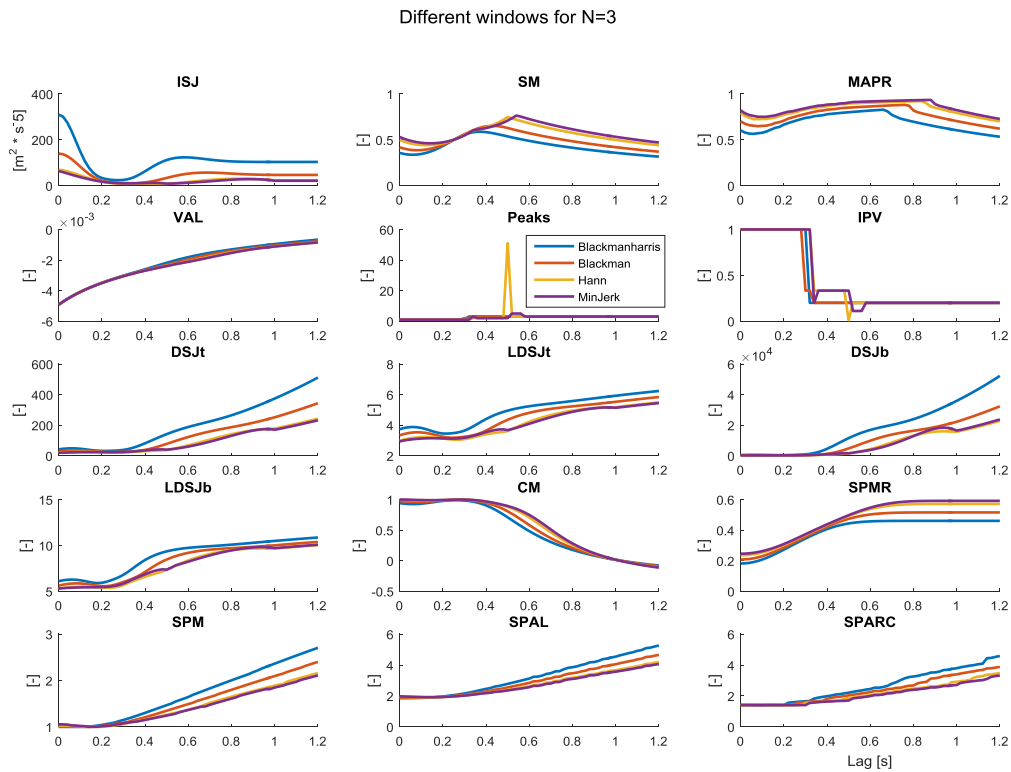


Figure E.6 - 3 sub-movements simulation. With integrated squared jerk (ISJ), speed metric (SM), movement arrest period ratio (MAPR), velocity arc length (VAL), number of peaks, inverse of number of peaks and valleys (IPV), Dimensionless squared jerk (DSJt and DSJb), log of DSJt and DSJb (LDSJb and LDSJt), correlation metric (CM), spectral metric (SPMR), spectral method (SPM), spectral arc length (SPAL) and spectral arc length with threshold (SPARC)

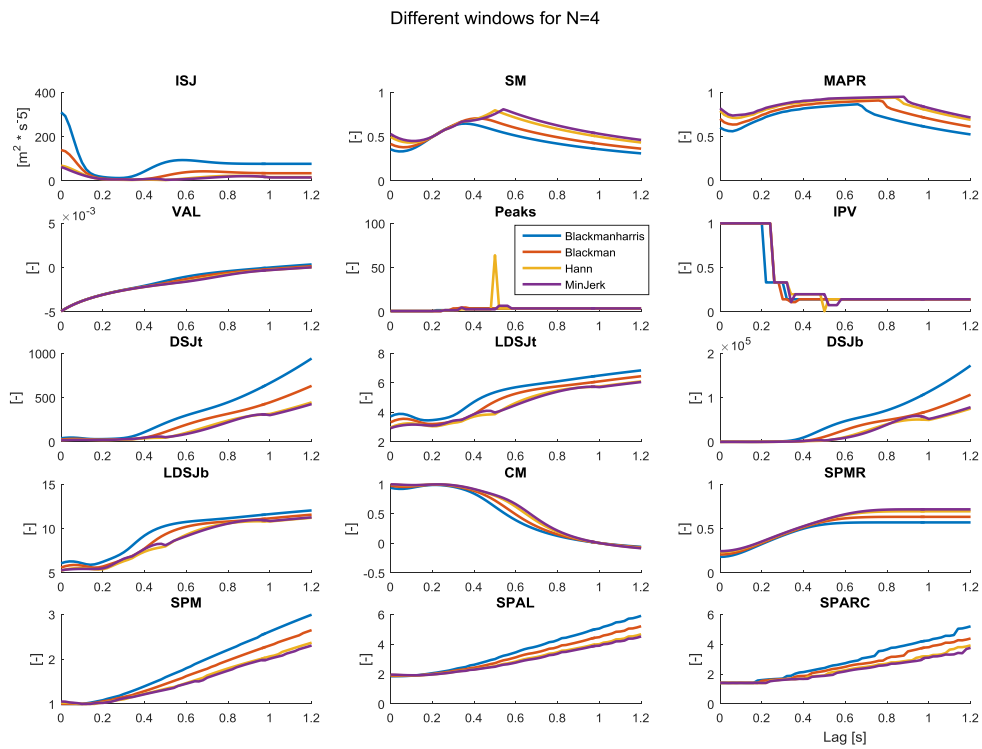


Figure E.7 - 4 sub-movements simulation. With integrated squared jerk (ISJ), speed metric (SM), movement arrest period ratio (MAPR), velocity arc length (VAL), number of peaks, inverse of number of peaks and valleys (IPV), Dimensionless squared jerk (DSJt and DSJb), log of DSJt and DSJb (LDSJb and LDSJt), correlation metric (CM), spectral metric (SPMR), spectral method (SPM), spectral arc length (SPAL) and spectral arc length with threshold (SPARC)

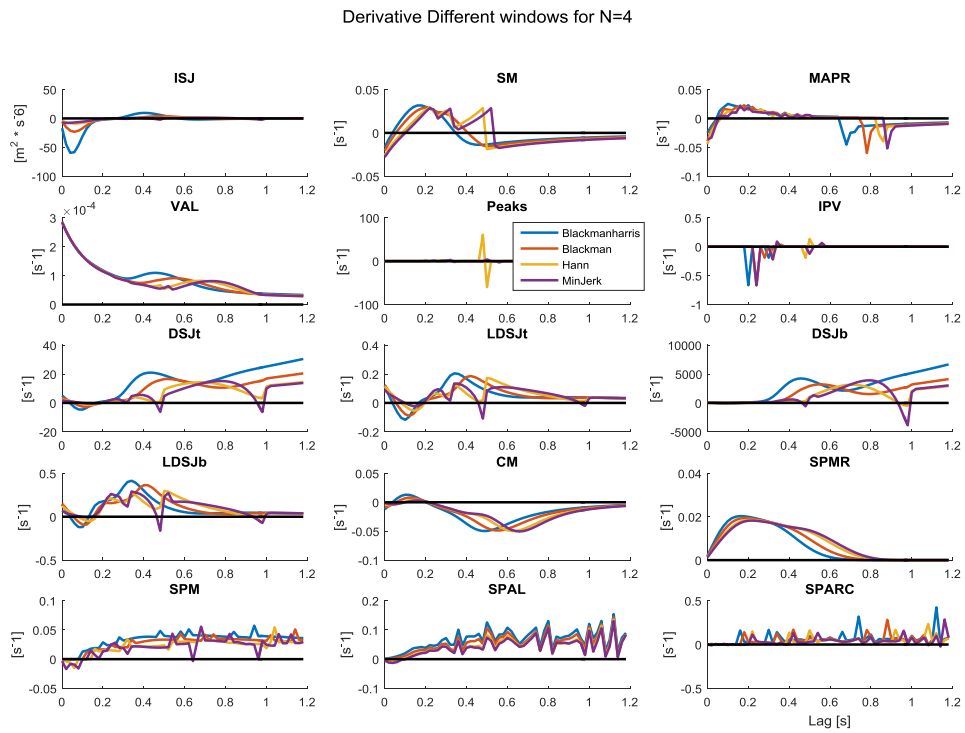


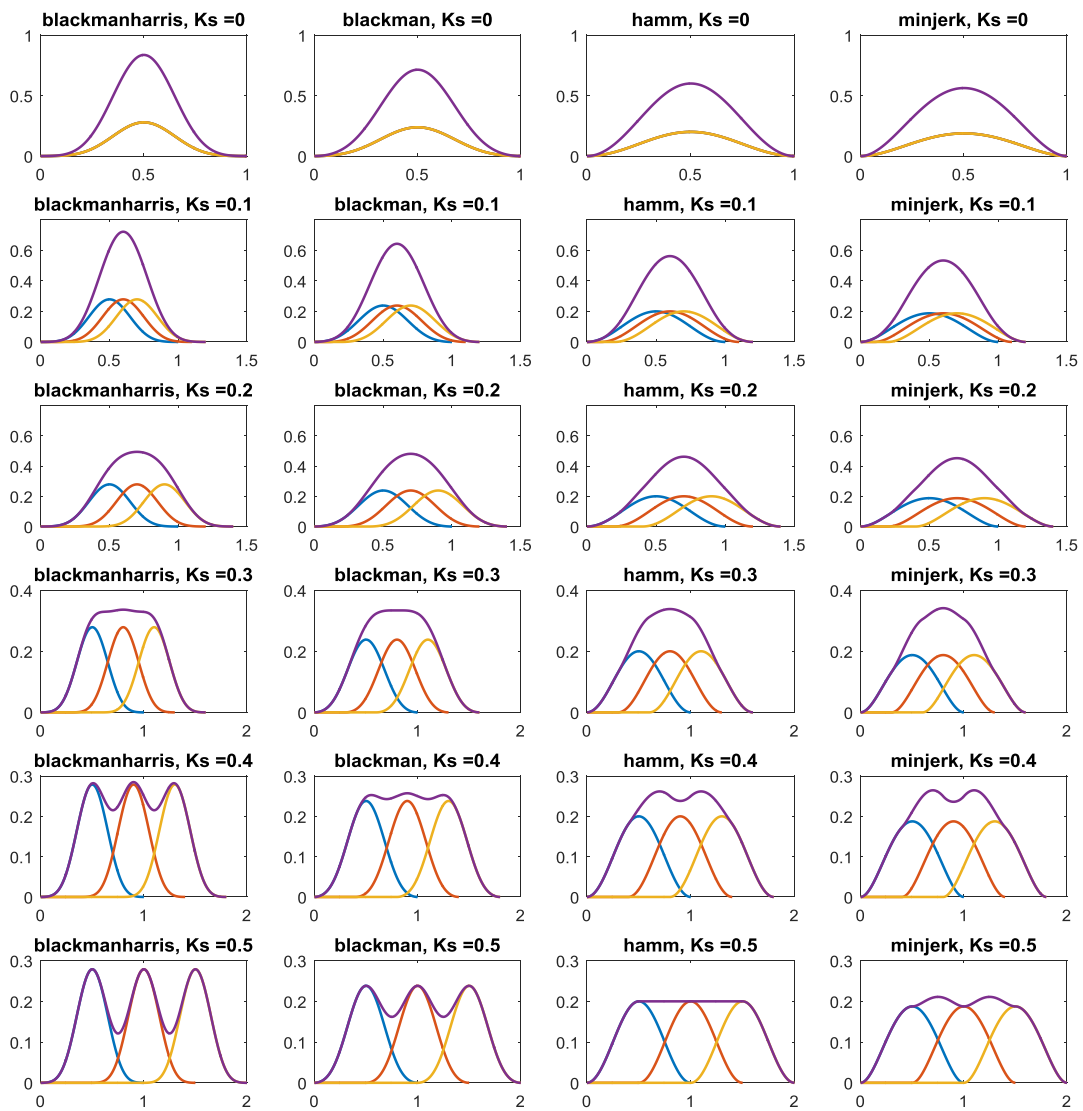
Figure E.8 - Derivative of simulation result with 4 sub-movements. With integrated squared jerk (ISJ), speed metric (SM), movement arrest period ratio (MAPR), velocity arc length (VAL), number of peaks, inverse of number of peaks and valleys (IPV), Dimensionless squared jerk (DSJt and DSJb), log of DSJt and DSJb (LDSJb and LDSJt), correlation metric (CM), spectral metric (SPMR), spectral method (SPM), spectral arc length (SPAL) and spectral arc length with threshold (SPARC)

Judging the monotonicity from the above simulations, it can be said that DSJt, LDSJt, DSJb and LDSJb are non-monotonic for some underlying sub-movements, but not for all.

3. Inspection of velocity profiles

Lastly, for $N=3$, the sub-movements are plotted as the sum (purple) and the single sub-movements (blue, red and yellow) to get a better image how the underlying sub-movements combine. This is shown in Figure E.9. In each column, another velocity profile is shown. In each row, another lag value is used. Ranging from 0 to 1.1 with steps of 0.1 seconds. Most difference between the four windows is visible around lag = 0.5s.

Note that there is a change in the length of the movement. As the spacing increases, the total length of the movement increases. A formula for the total length of the movement would be $D_s + (N_s - 1) * \text{lag}$. Where D_s is the duration of a sub-movement, N_s is the number of sub-movements and lag the time between the starting point of two consecutive sub-movements.



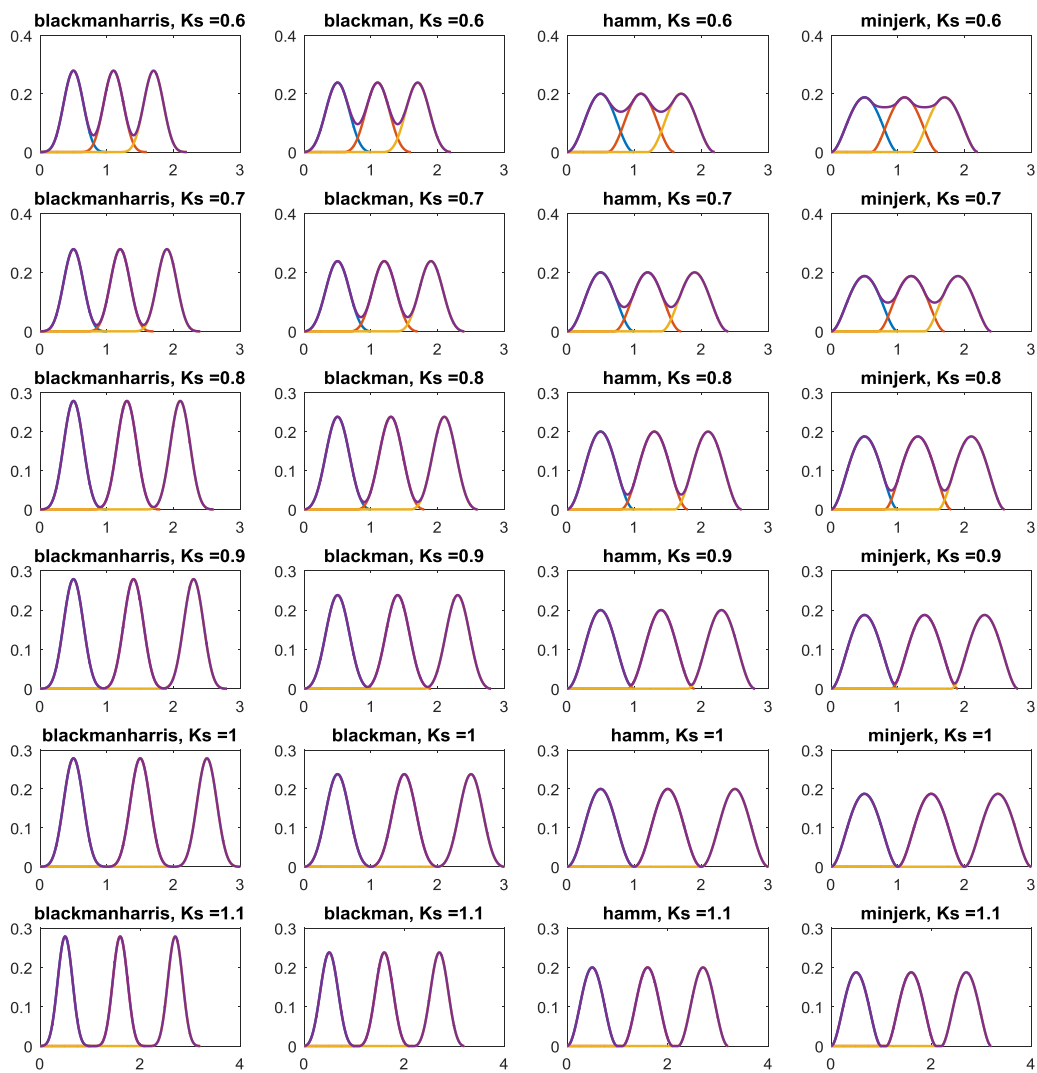


Figure E.9 – The different velocity profiles created with the different windows in each column and different lag values in each row. With time on the x-axis and velocity on the y-axis.

References

Rohrer, B., Fasoli, S., Krebs, H. I., Hughes, R., Volpe, B., Frontera, W. R., ... & Hogan, N. (2002). Movement smoothness changes during stroke recovery. *Journal of Neuroscience*, 22(18), 8297-8304.

Appendix F - Analyses of velocity profiles of the reach-to-grasp movement in healthy and stroke subjects

To inspect what would be a suitable choice for sub-movement in the simulation with sub-movements, it is decided to do a small study to the velocity profiles of healthy and stroke subjects. In this report, first different theoretical velocity profiles that can be used as sub-movement are explained. Then, these theoretical velocity profiles are fitted to real velocity profiles. It is studied which theoretical profile describes the executed velocity profile the best for healthy and for stroke subjects. Lastly, it is tested if the dimensionless jerk metrics for movement smoothness have a monotonic or non-monotonic response during the sub-movement simulation with the found theoretical velocity profiles.

1. Velocity profiles as sub-movement

Flash, T., & Hogan, N. (1985) showed that there is a good match between the minimal jerk model and healthy subjects in 2-dimensional unconstrained point-to-point reaching movements. However, in Figure F.1 the velocity profiles of a healthy subject are shown in a 3-dimensional reach-to-grasp movement. It can be clearly seen that this is a more skewed profile and the peak speed is not at half of the reaching time as it would be with symmetric velocity profiles.

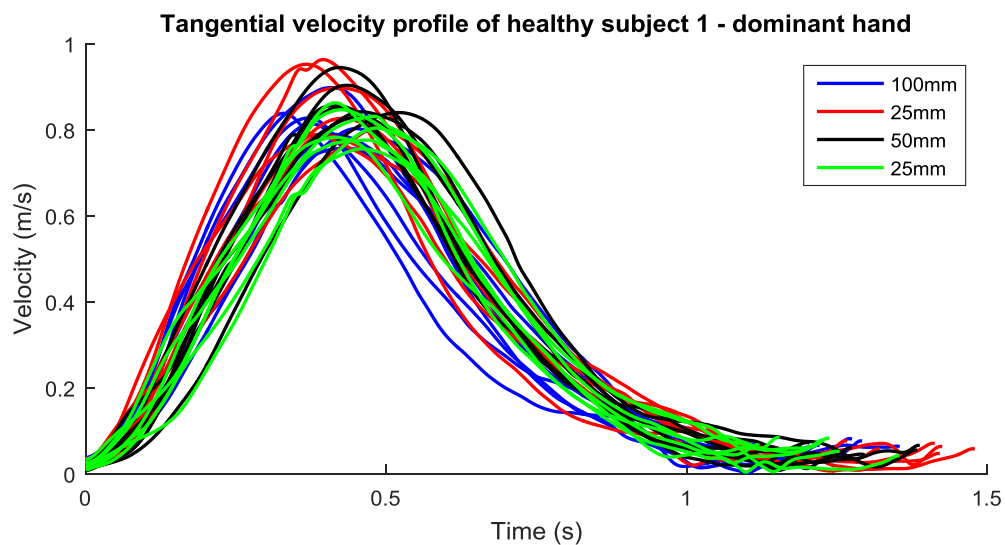


Figure F.10- Trails of the dominant hand of subject 1. The different colors represents the different block size of the grasp movement.

For subject 1, the peak is on average at 32.7% off the reaching movement. As the velocity profiles in Figure E.1 should be fitted, it would be more suitable to use a asymmetric curve. Currently only symmetric MATLAB windows and the minimum jerk trajectory are used as velocity profiles and these velocity profiles have the peak at 50% of the movement time.

To fit this asymmetric curve, new theoretical velocity profiles should be introduced.

Introducing asymmetric velocity profiles

There are multiple options to create a asymmetric profiles:

1. Using interpolation over specific values
2. Using a polynomial
3. Using the probability density function (PDF) of different MATLAB distributions

These three methods are tested and the result is shortly discussed.

1. Using interpolation over specific values

The idea here is to use knowledge about specific points to fit a curve trough these specific points. As both the end and the beginning of the movement have 0 velocity, these points can be used. It was also found that the peak was present at 32.7% of the total reaching time. By interpolating over these values a profile can be obtained.

A normalized profile was created with a duration of 1s and peak velocity of 1 m/s. The following coordinates were used over which the interpolation took place (0; 0), (0.327; 1) and (1; 0). Using MATLAB function `interp1` an interpolation was done. Although this interpolation went through the assigned coordinates, the derivatives were not correct. The derivatives are known to be 0 at the start, peak and end. All MATLABs interpolation methods were used but none gave the wished profile with the right derivatives.

2. Using a polynomial

As three coordinates are known, it is possible to fit these points using a polynomial. With this procedure, also the derivatives can be taken in to account. The following 6 conditions are created for the coordinates and derivatives and would also be seen for the normalized velocity profiles of subject 1.

Coordinates (x; y)	Derivatives (x; dy/dx)
(1) (0; 0)	(2) (0; 0)
(3) (0.327; 1)	(4) (0.327; 0)
(5) (1; 0)	(6) (1; 0)

As there are six conditions, a polynomial with 6 variables is expected to meet these conditions. This polynomial would be in the form of

$$y(x) = a + bx + cx^2 + dx^3 + ex^4 + fx^5.$$

Using the conditions stated above, the following equations can be made up:

- (1) $a = 0$
- (2) $b = 0$
- (3) $a + b0.327 + c0.327^2 + d0.327^3 + e0.327^4 + f0.327^5 = 1$
- (4) $b + 2c0.327 + 3d0.327^2 + 4e0.327^3 + 5f0.327^4 = 0$
- (5) $a + b + c + d + e + f = 0$
- (6) $b + 2c + 3d + 4e + 5f = 0$

By solving the set of equations, a solution is found. Although this velocity profile satisfies all the requirements, it does not have the wished shape of Figure E.1. This is shown in the dark blue curve in Figure E.2 (g=0). To create more freedom in this polynomial, an extra variable g is added.

The new polynomial becomes

$$y(x) = a + bx + cx^2 + dx^3 + ex^4 + fx^5 + gx^6.$$

If now the g variable is added to equations (1) – (6) and these are solved, multiple solutions can be found since there is redundancy in this set of solutions (7 variables, 6 equations). The effect of the value of parameter g is shown in Figure F.2.

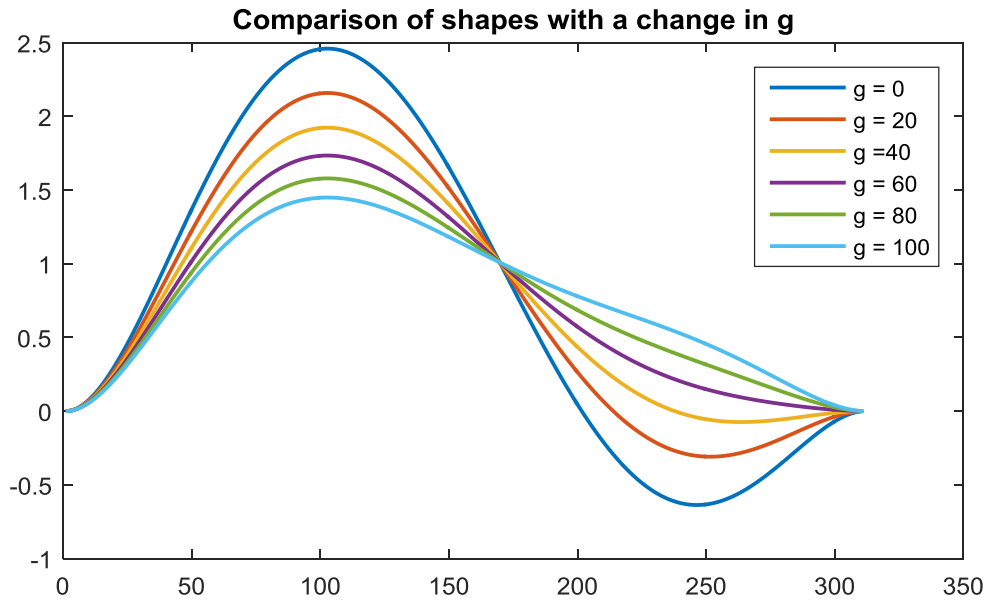


Figure F.2 - Effect of the parameter G on the shape of the velocity profile of the polynomial.

To optimize the value for parameter g , the error is calculated and optimized

$$error = \frac{\int |v - v_{fit}| dt}{\int v dt},$$

with v the mean velocity profile of subject 1 and v_{fit} the fitted velocity profile which is dependent on parameter g and the distance and duration of the reaching movement v . The mean velocity profile of subject 1 is derived by normalizing all trails to movement distance and duration. The the mean of all normalized trails was taken to create the mean velocity profile for subject 1. This error term is minimized using the MATLAB function *fmincon*. A g value of 54 was found to be the optimal value. This fit will be referred to as 'Polynomial 1'. This fit is shown in figure E.4.

To make the polynomial general to all subjects, all trails of all healthy subjects are normalized, as was done for subject 1, and the mean is taken. Before taking the mean it was seen that there were clearly 3 outlying velocity profiles. These are removed before taking the mean of the velocity profile. This mean velocity profile has however not a zero velocity and zero acceleration at the end and beginning of the movement.

Using the mean velocity profile, the previous described error function was minimized by changing the g parameter and also the location of the peak value, using *fmincon*. This resulted in a value of 81.5 for the g parameter and 0.3157 for the peak location. The error between the new found profile and the normalized mean velocity profile was 0.04. The main difference between these profiles is the value for g , which changes from 54 to 81.5.

The effect is that the slope after the peak is less steep, as seen in Figure E.2. To this polynomial will be referred as 'Polynomial 2'.

It was found that the difference between the two polynomial profiles is not that big. Over all trails, Polynomial 1, had an average error of 0.2369 while the general Polynomial had a slightly lower average error of 0.2169. In figure E.3 the two polynomials are plotted together with the generalized velocity profile.

3. Using PDF of MATLAB distributions

The probability density functions of different distributions can have all kind of shapes, also in the shape of the velocity profile as shown in Figure E.1. There are a lot of possible distributions that can fit the velocity profile of healthy subjects. The beta distribution is a bounded distribution between 0 and 1. The shape can be altered using two shape variables. Further, this distribution is supported by a MATLAB function and is therefore chosen to fit to the healthy velocity profile.

In the same fashion as Polynomial 2 is fitted, the beta distribution is fitted to the general velocity profile. This resulted in parameter α to be 0.27289 and β to be 4.4190. The error with the general velocity profile was 0.0859. The mean error with all trails 0.2294, which is comparable with the results of the polynomials. The beta distribution is also shown in figure F.3.

The Weibull distribution was used to replicate the velocity profile as well. The issue encountered here is that this optimization resulted in a shape that was non zero at the begin and end of the movement. That would be unsuitable for the simulations of smoothness metrics and it was decided to only use the beta distribution.

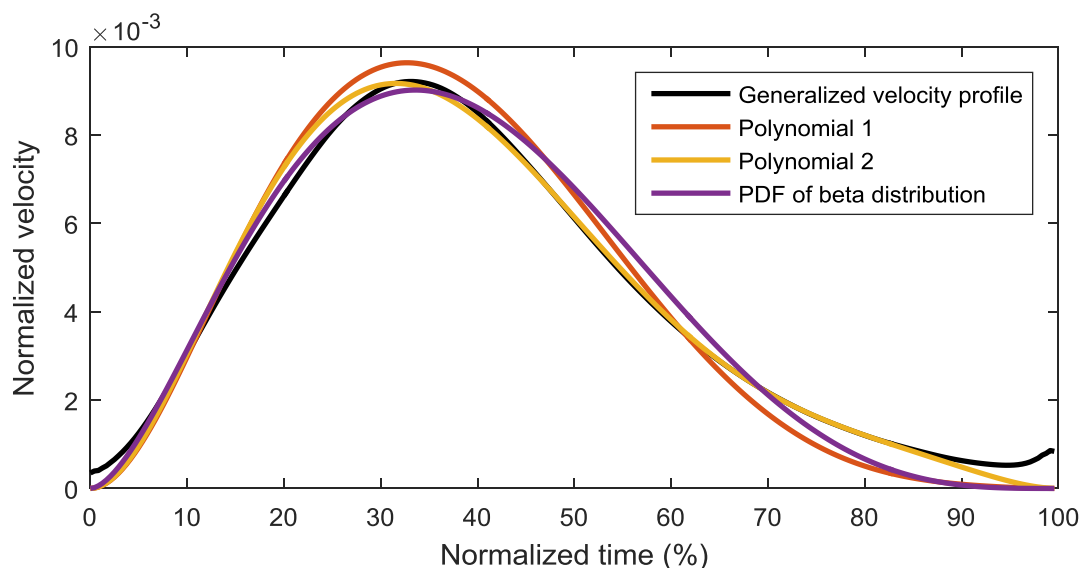


Figure F.3 – Comparison of the generalized velocity profile and the different methods to create a similar velocity profile.

2. Matching the different velocity profiles to the subjects

To compare the windows to the velocity profile of healthy subjects, it is chosen to use the integrated absolute error, divided by the total integral of the velocity profile, the same as done to optimize the parameters in the polynomial. Mathematically it is described as:

$$error = \frac{\int |v - v_{fit}| dt}{\int v dt}$$

With v the subjects velocity profile, v_{fit} the fitted velocity profile. The integral over the whole reaching movement is taken. Visually, this error can be seen as the surface between the fitted velocity profile and executed velocity profile.

The following profiles are used to match the executed velocity profile:

- Polynomial as explained above
- Minimal Jerk
- Gaussian
- Blackman
- Blackmanharris
- Hamming (or cosine)

They are shown Figure F.4 with the same duration and total reaching distance.

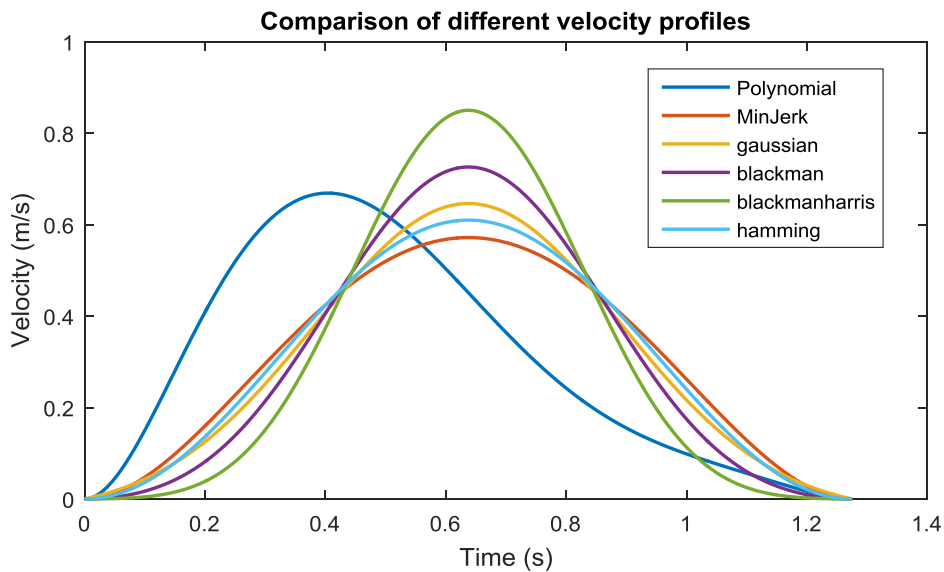


Figure F.4 - The different theoretical velocity profiles. Here polynomial 2 is shown in comparison with the symmetrical windows. The profiles are normalized such that the movement duration and distance is the same.

Healthy Subjects

The data of 12 healthy subjects is available, also present are the labels for the start and end point of the reach-to-grasp movement. In healthy subjects different aspects are studied. The main objective is to see which of the theoretical velocity profiles describes the executed velocity profiles the best for reach-to-grasp movements. Further, it is investigated if there is difference between the dominant and non-dominant hand, difference in the block size to which is grasped and lastly the variability between subjects studied.

For all healthy subjects for both dominant and non-dominant arm the best fit is determined and counted. The results are shown in table F.1. Clearly the polynomial is in most cases the best fit for bot dominant and non-dominant arm.

Table F.1 – Counts for best fit for the velocity profiles for healthy subjects.

Profile name	Polynomial	Minimal Jerk	Gaussian	Hamming	Blackmanharris	Blackman
Dominant hand	298	22	12	1	0	1
Non-dominant hand	293	24	10	7	0	0

In Figure F.5a, the dominant and non-dominant trails for all healthy subjects are shown with on the x-axis the movement duration and y-axis the error with the best fitted profile. No big differences are seen here. In Figure F.5b the different healthy subjects are plotted. It is seen that the trails of a subjects are consistent in movement duration. In Figure F.5c it is seen that it looks that the trails with 100mm and 25mm block sizes have both longer movement duration and a worse fit. In Figure F.6d it is seen that if an alternative for the polynomial fit is better, the error is in the same range as the error would be with the polynomial fit.

In Figure F.6 there is one clear outlier at movement duration of 2.2seconds. This velocity profile is inspected and it is found that at the end of this profile, the tangential velocity is for a second around 0.02m/s. This is also shown in Figure F.6. For the trails with a duration till 1 second, there is not a relation visible between movement duration and fit. For a duration of 1.4 seconds and longer it is clearly seen that a longer duration results in a worse fit. To investigate this, the velocity profile with a longer duration and high error are plotted in Figure F.6. It is seen that they have a relatively long period of low velocity near the end of the movement.

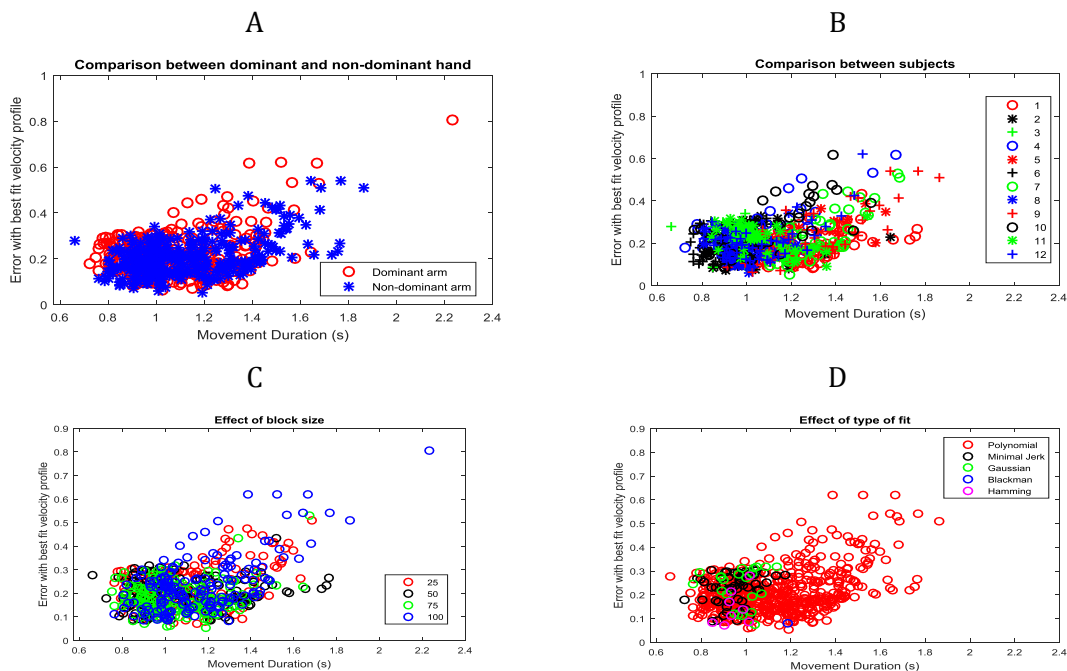


Figure F.5 (a) Effect of dominant hand and non-dominant hand (b) Intersubject differences, (c) the effect of the block size of the grasped block and (d) the effect of the type of fit on the error.

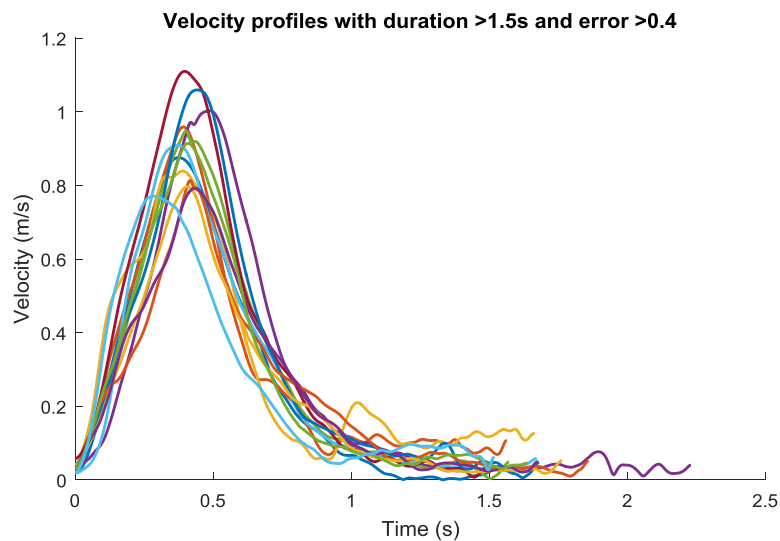


Figure F.6 – The velocity profiles with a longer duration and higher error are plotted

Stroke Subjects

For the 40 stroke subjects the velocity profiles of the trails 26 weeks after stroke are fitted with the theoretical velocity profiles, the same way as with healthy subjects. In the table F.2 the results of this are shown. Again it is seen that the polynomial fit represent the executed velocity profiles the best.

Table F.2 – Counts for best fit for the velocity profiles for stroke subjects.

Profile name	Polynomial	Minimal Jerk	Gaussian	Hamming	Blackmanharris	Blackman
Count	883	164	21	8	0	2

In Figure F.7a the movement duration is plotted with on the y-axis the error with the best fitted velocity profile. The values obtained are comparable with the healthy subjects for movements of a duration till 1.5 seconds. For the stroke group it is seen that there are more trails with a longer movement durations compared to healthy subjects. From the trails with a duration long than 1.5 seconds, it can be seen that longer movement durations are accompanied by a worse fit of the velocity profile.

In Figure F.7b it is seen that the higher FMA-UE scores (>60) are concentrated at a duration <1.5 seconds and an error <0.35. These values are comparable to healthy subjects as seen in Figure F.7.

In Figure F.8 the velocity profiles with a duration longer than 2 seconds and error greater than 0.7 are plotted. It is also here seen that at the end, the velocity is close to zero for a few seconds.

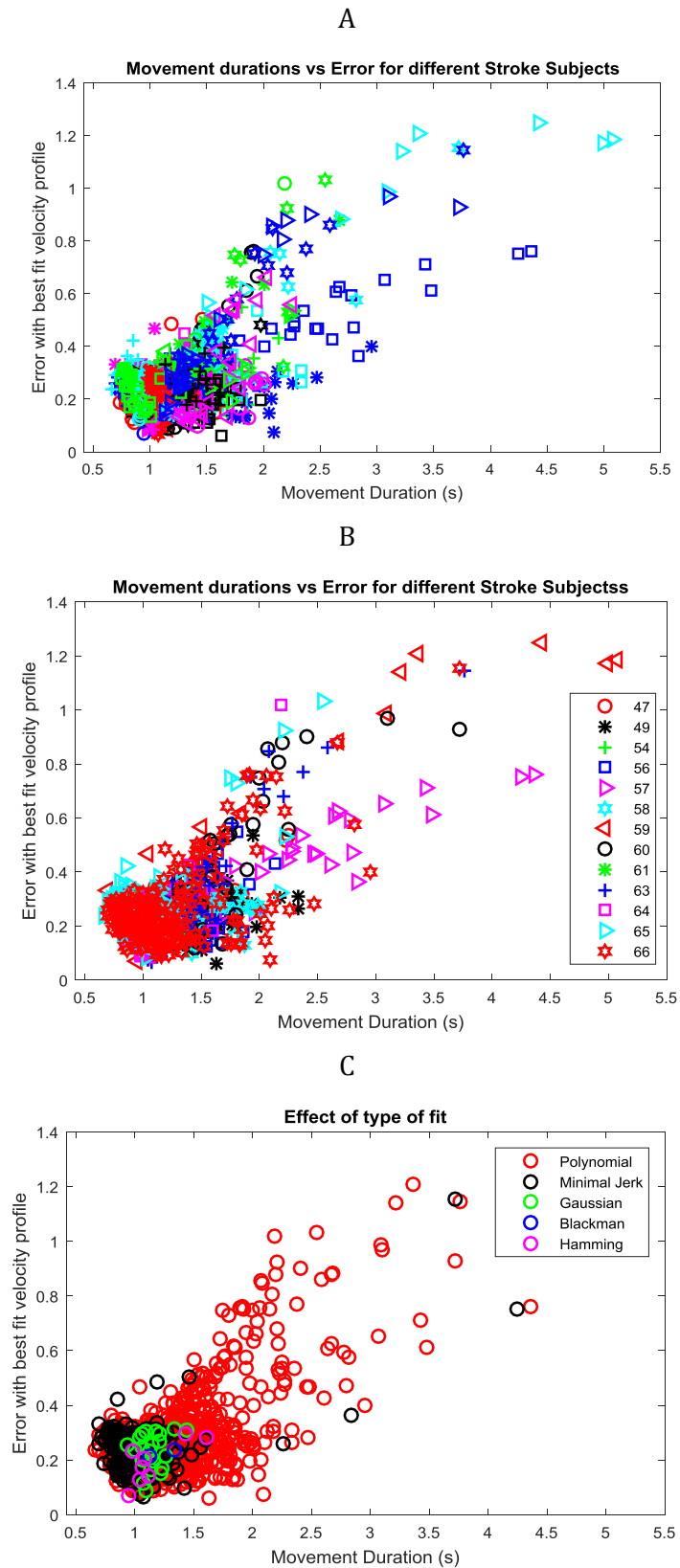


Figure F.7 (a) the movement duration and error with the best fit for all stroke subjects. All unique shape/color combinations represent a subject. (b) The same plot as (a) but now the color represents the FMA-UE score during the trail. In (c) the different best fits are presented by the color.

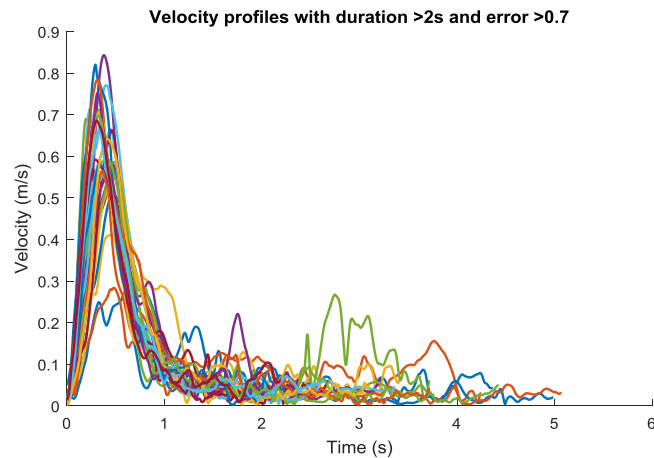


Figure F.8 - The velocity profiles with a longer duration and higher error are plotted

3. Monotonicity of dimensionless jerk metrics with the found profiles

In figure F.9 the effect of the asymmetric velocity profile on the sub-movement simulation is shown. As seen in F.9B, DSJb and LDSJb have a non-monotonic response on Polynomial 2 while the response is monotonic for the other sub-movements. Also remarkable is the response of CM. This metric had a monotonic response in symmetrical velocity profiles, but not for asymmetrical velocity profiles.

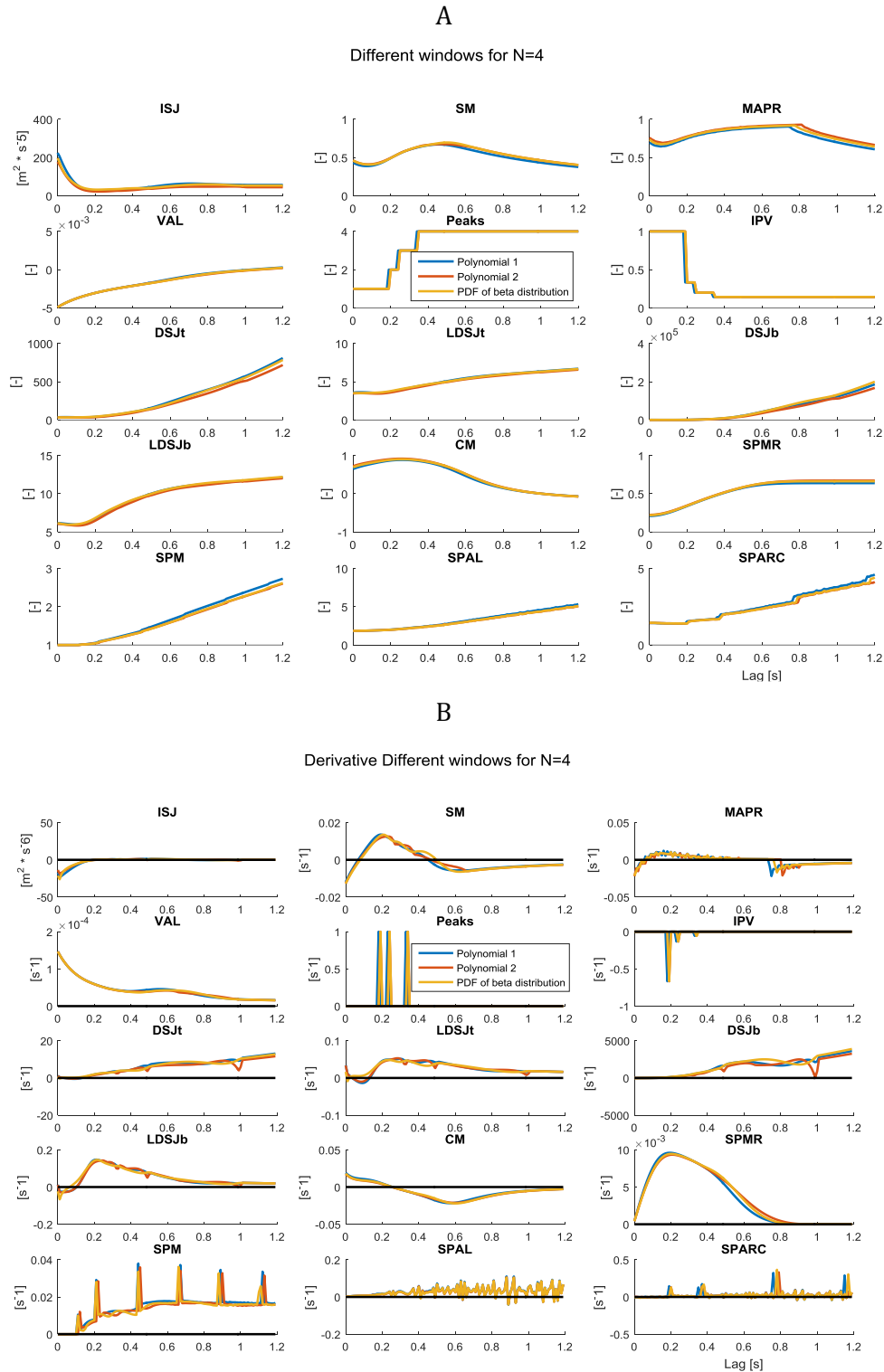


Figure F.9 – Check of monotonicity of the two polynomial fits and the probability density function (PDF) of the beta distribution. In figure F.9A the response of the simulation is seen. In B the derivative of this simulation is shown. A crossing of the 0 line would mean a non-monotonic response. It is seen that Polynomial 1 and the PDF of the beta distribution have a monotonic response. DSJb and LDSJb have a non-monotonic response on Polynomial 2. Also remarkable is the non-monotonicity for CM for all profiles. With integrated squared jerk (ISJ), speed metric (SM), movement arrest period ratio (MAPR), velocity arc length (VAL), number of peaks and valleys (IPV), Dimensionless squared jerk (DSJt and DSJb), log of DSJt and DSJb (LDSJb and LDSJt), correlation metric (CM), spectral metric (SPMR), spectral method (SPM), spectral arc length (SPAL) and spectral arc length with threshold (SPARC)

4. Conclusions

For both healthy and stroke subjects it was seen that the polynomial velocity profile represents the executed velocity profiles the best. It outperformed the minimal jerk trajectory which was the second best.

In healthy subjects it is seen that longer movement durations (>1.4 seconds) are accompanied by a worse fit. It is found that this is due to the long period of low velocity near the end of the movement. This raises the question whether the definition of the end point is well selected. This also opens the discussion that the way the end point is chosen influences the fit significantly.

For the stroke subjects it is seen that subjects with a FMA-UE score higher than 60 had an error and fit of the best fitted profile that was similar to the healthy subjects.

It was seen DSJb and LDSJb had a non-monotonic response for polynomial 2, while it was monotonic for polynomial 1 and the PDF of the beta distribution. This means that a subtle change in the underlying velocity profile would have big implication for the simulation. Also was seen that CM was clearly non-monotonic while it was monotonic for symmetrical velocity profiles.

References

Flash, T., & Hogan, N. (1985). The coordination of arm movements: an experimentally confirmed mathematical model. *Journal of neuroscience*, 5(7), 1688-1703.